A framework for predicting the effects of climate warming on arthropod disease vectors

Priyanga Amarasekare[1,3] **and Guilherme Casas Goncalves**[2]

[1] Independent researcher, Los Angeles, California, USA,

[2] Independent researcher, Sao Paulo, Brazil

[3] Corresponding author; E-mail: pamarasekare@gmail.com

ABSTRACT. Predicting the effects of climate warming on vector-borne disease transmission is a crucial research priority. Predictions that can reliably inform policy need to be based on vector biology, but models that incorporate biological realism are often difficult to test with the limited amount of information available for most disease vectors. Here we present a framework for predicting warming effects on vector population dynamics based solely on the vector's life history trait responses to temperature and the characteristics of the vector's thermal environment. We show that life history trait responses alone can make reasonably accurate predictions of a vector population's propensity for extinction under warming, while trait responses combined with the life stage at which density-dependence operates can predict whether vector populations exhibit intrinsic cycles in the absence of temperature variation. By incorporating the vector's life history traits into a population model that explicitly incorporates the vector's developmental delay, we show that the interplay between intrinsic cycles and temperature variation can lead to distinctive signatures in vector abundance patterns that can be detected in time series data without having to fit the model to such data. Importantly, we can use the model to predict the level of warming at which population regulation fails altogether, causing vector extinction. We find that the threshold warming level for extinction is lower when warming is driven by hot extremes compared to other scenarios.

Keywords: Climate warming, developmental delays, disease vectors, ectotherm, thermal niche, life history traits, population regulation

Introduction

Vector-borne diseases pose significant risks to public health and wildlife management on a global scale (Caminade et al., 2016). Most disease vectors are arthropods (e.g., mosquitoes, ticks, flies) with complex life cycles consisting of distinct life stages (e.g., eggs, larvae/nymphs, adults). The time delay induced by development from egg to adult is a distinctive feature of such life cycles. Developmental

delays drive phenology, the seasonal timing of life history events (Scranton and Amarasekare, 2017). They also induce delays in the operation of density-dependent feedbacks underlying population regulation, generating intrinsic oscillations in the absence of any environmental variation (Gurney et al., 1983; Nisbet and Gurney, 1983; Nisbet, 1997; Murdoch et al., 2003). Because arthropods are ectotherms whose body temperature depends on the environmental temperature, climate warming is likely to have direct and immediate effects on vector developmental delays. If we are to make reliable predictions about warming effects on vector-borne disease transmission, we need to understand how temperature effects on vector developmental delays translate into vector phenology and population dynamics.

Delay differential equations (DDEs) provide a natural mathematical context for incorporating developmental delays into models of population dynamics. Such models have a long history in the study of insect population dynamics and host-parasitoid interactions (Gurney et al., 1983; Nisbet and Gurney, 1983; Nisbet, 1997; Murdoch, 1992; Murdoch et al., 2003, 2006). They have also been used in investigations of vector population dynamics (Beck-Johnson et al., 2013; Ewing et al., 2016; Beck-Johnson et al., 2017). However, the biological realism afforded by DDE models also makes them mathematically complex, making it difficult to fit them to time series data. The challenge is to leverage the realism of DDE models to generate predictions that can be tested with the minimum amount of empirical information.

Here we present a theoretical framework for predicting warming effects on vector phenology and population dynamics based solely on the vector's life history trait responses to temperature and the characteristics of the vector's thermal environment (e.g., mean temperature and amplitude of seasonal fluctuations). We show that life history trait responses alone can make reasonably accurate predictions of a vector population's propensity for extinction under warming, while trait responses combined with the life stage at which density-dependence operates can predict whether developmental delays can generate intrinsic population cycles. By incorporating the temperature responses of life history traits

and competition into a DDE model, we can identify qualitatively distinctive patterns of phenology and population dynamics, the signatures of which can be detected in time series data.

Conceptual framework

Our goal is to develop a framework for generating predictions about warming effects based on the vector's life history and its thermal environment. To this end, we focus on vector biology and defer the mathematical details to the Supplementary Information. We begin by showing how we can use the vector's life history trait responses to temperature to predict its fundamental thermal niche. We next investigate vector population dynamics in the absence of temperature variation, identifying the conditions under developmental delays generate intrinsic population cycles. We end with an analysis of vector population dynamics under seasonal variation and warming, making testable predictions about how the interplay between intrinsic cycles and temperature variation influences vector phenology and population dynamics.

Temperature responses of vector life history traits

Most disease vectors are ectotherms whose body temperature depends on the environmental temperature. Their life history traits exhibit plastic responses to temperature variation (thermal reaction norms; Stearns, 1992; Roff, 1992) arising from temperature effects on the underlying biochemical processes (Johnson and Lewin, 1946; Sharpe and DeMichele, 1977; Schoolfield et al., 1981; Van der Have and de Jong, 1996; Ratkowsky et al., 2005). This biochemical dependence allows us to derive mechanistic descriptions of trait responses based on first principles of thermodynamics (Johnson and Lewin, 1946; Sharpe and DeMichele, 1977; Schoolfield et al., 1981; Van der Have and de Jong, 1996; Van der Have, 2002; Van der Have and de Jong, 1996; Ratkowsky et al., 2005) (Appendix A). This characterization reveals two distinct types of life history trait responses to temperature. Rate-controlled responses, which are driven primarily by temperature effects on biochemical rate processes (e.g., reaction kinetics, en-

zyme inactivation), exhibit monotonic or left-skewed responses to temperature (Sharpe and DeMichele, 1977; Schoolfield et al., 1981; Van der Have and de Jong, 1996; Van der Have, 2002; Kingsolver, 2009; Kingsolver et al., 2011). For instance, above the low temperature threshold for viability, the mortality rate increases with increasing temperature while the maturation rate increases to a maximum followed by a rapid decline (Appendix A). Regulatory responses, which are driven by biochemical regulatory processes that prevent reactions from proceeding to their maxima (e.g., neural and hormonal regulation; Hochachka and Somero 2002; Long and Fee 2008; Nijhout 1994), exhibit more symmetrically unimodal responses to temperature (e.g., the birth rate; Appendix A). Several large-scale data analyses show that the qualitative nature of life history trait responses (e.g., monotonic, left-skewed, Gaussian) is conserved across ectotherm taxa Gillooly et al. (2001, 2002); Savage et al. (2004); Dell et al. (2011); Englund et al. (2011). This allows us to develop a mechanistic framework for predicting warming effects on ectotherm disease vectors that can apply broadly across taxa, habitats and latitudes.

The vector's fundamental thermal niche

The vector's fundamental thermal niche is the range of temperatures within which it can maintain a positive intrinsic growth rate. When population growth is density-independent, the long-run growth rate of the population constitutes its intrinsic growth rate (Amarasekare and Coutinho, 2013). When the thermal environment is invariant, i.e., the vector population experiences the same temperature, on average, with few or no fluctuations around the mean, we can derive the temperature dependence of the intrinsic growth rate in terms of the temperature responses of its constituent life history traits:

$$r(T) = -d_A(T) + \frac{W\left(b(T)\tau_J(T)e^{(d_A(T)-d_J(T))\tau_J(T)}\right)}{\tau_J(T)} \tag{1}$$

where W is the principal (positive) branch of the Lambert W function or the product logarithm (Corless et al., 1996), $\tau_J(T)$ is the temperature-dependent developmental delay, $b(T)$ and $d_X(T)$ $(X = J, A)$ are the temperature responses of birth and and mortality rates, and $m_J(T) = \frac{1}{\tau_J(T)}$ is the maturation rate (see Appendix A for details).

Note that $r(T)$ is the sum of two components, with a negative contribution through adult mortality ($d_A(T)$) and a positive contribution through the multiplicative effects of birth, juvenile mortality, adult mortality, and the developmental delay. Importantly, the lower and upper temperature limits at which the negative contribution equals the positive contribution constitute the thermal limits above and below which the vector population goes extinct ($T_{min_{r=0}}$ and $T_{max_{r=0}}$), and the temperature at which the positive contribution exceeds the negative contribution by the greatest amount constitutes the temperature at which $r(T)$ is maximized ($T_{\mathrm{r_{max}}}$). Knowing the $T_{\mathrm{r_{max}}}$ for a given vector species is important because it is the temperature at which the vector can recover from low density at the fastest rate.

The key point is that we can characterize the FTN of any ectotherm disease vector based solely on the temperature responses of its life history rates. By comparing the upper thermal limit to viability and the temperature at which $r(T)$ is maximized with the mean and maximum temperatures under a given warming scenario, we can predict whether a given vector population is likely to go extinct under that warming scenario.

Vector population dynamics in constant thermal environments

Vector populations are regulated by negative density-dependent feedbacks driven by intra-specific competition at the juvenile or adult stage. In mosquito vectors for example, competition between adult females for blood meals from hosts can cause vector birth rate to decline with increasing adult density; competition between larvae for food can cause the juvenile mortality rate to increase with increasing juvenile density. Importantly, because vector life cycles are characterized by a developmental delay,

there can be a delay in the operation of these negative feedback mechanisms, leading to population cycles even in the absence of any abiotic environmental variation (Gurney et al., 1983; Nisbet and Gurney, 1983; Nisbet, 1997; Murdoch et al., 2003).

The mechanisms underlying population cycles are as follows. When density-dependence operates through the birth rate, its effects on the adult population is delayed by a generation because of the time delay due to juvenile development. When lifetime fecundity (birth rate * adult longevity) is high and the developmental delay is long relative to adult longevity, this leads to delayed feedback cycles with a period $2-4$ times the developmental delay (Murdoch et al., 2003). When density-dependence operates through juvenile mortality, its effects are felt immediately on the juvenile population. When lifetime fecundity is high, this can lead to direct feedback cycles with a period $1-1.5$ times the developmental delay (Murdoch et al., 2003).

We can make two predictions based on these findings. First, we expect vector species with high lifetime fecundity and long juvenile developmental periods relative to adult longevity to exhibit population cycles even in the absence of temperature variation (Appendix B). Second, vector populations in which females are more limited by hosts than larvae are by their food resources are more likely to exhibit delayed feedback cycles while populations in which larvae are more food-limited than adults are host-limited are more likely to exhibit generation cycles.

Vector population dynamics in variable thermal environments

When temperature varies over time, the developmental delay varies with both temperature and time. In this case, modelling vector population dynamics requires using DDE models with variable time delays (Appendix C). The key question is how temperature variation affects the negative feedback processes that underlie population regulation, especially when delays in the operation of these feedbacks lead to intrinsic cycles.

We expect vector populations experiencing direct or delayed negative feedback to exhibit bounded growth under typical seasonal variation (i.e., populations do not drift to zero or reach outbreak densities). We also expect vector populations exhibiting intrinsic cycles in the absence of temperature variation to retain the signature of those cycles under typical seasonal variation. For instance, populations may still cycle with the same period and amplitude but attain higher maximum and minimum abundances during favorable periods and *vice versa* during unfavorable periods. We expect vector populations that attain stable point equilibria in the absence of temperature variation to follow the seasonal pattern of temperature variation with a single peak in abundance during the most favorable time of the year.

We expect climate warming to weaken the negative feedback processes that underlie population regulation, altering phenological patterns and disrupting bounded population growth. In populations exhibiting intrinsic cycles in the absence of temperature variation, higher mortality and longer developmental delays should cause abundances to fall below the cycle minima during the hottest parts of the year and to increase above the cycle maxima during the cooler parts of the year, with prolonged periods below cycle minima as warming proceeds. In populations exhibiting stable point equilibria in the absence of temperature variation, we expect longer periods of low abundances during the hottest periods the year and smaller peaks in abundance during the cooler periods as warming increases.

Our framework is general and its predictions apply to any ectotherm disease vector. We use the Malaria vector as a case study to illustrate how it can be used to predict the vector's FTN, its propensity for intrinsic cycling, and population dynamics under seasonal variation and warming based solely on information on the vectors life history trait responses to temperature and characteristics of its thermal environment.

Methods

Biology and previous studies of the Malaria vector (*Anopheles* species)

The malaria vector has a stage-structured life cycle with juvenile (eggs, larvae, pupae) and adult stages. Intra-specific competition can occur at the adult stage when females compete for blood meals from hosts and/or at the larval stage when larvae compete for their food resources (Beck-Johnson et al., 2013, 2017). Yamana et al. (2016) investigated the effects of climate warming on malaria prevalence in four geographic subregions in west Africa. They used extensive field observations to develop a mechanistic model of malaria transmission that included temperature, hydrology, and an agent-based model of vector population dynamics. Based on their findings, Yamana et al. (2016) predicted hotter and drier conditions in subregion (i), with an attendant decrease in malaria outbreaks. In subregion (ii) where vector reproduction and survival were already limited due to hot and dry conditions, they predicted malaria transmission to be unsustainable under future climate conditions. In subregion (iv) where the climate was highly suitable for disease transmission, Yamana et al. (2016) predicted future temperature increases to have minimal effect. They considered subregion (iii) the most critical because of strong inter-annual variability in transmission and because the increase in mosquito breeding due to projected increases in rainfall was similar in magnitude to the increase in mortality due to increases in temperature, thus making future outcomes uncertain. Based on these findings, Yamana et al. (2016) predicted that climate warming was unlikely to increase malaria burden in west Africa.

Temperature responses of life history traits

We used non-linear regression (nls package in R; R Core Team, 2016) to fit mechanistic response functions (Appendix A) to published data on temperature responses of life history traits for the Malaria vector (*Anopheles* species; Mordecai et al., 2013; Ciota et al., 2014; Shapiro et al., 2017). We used the nls.multstart package (Padfield et al., 2020) to allow for multiple initial conditions for each parameter.

This analysis assumes Gaussian error around predictions of trait means and a reference trait value measured at a temperature typically determined by the investigator.

We used trait response parameters to calculate the malaria vector's developmental delay, adult longevity, lifetime fecundity and the fraction of juveniles surviving to adulthood at the mean habitat temperature for eight locations across the four subregions in west Africa previously studied by Yamana et al. (2016) (Table 1).

Temperature response of the vector's fundamental thermal niche (FTN)

We incorporated life history trait response parameters into Equation (1) to characterize the FTN of the malaria vector. We calculated the lower and upper thermal limits to population viability and the temperature at which the intrinsic growth rate is maximized.

Vector population dynamics in constant thermal environments

We used the DDE model with fixed developmental delays (Appendix B) to investigate vector population dynamics in the absence of temperature variation. We parameterized the model with trait response data at the mean habitat temperature for each location to determine whether vector populations exhibited direct or delayed feedback cycles (see Appendix B for details). We calculated the amplitude and cycle period for each population that exhibited intrinsic cycles.

Vector population dynamics in variable thermal environments

We used the stage-structured DDE model with time-varying developmental delays (Appendix C) to investigate vector phenology and population dynamics under typical seasonal variation and warming. We parameterized the model with trait response parameters and simulated population dynamics at each locality over 75 years.

Characterizing temperature variation

We obtained monthly temperature data for the eight locations in west Africa from the NOAA climate prediction center (https://www.cpc.ncep.noaa.gov) and records from local weather stations closest to each location (Yamana et al., 2016). We depicted seasonal temperature variation using the sinusoidal function $T(t) = M_T - A_T \cos\frac{2\pi t - S}{yr}$ where t is the time in days, M_T is the mean habitat temperature in K, A_T is the amplitude of seasonal fluctuations, S is the phase shift when the warmest day occurs later in the year, and $yr = 365$ days. Taking the Julian date of the mid-point of each month as the independent variable (time), we estimated M_T, A_T and S for each of the eight locations using non-linear least squares regression (R Core Team, 2016) and allowing for multiple initial conditions with the nls.multstart package (Padfield et al., 2020).

We depict climate warming by modifying the seasonal temperature regime as follows: $T(t) = (M_T + m\,t) - (A_T + a\,t)\cos\frac{2\pi t - S}{yr}$ where $m = (\text{mhigh} - \text{mlow})/2$ and $a = (\text{mhigh} - \text{mlow})/2$ represent respectively, the daily rate of increase in mean and amplitude. The quantities $\text{mlow} = s_1/(n * yr)$ and $\text{mhigh} = s_2/(n * yr)$ where s_1 and s_2 are, respectively, the number of degrees by which minimum and maximum temperatures increase in n years.

We consider warming to manifest as an increase in the mean annual temperature and/or an increase in minimum and maximum temperatures. We consider three scenarios:

1. Baseline: minimum and maximum temperatures increase at the same rate ($s_1 = s_2$), resulting in an increase in the mean temperature while the amplitude stays the same.

2. Higher minimum temperature: the minimum temperature increases faster than the maximum temperature ($s_1 > s_2$), resulting in an increase in the mean temperature and a decrease in the amplitude. We term this the warmer winters scenario.

3. Higher maximum temperature: the maximum temperature increases faster than the maximum

temperature ($s_1 < s_2$), resulting in an increase in both the mean temperature and amplitude. We term this the hot extremes scenario.

According to the latest IPCC predictions (IPCC, 2023), the best estimate for warming is a 1.4° C increase in the mean habitat temperature (M_T) by year 2100 (75 years), the intermediate is 2.7° C, and the worst estimate is 4.4° C. We implement the three warming scenarios such that M_T increases by $1.4 - 4.4°$ over period of 75 years. For example, in the hot extremes (warmer winters) scenario, the mean increases by 2.7° when the maximum temperature increases by 3.6° (1.8°) and the minimum temperature by 1.8° (3.6°). We get the baseline scenario when both minimum and maximum temperatures increase by 2.7° over 75 years.

We use the DDE model with variable time delays (Appendix C) to generate predictions on the effects of these warming scenarios on the malaria vector the four subregions in west Africa. We compare our predictions with those made by (Yamana et al., 2016) in their study.

Results

Temperature responses of vector life history traits

The mechanistic temperature response functions (Appendix A) provide an excellent fit to data on the malaria vector's birth, maturation and mortality rates (Fig.1a-d). The mean habitat temperatures of the eight locations are at or near the optimal temperature for the birth rate (28.2° C; Fig. 1a) and below the temperature at which the maturation rate is maximal (30° C; Fig. 1b). The high mean temperatures mean that the vector experiences high juvenile and adult mortality, with juvenile mortality increasing faster with increasing temperature compared to adult mortality (Fig.1c-d, Table A1). These data suggest that even a small increase in mean temperature could lead to declines in birth and maturation and increases in juvenile and adult mortality (Fig.1a-d), with detrimental consequences for population viability.

The vector's fundamental thermal niche

By parameterizing Equation (1) with life history trait response data, we find that the temperature at which $r(T)$ is maximized ($T_{r_{max}}$) is 28.2° C, the same temperature as the birth rate optimum (T_{opt_b}), and the upper thermal limit for viability ($T_{max_{r=0}}$) is 33.9° C, barely 1° above the temperature above which the maturation rate starts to decline with increasing temperature ($T_{H_{m_J}} = 33.0°$ C; Table A1). These findings suggest that T_{opt_b} and $T_{H_{m_J}}$ can provide good approximations of $T_{r_{max}}$ and $T_{max_{r=0}}$. Importantly, this means that we can use life history trait response data to predict the temperature at which the vector population can increase from low densities at the fastest rate ($T_{r_{max}}$) and the temperature at which warming will cause deterministic extinction of the vector population ($T_{max_{r=0}}$).

By comparing the vector's $T_{r_{max}}$ and $T_{max_{r=0}}$ with the mean habitat temperature (M_T) and amplitude of seasonal fluctuations (A_T), we can predict the effects of warming on the population viability of the malaria vector. Save for the two locations in subregion (iv), vector populations in all other locations have $M_T > T_{r_{max}}$ indicating slower recovery from low abundances. Populations in subregion (ii) exhibit the largest seasonal fluctuations with maximum temperatures exceeding $T_{max_{r=0}}$ even in the absence of warming (Fig. 1e-l; Table 1). Populations within subregions (i) and (iii) also differ in seasonal fluctuations, with those exhibiting higher fluctuations exhibiting maximal temperatures closer to $T_{max_{r=0}}$ (Fig. 1e-l).

Based on this comparison, we expect even a moderate increase in M_T (e.g., M_T increasing by 2.7° over 75 years; see above) to cause vector extinction in subregion (ii) even without an increase in A_T due to hot extremes. We expect a moderate increase in M_T coupled with hot extremes to cause extinction in regions (i) and (iii). We do not expect warming-induced extinction in subregion (iv) where $M_T \ll T_{r_{max}}$ and seasonal fluctuations are sufficiently small that maximum temperatures are unlikely to exceed $T_{max_{r=0}}$ even when a moderate increase in M_T is coupled with hot extremes (Fig. 1m-t).

Vector population dynamics in constant thermal environments

As noted above, the vector's developmental delay can cause delays in the operation of density-dependent feedbacks, leading to intrinsic population cycles even in the absence of temperature variation. Importantly, we can predict a given vector population's propensity to exhibit such cycles based solely on the temperature responses of its life history traits and the mean habitat temperature.

We see that lifetime fecundity of the malaria vector is high even in the warmest locations, and that the developmental delay exceeds adult longevity in the warmer locations and slightly exceeds unity in the coolest locations (subregion (iv); Fig. 1m). The reason why the delay and longevity are more similar in the coolest locations is because the mean habitat temperature is well below the temperature at which the delay is minimized (and the maturation rate is maximized; Fig. 1n) and hence the delay and longevity are both decreasing with increasing temperature. Since the rate at which this decrease occurs decelerates as the delay approaches its minimum while longevity continues to decline exponentially, the delay starts to exceed longevity in the warmer locations (Fig. 1n). Based on these findings, we expect vector populations in all eight locations to exhibit intrinsic cycles.

Verifying the accuracy of this prediction with the fixed-delay the DDE model parameterized with the vector's trait response data (Appendix B) shows that when density-dependence operates on the adult stage (e.g., females competing for blood meals from hosts causing the birth rate to decrease with increasing adult density), populations from all eight locations exhibit delayed feedback cycles with periods approximately four times the developmental delay at the mean habitat temperature (Table 1, Figure 2). When density-dependence operates on the juvenile stage (e.g., when larvae compete for food), all eight populations reach stable point equilibria (Figure 2).

Knowing a vector population's propensity for intrinsic cycles in the absence of temperature variation is important for predicting its populations dynamics under seasonal variation and warming. Since temperature variation can only affect the strength of density-dependence but not the life stage it op-

erates at (e.g., juvenile vs. adult) or its nature (e.g., delayed vs. direct negative feedback), we expect signatures of direct and delayed density-dependent feedbacks to be evident in vector abundance patterns under typical seasonal variation. We also expect such signatures to be retained under warming until and unless warming is strong enough to weaken density-dependence to a level at which bounded growth no longer occurs.

It is difficult in practice to determine which life stage density-dependence operates on or how strong the negative feedback is. We can, however, make inferences based on available information. For instance, we can use data on human population density in different locations to determine whether competition for blood meals is likely to be the main source of population regulation. We expect weaker competition for blood meals in locations of high human density and *vice versa*. For example, human population density is high in locations within subregion (iv), low in subregions (i) and (ii), and variable in subregion (iii) with low to moderate densities (Yamana et al., 2016). Since adult females are unlikely to be limited by blood meals in high density locations, we expect larval competition to be the main source of population regulation in such locations. If this is the case, we expect vector populations in locations of low human density to exhibit delayed feedback cycles and populations in locations of high human density to attain stable point equilibria in the absence of temperature variation. We therefore expect distinct differences in phenology and population dynamics between these locations.

Vector population dynamics under seasonal variation

We used the DDE model with variable developmental delays (Appendix C) to investigate vector population dynamics under typical seasonal variation in the eight locations. As predicted, we find signatures of delayed and direct density-dependent feedback in the time series of vector abundances (Fig. 2, Fig. C1).

Density-dependence operates on vector birth rate

When density-dependence operates on the vector's birth rate, we see seasonal variation superimposed on delayed feedback cycles such that delay cycles retain the same period but have lower minima and maxima during the warmest part of the year and higher minima and maxima during the cooler parts of the year. Signatures of delay cycles are strongest in the two locations experiencing the lowest mean temperature (subregion (iv), Fig.2(g), Fig. C1(g) and (h)) and weakest in the two locations experiencing the highest amplitude of seasonal fluctuations (subregion (ii), Fig.2c), Fig. C1c and d). In subregion (iv), delay cycles persist throughout the year. While the minimum abundance drops slightly below the cycle minimum during the warmest part of the year, the maximum abundance never exceeds the cycle maximum (Fig.2(g), Fig. C1(g) and (h)). In subregion (ii), delay cycles are suppressed during the warmest period of the year, leading to extended periods of abundances falling well below the cycle minima followed by a single short peak of high abundance (Fig. 2c, Fig. C1(c) and (d)). In subregion (i), the population experiencing larger seasonal fluctuations exhibits a longer period of abundances below the cycle minimum (compare Fig. 2a, Fig. C1(a) and (b)), while in subregion (iii), the population experiencing lower fluctuations but the highest mean temperature of all locations (Koure, Niger) exhibits a longer period of abundances below the cycle minimum (compare Fig. C1(e) and (f)).

Higher temperatures suppress delay cycles via the following mechanism. Juvenile mortality increases and the maturation rate decreases with increasing temperature (Fig. 1b and c), leading to a smaller fraction of juveniles surviving to adulthood. At the same time, higher adult mortality means a smaller adult population and weaker competition for blood meals, weakening negative feedback and suppressing delay cycles. Since the birth rate is also lower at higher temperatures, the adult population remains low during the warmer period, recovering only after temperatures drop to levels at which birth and maturation can exceed mortality.

Density-dependence operates on vector's juvenile mortality rate

As predicted, when density-dependence operates on juvenile mortality and vector populations reach stable point equilibria in the absence of temperature variation, we see only seasonal cycles with abundances reaching a maximum during the cooler part of the year and a minimum during the warmer part of the year (Fig. 2b, d, f and h, Fig. C2) However, these seasonal cycles retain signatures of direct density-dependent feedback. In locations where $M_T < T_{r_{max}}$ (subregion (iv)), minimum seasonal abundance does not fall below the equilibrium abundance; this is also the case in locations within subregions (i) and (iii) where $M_T > T_{r_{max}}$ but A_T is low. In locations where $M_T < T_{r_{max}}$ but A_T is high (subregion (ii)), abundances fall below the equilibrium abundance during the warmest months of the year (Fig. 2f, Fig. C2).

As in the case when density-dependence operates on the birth rate, populations in subregion (ii) exhibit long periods of low abundances followed by a short period of high abundances. Similarly, the population experiencing larger seasonal fluctuations in region (i) (Dire, Mali) and the population with the highest mean temperature in subregion (iii) (Koure, Niger) show longer periods of low abundances compared to their counterparts within the same subregion.

Of note, when density-dependence operates on juvenile mortality, adult vector abundances are lower than when density-dependence operates on the birth rate. This is because vector populations experience high juvenile mortality even at their current mean habitat temperatures (Fig. 1c), further increases in mortality due to competition reduces the fraction of juveniles surviving to adulthood. Vector populations in subregion (iv), which experience the lowest mean temperatures, exhibit the highest adult abundance.

Combining this information with existing data on human population density (Yamana et al., 2016), we can predict the type of phenological pattern we expect to see in the different locations. In subregions (i) and (ii) where human population density is low and delayed feedback cycles are likely, we expect a

pattern driven by seasonal forcing of the delay cycles (Fig. 2a,d). In subregion (iv) where population human density is high and feedback cycles are unlikely, we expect a pattern dominated by seasonal variation (Fig. 2g,Fig. C2g and h). In subregion (iii) where human population density is variable, the location with the lower density (Tanout, Niger) is likely to exhibit feedback cycles (Fig. 2e, Figs. C2e and f) and hence a phenological pattern similar to subregion (i), while the location with higher density (Koure, Niger) is likely to exhibit a pattern similar to subregion (iv) (Fig. C2f and g).

Detecting signatures of population dynamics in census data

A key question is whether we can detect the signatures predicted by the DDE model in vector census data. Using the daily time series from the model to calculate monthly vector abundances, we find that when density-dependence operates on the birth rate, monthly census data can accurately capture the distinctive abundance pattern arising from the interplay between delay cycles and seasonal temperature variation. However, monthly data, while accurately capturing population minima, tend to underestimate the maxima (Fig. 5). We find that biweekly census data can more accurately capture population maxima. When density-dependence operates on juvenile mortality, monthly data are sufficient to capture the peaks and troughs driven by seasonal variation (Fig. 5).

Vector population dynamics under climate warming

We find that low levels of warming (e.g., M_T increasing by 1.4° C over 75 years) do not cause vector extinctions in any of the eight locations (Fig. 3, Figs. C3 and C4). This is true regardless of whether density-dependence operates on the vector's birth rate or the juvenile mortality rate. Warming does amplify the seasonal pattern of lower abundances during the hottest months and higher abundances during the cooler months. An increase in M_T accompanied by an increase in A_T due to hot extremes is the most detrimental warming scenario, causing long periods of extremely low abundances followed short-period outbreaks in subregion (ii). Populations in the coolest locations (subregion (iv)) are largely

immune to these warming effects.

As predicted based on the vector's FTN, moderate levels of warming (2.7° C) cause five out of eight populations to go extinct due to hot extremes by 2100 (Fig. 4, Figs. C5 and C6). Two out of eight populations go extinct under all three warming scenarios. These include one population in subregion (ii) with high M_T and A_T, and one in subregion (iii) with the highest M_T of all locations. Also as predicted based on the vector's FTN, vector populations in subregion (iv) persist under all warming scenarios but with abundances falling below cycle minima during the warmest months of the year. Hot extremes cause longer periods of low abundances compared to other warming scenarios. These outcomes ensue regardless of which life stage density-dependence operates on. The one exception to our predictions is the remaining population in subregion (iii) (Tanout, Niger), which persists under all warming scenarios albeit with an extended period of low abundances followed by short-period outbreaks under baseline and hot extremes scenarios (Fig. 4, Figs. C5 and C6). This is likely due to the fact that this population exhibits the highest $r_{T_{\max}}$ of all locations, which gives it the ability to recover from low densities at the fastest rate.

High levels of warming (4.4° C over 75 years) cause the extinction of all but the two populations in subregion (iv). These two populations, though extant, experience warming-induced disruption of bounded growth. Vector abundances fall below cycle minima for extended periods of time and increase above cycle maxima to outbreak levels under baseline and hot extremes scenarios (Fig. C7 and C8). Across all levels of warming, the warmer winters scenario is the least detrimental to vector population viability.

In comparing our findings with the predictions made by Yamana et al. (2016), the vector's FTN provides reasonably accurate predictions of its ability to sustain malaria transmission. For instance, we find that vector populations in subregion (i) are likely to go extinct due to hot extremes even under moderate levels of warming, consistent with Yamana et al. (2016)'s predicttion of significantly reduced

malaria transmission in this subregion. The FTN shows that vector populations in subregion (ii) already experience temperatures near the upper limit of population viability, supporting the Yamana et al. (2016)'s previous prediction that malaria transmission is unlikely to sustainable in this region. Interestingly, we also find subregion (iii) to exhibit the most variable outcomes, with one population remaining viable even when moderate levels of warming are accompanied by hot extremes while the other goes extinct. In the case of subregion (iv) which was predicted to exhibit no change, we find that hot extremes can disrupt bounded population growth leading to prolonged periods of low abundances during which the vector population could go extinct due to demographic stochasticity. This comparison shows that our trait-based approach can provide reasonably accurate predictions of warming effects on field populations of disease vectors.

Summary of results

We find that the vector's life history trait responses and the characteristics of the vector's thermal environment are sufficient to predict warming effects on vector population dynamics and persistence.

1. Data on the vector's life history trait responses to temperature are sufficient to predict vector extinction under warming. Using trait response data for the malaria vector, we find that the temperatures at which birth and maturation rates are maximized (T_{opt_b} and $T_{H_{m_J}}$) provide good approximations of the temperature at which the vector can recover from low densities at the fastest rate ($T_{r_{max}}$) and the upper thermal limit for viability ($T_{max_{r=0}}$).

   By comparing these metrics with the mean habitat temperature (M_T) and the amplitude of seasonal fluctuations (A_T), we can predict which vector populations are likely to go extinct under different levels (M_T increasing by $1.4^\circ, 2.7^\circ$ or 4.4° over 75 years) and scenarios (baseline, warmer winters, hot extremes) of warming. These predictions are borne out by the analyses of a DDE model that incorporates trait response data and the life stage at which density-dependence

operates.

2. Life history trait response data can predict whether vector populations exhibit intrinsic cycles in the absence of temperature variation. High lifetime fecundity and a long developmental delay relative to adult longevity can lead to delayed feedback cycles when density-dependence operates at the adult stage and direct feedback cycles when density-dependence operates at the juvenile stage.

   The malaria vector exhibits high lifetime fecundity and a long developmental delay in all eight locations, indicating the propensity for intrinsic cycles. A DDE model parameterized with trait response data shows that all eight populations exhibit delayed feedback cycles when females compete for host blood meals, and stable point equilibria when larvae compete for food resources. Using data on human population density in different locations, we can predict which vector populations are likely exhibit delayed feedback cycles and which are likely to attain stable equilibria in the absence of temperature variation.

3. The combination of life history trait response data and characteristics of the thermal regime are sufficient to predict vector population dynamics under seasonal variation and warming.

   We find that locations in which vector populations are likely to undergo delayed feedback cycles exhibit a qualitatively different phenological pattern under seasonal variation compared to locations in which vector populations attain stable point equilibria.

   We find that vector populations experiencing warming tend to exhibit qualitatively similar abundance patterns as under typical seasonal variation when density-dependence operates at the juvenile stage and qualitatively different patterns when density-dependence operates at the adult stage.

4. We find that monthly census data of vector abundances are sufficient to detect which life stage density-dependence is likely to be strongest at and whether a given population is likely to exhibit intrinsic population cycles.

Discussion

Vector-borne diseases comprise a significant portion of the global disease burden (Caminade et al., 2016; World Health Organization, 2019). Predicting whether climate warming will increase or decrease this burden is a crucial priority for public health and wildlife management. Predictions that can reliably inform policy need to be based on vector biology, but models that incorporate biological realism are often difficult to test with the limited amount of information available for most disease vectors. For instance, most disease vectors are arthropods with complex life cycles characterized by developmental delays that drive both vector phenology and population dynamics. Population models that can incorporate developmental delays can generate predictions on phenology and dynamics. But, their biological realism comes at the cost of being parameter-rich, making it difficult to fit these models to census data.

Here we present a theoretical framework for predicting warming effects on disease vectors based solely on the temperature responses of the vector's life history traits and characteristics of the vector's thermal environment. Its novelty lies in elucidating mechanisms underlying warming effects on vector phenology and population dynamics from first principles rather than inferring mechanisms from data. It has the advantage of identifying qualitative signatures of warming effects on vector abundance patterns that can be detected in time series data, without having to fit complex models to such data. Perhaps most important, it shows us that the vector species' life history features contain insights that are crucial for predicting their ability to transmit diseases in the face of climate warming.

Our key findings are as follows. First, by characterizing the vector's fundamental thermal niche (FTN) based on its constituent life history traits (birth, maturation, mortality) we can predict the ther-

mal limits to vector population viability and the temperature at which the population can recover from low densities at the fastest rate. This allows us to predict the vector's propensity to go extinct under a given climate warming scenario, and whether or not it can recover from warming-induced decreases in abundance. Second, by comparing the vector's developmental delay with its lifetime fecundity and adult longevity, we can predict whether vector populations are prone to intrinsic population cycles. Third, by incorporating the vector's life history traits into a population model that explicitly incorporates the vector's developmental delay, we can predict the time to vector extinction under a given climate warming scenario and expected patterns of population dynamics when vector populations exhibit intrinsic cycles as opposed to stable point equilibria in the absence of temperature variation. We show that the interplay between intrinsic cycles and temperature variation can lead to distinctive signatures in vector abundance patterns that can be detected in time series data without having to fit the model to such data.

By testing the applicability of our framework with temperature response data for the malaria vector (*Anopheles* species), we find that the optimal temperature for the birth rate and the upper temperature limit above which the maturation rate starts to decrease with increasing temperature provide reasonably accurate predictions of the temperature at which the vector population can recover from low densities at the fastest rate and the upper thermal limit for vector viability. By incorporating the vector's life history trait responses to temperature into a stage-structured population model constructed with delay differential equations (DDEs), we find that the vector's FTN, which can be characterized using life history trait response data alone, can accurately predict the vector's propensity to go extinct under a given climate change scenario. We also find that the vector's developmental delay relative to its lifetime fecundity and adult longevity can accurately predict its propensity to exhibit delay-driven population cycles, and that for the malaria vector's trait response parameters, we expect to see delayed feedback cycles with a period of approximately four times the developmental delay when density-dependence operates on at

the adult stage (through competition for host blood meals by females), and stable point equilibria when density-dependence operates on the juvenile stage (through larval competition for food resources). The model predicts qualitatively distinct patterns of vector phenology and abundance depending on whether competition occurs at the adult or juvenile stages. Importantly, signatures of these qualitative differences can emerge in monthly census data, allowing us to infer what life stage density-dependence is most likely to operate at and whether vector populations exhibit intrinsic population cycles in the absence of temperature variation. The key point is that by elucidating mechanisms from first principles rather than inferring them from the data, we can make informed predictions about warming effects on disease vectors without having to fit complex models to time series data.

Given that this framework hinges on life history trait responses to temperature, the question arises as to the feasibility of quantifying these responses for disease vectors and the applicability of trait response data obtained in laboratory experiments to real world situations. As for feasibility, temperature responses of vector life history traits and disease transmission rates have been quantified for a number of Dipteran and Hemipteran vectors, and used to predict thermal limits to viability and Basic Reproductive Number (R_0; Mordecai et al. (2013); Ciota et al. (2014); Shapiro et al. (2017)). As for applicability, applying our framework to the malaria vector shows that life history trait response data can be reliably used to characterize real vector populations. For instance, we used laboratory-measured trait responses to predict the temperature at which the malaria vector's intrinsic growth rate is maximized ($T_{r(T)_{\max}}$), which is also the temperature at which the vector population can increase from low densities the fastest. When we compare $T_{r_{max}}$ with the mean habitat temperatures of vector populations across the four subregions previously studied by Yamana et al. (2016), we find that all populations have mean temperatures at or near $T_{r(T)_{\max}}$, exactly what we would expect for tropical ectotherms adapted to their typical thermal environment (Deutsch et al., 2008; Amarasekare and Savage, 2012). We also find that the maximum intrinsic growth rate ($r(T)_{\max}$) is higher for vector populations experiencing mean habi-

tat temperatures closer to $T_{r(T)_{\max}}$, also what we would expect for tropical ectotherms (Deutsch et al., 2008; Amarasekare and Savage, 2012; Amarasekare and Johnson, 2017). Moreover, we find that the upper thermal limit for viability predicted by trait response data coincides with the observed maximum habitat temperature for all vector populations, except those in subregion (ii) that experience higher-amplitude seasonal fluctuations than are typical for tropical habitats. Lastly, laboratory-measured trait response data can also correctly predict the propensity for intrinsic population cycles. Taken together, these findings suggest that trait response data measured in laboratory experiments can reliably be used to predict the viability, phenology and population dynamics of real vector populations. Indeed, there is a long tradition of using such data to predict the prevalence and transmission of vector-borne diseases (Mordecai et al., 2013, 2017; Johnson et al., 2015; Shocket et al., 2018, 2020; Tesla et al., 2018; Cator et al., 2020).

A related issue is whether knowledge of vector population dynamics in the absence of temperature variation, particularly whether populations exhibit intrinsic cycles, is useful for predicting warming effects on real vector populations. There are two reasons why this knowledge is important. The first is population regulation. Populations cannot persist in the absence of regulation via density-dependent feedbacks. These feedbacks enable populations to increase when rare and decrease when abundant, such that they exhibit bounded growth. Knowing what these bounds are is essential for predicting how well regulated a given population is in its typical thermal environment, and how severe warming would have to be to disrupt regulation altogether. For instance, life history trait data suggest that malaria vector populations in all four subregions have the propensity to exhibit delayed feedback cycles at their respective mean habitat temperatures. By comparing the maximum daily/monthly temperature each population is likely to experience with the upper thermal limit for viability, we can predict how many days/months of the year the population is likely to experience temperatures above this limit. We would expect abundances to fall below cycle minima during this period, and that is exactly what we find when

we simulate a DDE model parameterized with trait response data for each vector population. The key point is that knowing the bounds of population growth dictated by density-dependent feedbacks allows us to predict how severe warming would have to be for population regulation to fail.

It has been shown that as long as populations are regulated by density-dependent feedbacks, they will converge to a time-dependent asymptotic trajectory even in a nonstationary environment (AEDT; Chesson 2017, 2019). We do indeed see this when we simulate the DDE model parameterized with trait response data for various levels of climate warming. For low levels of warming, vector populations do indeed converge to qualitatively distinct trajectories depending on whether they attain stable point equilibria or delayed feedback cycles in the absence of temperature variation. We find that higher levels of warming progressively weaken density-dependent feedbacks, leading to long periods of low abundances followed by short-period outbreaks, a prediction we can test with information we can obtain with monthly censuses of vector abundances. Importantly, we can use the DDE model to predict the level of warming at which population regulation fails altogether, causing vector extinction. We find that the threshold warming level for extinction is lower when warming is driven by hot extremes compared to other scenarios.

The second reason why it is important to characterize vector population dynamics in the absence of temperature variation is because populations with a propensity for intrinsic cycles lead to qualitatively distinct phenological patterns compared to those that do not. Importantly, these differences can be detected in population census data, allowing us to infer which life stage density-dependence is most likely to operate on, information that cannot otherwise be obtained without detailed field studies. By comparing monthly census data with predicted trajectories of bounded growth from a DDE model, we can determine whether abundances fall below expected cycle minima and how long it takes the population to recover. By comparing the time spent below cycle minima in the observed time series with those predicted by a DDE model that incorporates climate warming scenarios, we can gauge how

susceptible a given vector population is to warming-induced extinction. The point is that we can learn a great deal about a vector population's susceptibility to extinction through information on its FTN and bounded population growth, without having to fit a complex population model to census data.

As noted in the Introduction, delay differential equations (DDEs) provide the most biologically realistic mathematical approach for modelling the dynamics of disease vectors and other arthropods whose life cycles are characterized by developmental delays. They are mathematically complex, particularly when developmental delays vary over time due to seasonal variation and warming. But they are necessary for making informed predictions about warming effects because models based on ordinary differential equations (ODEs) cannot capture the delay-induced phenological patterns that underlie patterns of disease transmission. There are well-developed numerical methods for simulating DDE models (e.g., the pydde package in Python) that are freely available. The great advantage of a DDE-based framework is that we can leverage the realism of DDE models to both generate and test predictions with the minimum amount of empirical information.

In conclusion, we have presented a theoretical framework for predicting the effects of climate warming on arthropod disease vectors that utilizes information on vector life history traits and characteristics of the vector's thermal environment to make predictions that can be tested with census data without having to fit models to data. The framework is general and can be applied to insect pests and pollinators in addition to arthropod disease vectors. In ongoing work we have successfully applied the framework to predict warming effects on west Nile vector populations across different latitudes and climate regimes (Amarasekare and Goncalves in Prep.), and we plan to apply it to insect pests from tropical, Mediterranean and temperate latitudes.

References

Amarasekare, P., and R. Coutinho. 2013. The intrinsic growth rate as a predictor of population viability under climate warming. Journal of Animal Ecology 82:1240–1253.

Amarasekare, P., and C. Johnson. 2017. Evolution of thermal reaction norms in seasonally varying environments. American Naturalist 189:E31–E45.

Amarasekare, P., and V. Savage. 2012. A mechanistic framework for elucidating the temperature dependence of fitness. American Naturalist 179:178–191.

Beck-Johnson, L., W. Nelson, K. Paaijmans, A. Read, M. Thomas, and O. Bjornstad. 2013. The effect of temperature on anopheles mosquito population dynamics and the potential for malaria transmission. PLoS One 8:e79276.

———. 2017. The importance of temperature fluctuations in understanding mosquito population dynamics and malaria risk. Open Science 4:160969.

Caminade, C., M. McIntyre, and A. Jones. 2016. Climate change and vector-borne diseases: Where are we next heading? The Journal of Infectious Diseases 214:1300–1301.

Cator, L. J., L. R. Johnson, E. A. Mordecai, F. El Moustaid, T. R. Smallwood, S. L. LaDeau, M. A. Johansson, P. J. Hudson, M. Boots, M. B. Thomas, A. G. Power, and S. Pawar. 2020. The role of vector trait variation in vector-borne disease dynamics. Frontiers in Ecology and Evolution 8.

Chesson, P. 2017. Aedt: A new concept for ecological dynamics in the ever-changing world. PLoS biology 15.

———. 2019. Contributions to nonstationary community theory. Journal of Biological Dynamics 13:123–150.

Ciota, A., A. Kilpatrick, and L. Kramer. 2014. Modelling the effect of temperature on the seasonal
616 population dynamics of temperate mosquitoes. Journal of Medical Entomology 51:55–62.

Corless, R., G. Gonnet, D. Hare, D. Jeffrey, and D. Knuth. 1996. On the lambert w function. Advances
618 in Computational Mathematics 5:329–359.

Dell, A., S. Pawar, and V. M. Savage. 2011. Systematic variation in the temperature dependence of
620 physiological and ecological traits. Proceedings of the National Academy of Sciences 108:10591–
10596.

622 Deutsch, C. J., J. Tewksbury, R. B. Huey, K. Sheldon, C. Ghalambor, D. Haak, and P. R. Martin.
2008. Impacts of climate warming on terrestrial ectotherms across latitude. Proc Natl Acad Sci USA
624 105:6668–6672.

Englund, G., G. Ohlund, C. Hein, and D. S. 2011. Temperature dependence of the functional response.
626 Ecology Letters 14:914–921.

Ewing, D., C. Cobbold, B. Purse, M. Nunn, and S. White. 2016. Modelling the effect of temperature on
628 the seasonal population dynamics of temperate mosquitoes. Journal of Theoretical Biology 400:65–
79.

630 Gillooly, J. F., J. H. Brown, G. B. West, V. M. Savage, and E. L. Charnov. 2001. Effects of size and
temperature on metabolic rate. Science 293:2248–2251.

632 Gillooly, J. F., E. L. Charnov, G. B. West, , V. M. Savage, and J. H. Brown. 2002. Effects of size and
temperature on developmental time. Science 293:2248–2251.

634 Gurney, W., R. Nisbet, and J. Lawton. 1983. The systematic formulation of tractable single-species
population models incorporating age structure. Journal of Animal Ecology 52:479–495.

636 Hochachka, P., and G. Somero. 2002. Biochemical Adaption. Oxford University Press.

IPCC. 2023. Climate Change 2023: Synthesis Report. Contribution of Working Groups I, II and III
638 to the Sixth Assessment Report of the Intergovernmental Panel on Climate Change [Core Writing Team, H. Lee and J. Romero (eds.)]. IPCC, Geneva, Switzerland.

640 Johnson, F., and I. Lewin. 1946. The growth rate of e. coli in relation to temperature, quinine and coenzyme. Journal of Cellular and Comparative Physiology 28:47–75.

642 Johnson, L., T. Ben-Horin, K. Lafferty, A. McNally, E. Mordecai, K. Paaijmans, S. Pawar, and S. Ryan. 2015. Understanding uncertainty in temperature effects on vector-853 borne disease: a bayesian
644 approach. Ecology 96:203–213.

Kingsolver, J. 2009. The well-temperatured biologist. American Naturalist 174:755–768.

646 Kingsolver, J., A. Woods, L. B. Buckley, L. Potter, H. MacLean, and J. Higgins. 2011. Complex life cycles and the responses of insects to climate change. Integrative and Comparative Biology 51:719–
648 732.

Long, M., and M. Fee. 2008. Using temperature to analyse temporal dynamics in the songbird motor
650 pathway. Nature 456:189–194.

Mordecai, E. A., J. M. Cohen, M. V. Evans, P. Gudapati, L. Johnson, C. A. Lippi, K. Miazgowicz,
652 C. C. Murdock, J. R. Rohr, S. J. Ryan, V. M. Savage, M. S. Shocket, A. S. Ibarra, M. B. Thomas, and D. P. Weikel. 2017. Detecting the impact of temperature on transmission of zika, dengue, and
654 chikungunya using mechanistic models. PLOS Neglected Tropical Diseases 11.

Mordecai, E. A., K. Paaijmans, L. Johnson, C. Balzer, T. Ben-Horin, E. Moor, M. A., S. Pawar, S. Ryan,

656 T. Smith, and K. Lafferty. 2013. Optimal temperature for malaria transmission is dramatically lower than previously predicted. Ecology Letters 16:22–30.

658 Murdoch, W. 1992. Ecological theory and biological control. Pages 197–221 *in* S. Jain and L. Botsford, eds. Applied Population Biology. Kluwer Academic Publishers.

660 Murdoch, W., C. J. Briggs, and N. R. M. 2003. Consumer resource dynamics. Princeton University Press, Princeton New Jersy.

662 Murdoch, W. W., S. Swarbrick, and C. J. Briggs. 2006. Biological control: lessons from a study of calofornia red scale. Population Ecology 48:297–305.

664 Nijhout, H. 1994. Insect hormones. Princeton University Press.

Nisbet, R. 1997. Sdelay-differential equations for structured populations. Pages 89–116 *in* S. Tul-
666 japurkar and H. Caswell, eds. Structured-population models in marine, terrestrial, and freshwater systems. Chapman and Hall, New York.

668 Nisbet, R. M., and W. Gurney. 1983. The systematic formulation of population-models for insects with dynamically varying instar duration. Theoretical Population Biology 23:114–135.

670 Padfield, D., H. O'Sullivan, and S. Pawar. 2020. rtpc and nls.multstart: A new pipeline to fit thermal performance curves in r. Methods in Ecology and Evolution 12:1138–1143.

672 R Core Team. 2016. R: A language and environment for statistical computing. R Foundation for Statistical Computing, Vienna .

674 Ratkowsky, D., J. Olley, and T. Ross. 2005. Unifying temperature effects on the growth rate of bacteria and the stability of globular proteins. Journal of Theoretical Biology 233:351–362.

676 Roff, D. 1992. The evolution of life histories: theory and analysis. Chapman and Hall.

Savage, V. M., J. F. Gillooly, J. H. Brown, G. B. West, and E. L. Charnov. 2004. Effects of body size
678 and temperature on population growth. American Naturalist 163:429–441.

Schoolfield, R., J. Sharpe, and C. Magnuson. 1981. Non-linear regression of biological temperature-
680 dependent rate models based on absolute reaction-rate theory. Jounal of Theoretical Biology 88:719–731.

682 Scranton, K., and P. Amarasekare. 2017. Predicting phenological shifts in a changing climate. Proceedings of the National Academy of Sciences 114:13212–13217.

684 Shapiro, L. L. M., S. A. Whitehead, and M. B. Thomas. 2017. Quantifying the effects of temperature on mosquito and parasite traits that determine the transmission potential of human malaria. PLoS
686 biology 15:e2003489.

Sharpe, P., and D. DeMichele. 1977. Reaction kinetics of poikilotherm development. Journal of Theo-
688 retical Biology 64:649–670.

Shocket, M. S., S. J. Ryan, and E. A. Mordecai. 2018. Temperature explains broad patterns of ross
690 river virus transmission. Elife 7:e37762.

Shocket, M. S., A. B. Verwillow, M. G. Numazu, H. Slamani, J. M. Cohen, F. El Moustaid, J. Rohr, L. R.
692 Johnson, and E. A. Mordecai. 2020. Transmission of west nile and five other temperate mosquito-borne viruses peaks at temperatures between 23 c and 26 c. Elife 9.

694 Stearns, S. 1992. The Evolution of Life Histories. Oxford University Press.

Tesla, B., L. R. Demakovsky, E. A. Mordecai, S. J. Ryan, M. H. Bonds, C. N. Ngonghala, M. A. Brind-

ley, and C. C. Murdock. 2018. Temperature drives zika virus transmission: evidence from empirical and mathematical models. Proceedings of the Royal Society B: Biological Sciences 285:20180795.

Van der Have, T. 2002. A proximate model for thermal tolerance in ectotherms. Oikos 98:141–155.

Van der Have, T. M., and G. de Jong. 1996. Adult size in ectotherms: temperature effects on growth and differentiation. Journal of Theoretical Biology 183:329–340.

World Health Organization. 2019. World Malaria Report 2019. World Health Organization.

Yamana, T., A. Bomblies, and E. Eltahir. 2016. Climate change unlikely to increase malaria burden in west africa. Nature Climate Change 6:1012–1016.

Table 1: Characteristics of vector populations in the four geographical subregions of west Africa[1].

Sub-region	Location	MT	AT	S	r(MT)	Transmission category	Human density	Cycle period	Cycle amplitude
(i)	Dire, Mali	302.35	3.79	-122.22	0.3339	Moderate	Low	35	594
(i)	Linguere, Senegal	302.59	2.43	-51.18	0.3291	Moderate	Low	35	620
(ii)	Kidal, Mali	301.88	6.85	45.41	0.3407	Low	Low	37	218
(ii)	Agadez, Niger	302.23	6.50	9.73	0.336	Low	Low	36	581
(iii)	Tanout, Niger	301.57	3.81	-101.63	0.3432	Moderate	Low	37	206
(iii)	Koure, Niger	303.00	2.71	-143.53	0.318	Moderate	Medium	35	666
(iv)	Kano, Nigeria	299.50	4.07	-201.11	0.3315	High	High	44	743
(iv)	Karan, Mali	300.16	2.18	-423.52	0.3395	High	Medium	42	407

[1] Subregions, locations, and data on transmission category and human population density are from Yamana *et al.,* (2016).

Figure legends

Figure 1. Life history trait responses, fundamental thermal niche (FTN) and propensity for intrinsic cycles in malaria vector populations across four geographic subregions in west Africa. Panels (a)-(d) depict, respectively, the temperature responses of the vector's birth, maturation, juvenile, mortality, and adult mortality rates. In panels (a) and (c), the vertical dashed line depicts the optimal temperature for

the birth rate and in panels (b) and (e), upper temperature threshold for the maturation rate. Panels (e)-(l) depict the FTN of eight populations in the four subregions. In these panels, the solid circle depicts the mean habitat temperature (M_T) of the focal population, the blue shaded region depicts the range of M_T across the eight populations, and the pink region, the expected range under a 2.7° increase in M_T due to hot extremes. Panel (m) depicts the vector's lifetime fecundity (black curve) and the ratio of adult longevity to the developmental delay (red curve) as a function of temperature (in K), and panel (n), adult longevity (black curve) and developmental delay as a function of temperature. In panel (m), the blue vertical line depicts the optimal temperature for reproduction, and in panel (n), the upper temperature limit above which the developmental delay starts to increase with increasing temperature. In both panels, the points on each curve correspond to the mean habitat temperature experienced by the eight vector populations. Parameter values are given in Tables 1 and A1.

Figure 2. Population dynamics of the malaria vector in constant and seasonal thermal environments when density-dependence operates on the vector's birth rate (left column) and juvenile mortality rate (right column). Dynamics are shown for four populations for each of the four subregions. Dynamics for all eight populations are given in Figs. C1 and C2. Parameter values are given in Tables 1 and A1.

Figure 3. Malaria vector population dynamics under low levels of warming (increase in mean temperature by 1.4° over 75 years) for the warmer winters (blue), baseline (orange) and hot extremes (red) scenarios when density-dependence operates on the vector's birth rate (left column) and juvenile mortality rate (right column). Dynamics for all eight populations across the four subregions are given in Figs. C3 and C4. Parameter values are given in Tables 1 and A1.

Figure 4. Malaria vector population dynamics under moderate levels of warming (increase in mean temperature by 2.7° over 75 years) for the warmer winters (blue), baseline (orange) and hot extremes (red) scenarios when density-dependence operates on the vector's birth rate (left column) and juvenile mortality rate (right column). Dynamics for all eight populations across the four subregions are given

in Figs. C5 and C6. Parameter values are given in Tables 1 and A1.

734 Figure 5. Average monthly and biweekly abundances of malaria vector populations calculated from the daily time series predicted by the DDE model when density-dependence operates on the birth 736 rate (left column) or the juvenile mortality rate (right column). The solid blue points denote monthly abundances and the red points, biweekly abundances. The points are connected for ease of comparison 738 with the daily time series (gray). Parameter values are given in Tables 1 and A1.

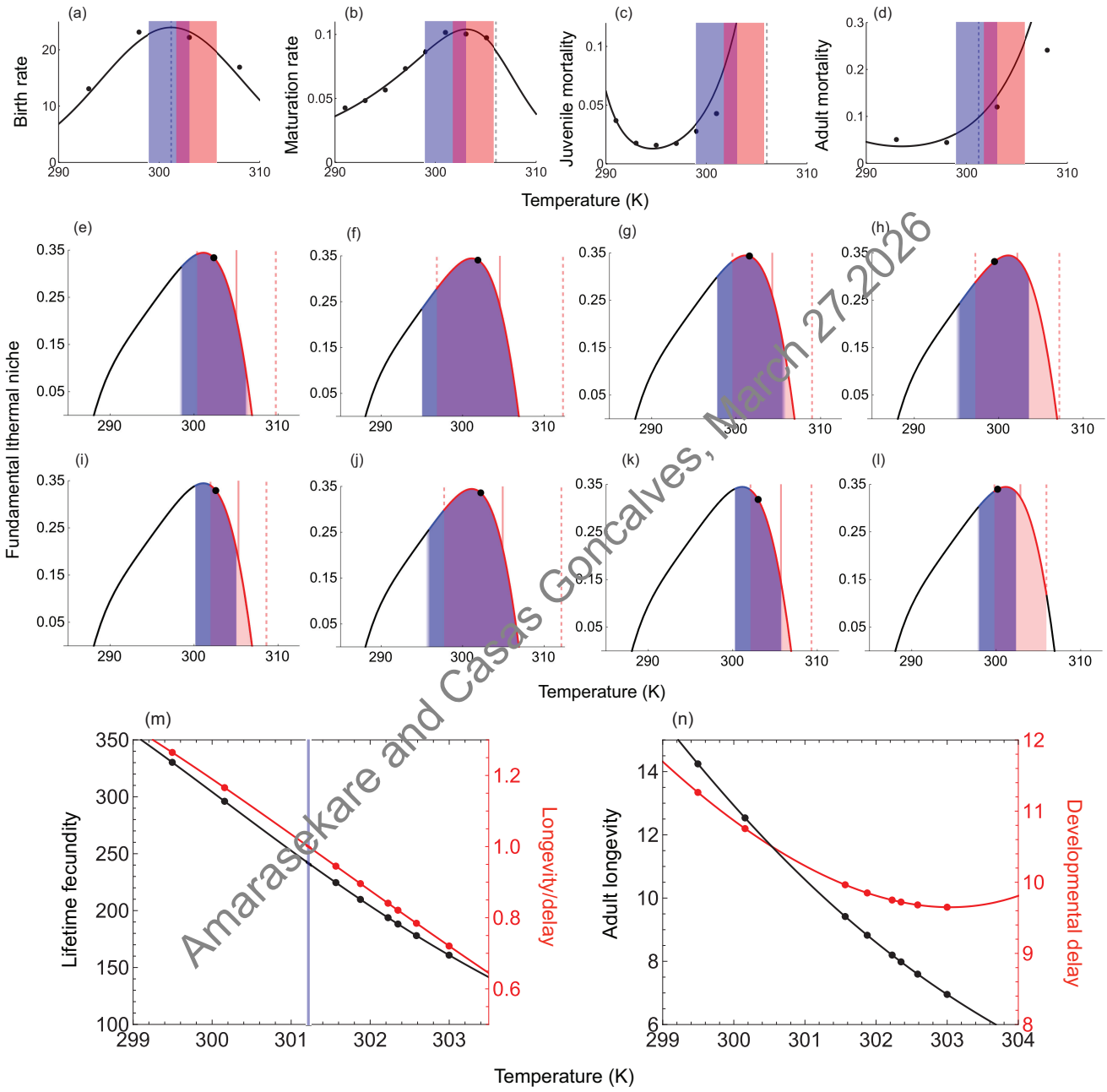

Figure 1

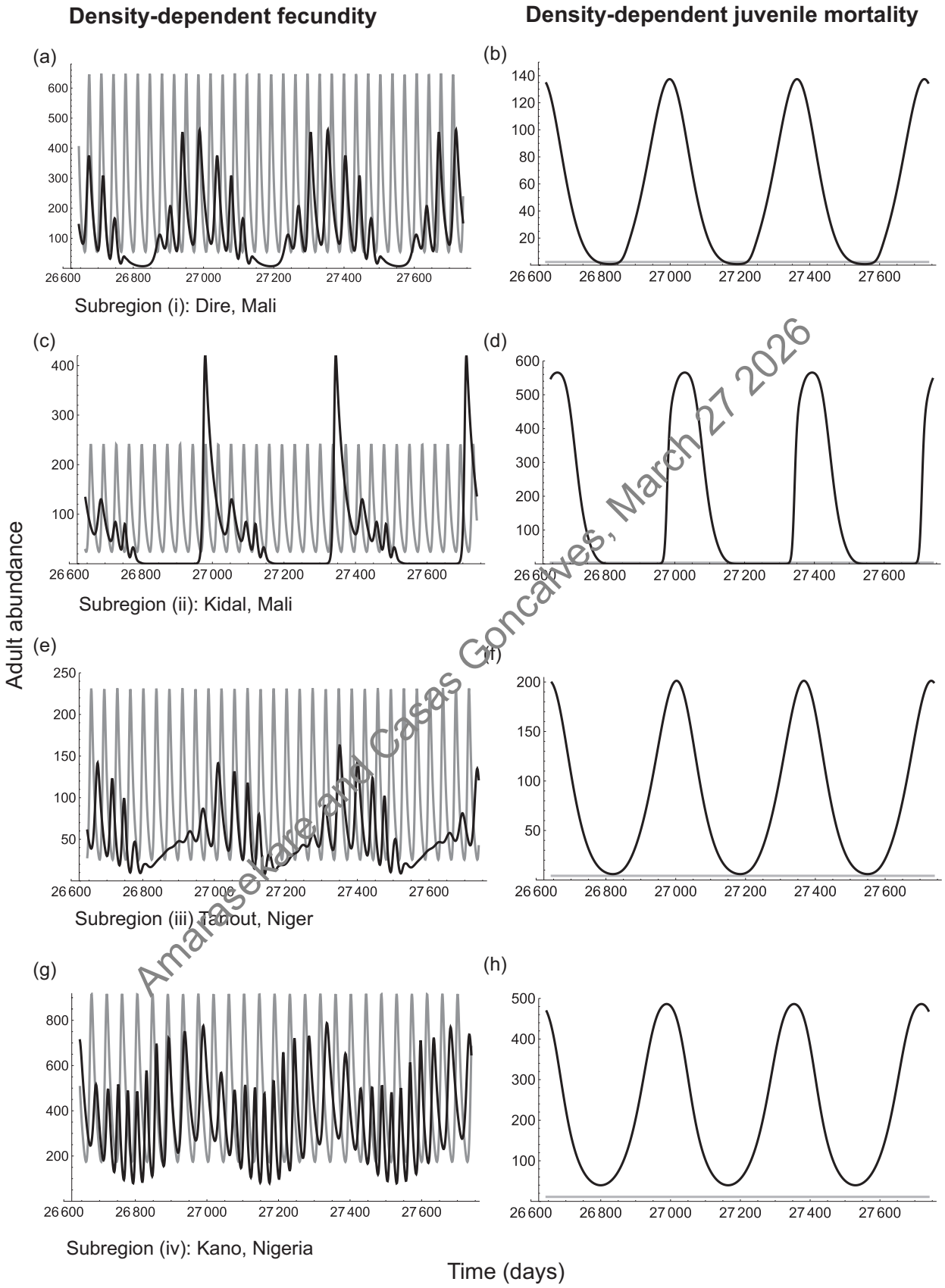

Figure 2

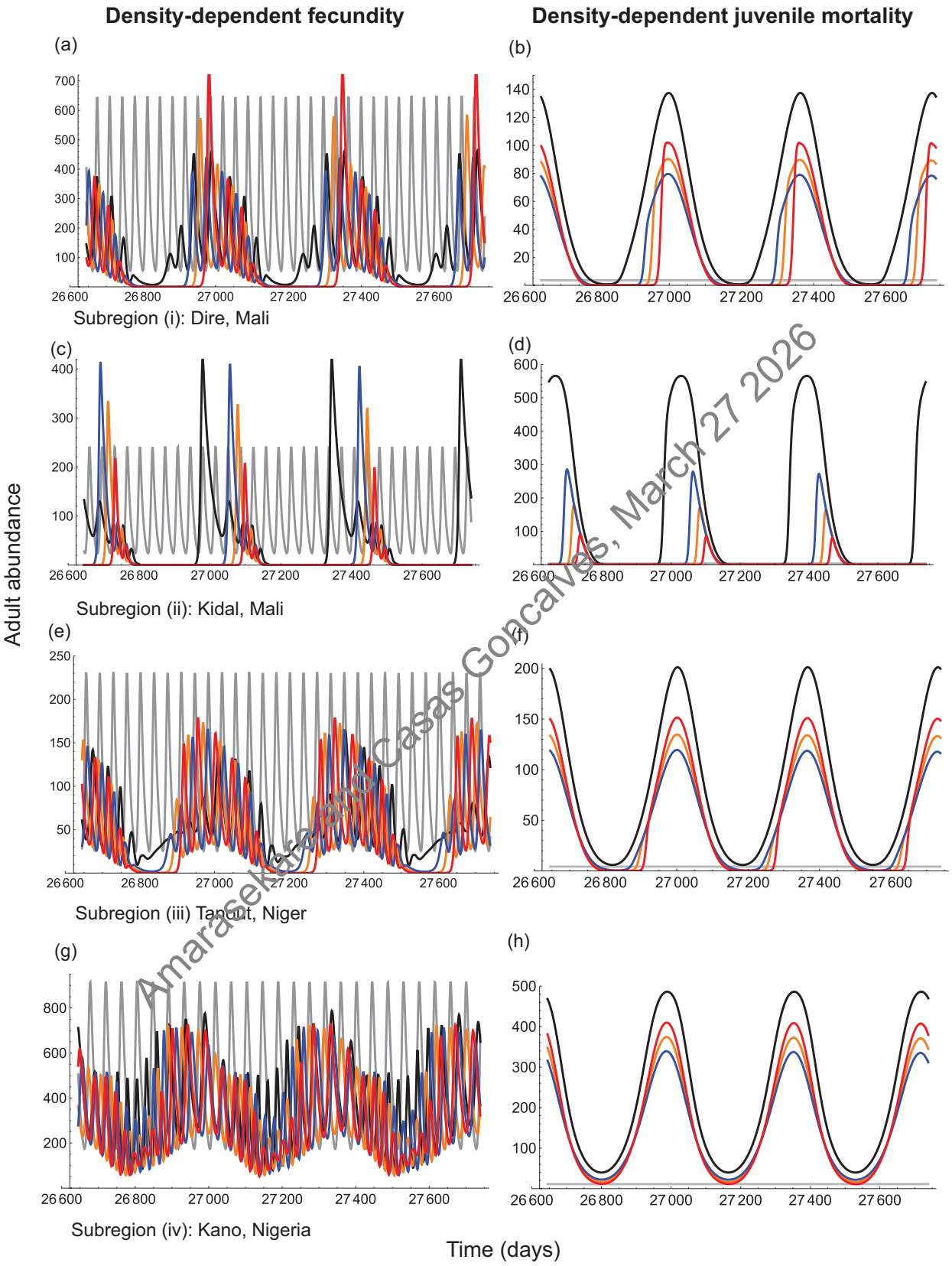
Density-dependent fecundity
Density-dependent juvenile mortality
(a)
(b)
(c)
(d)
(e)
(f)
(g)
(h)
Subregion (i): Dire, Mali
Subregion (ii): Kidal, Mali
Subregion (iii) Tanout, Niger
Subregion (iv): Kano, Nigeria
Adult abundance
Time (days)
Amaraseka Perera and Casas Goncalves, March 27 2026

Figure 3

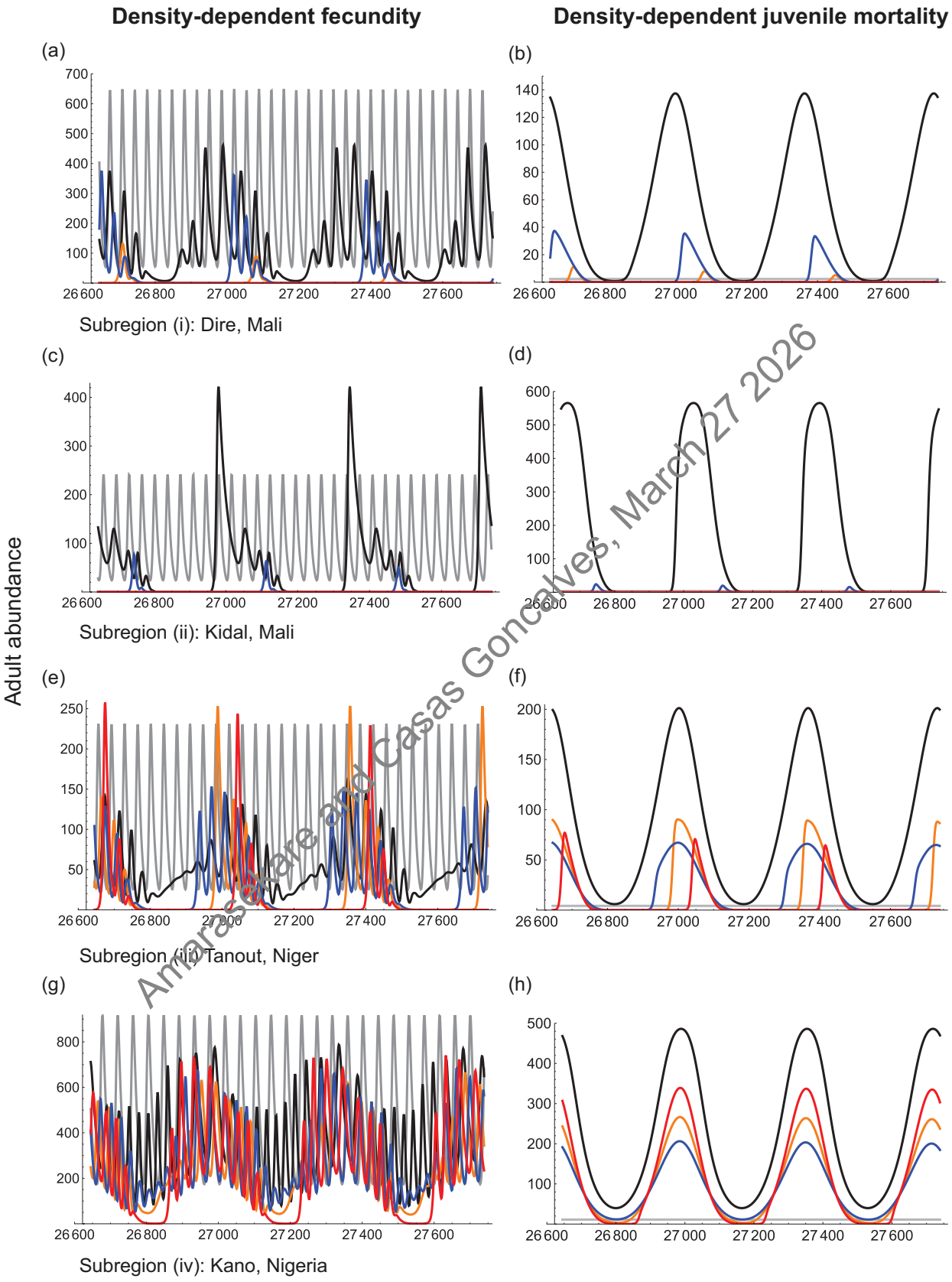

Figure 4

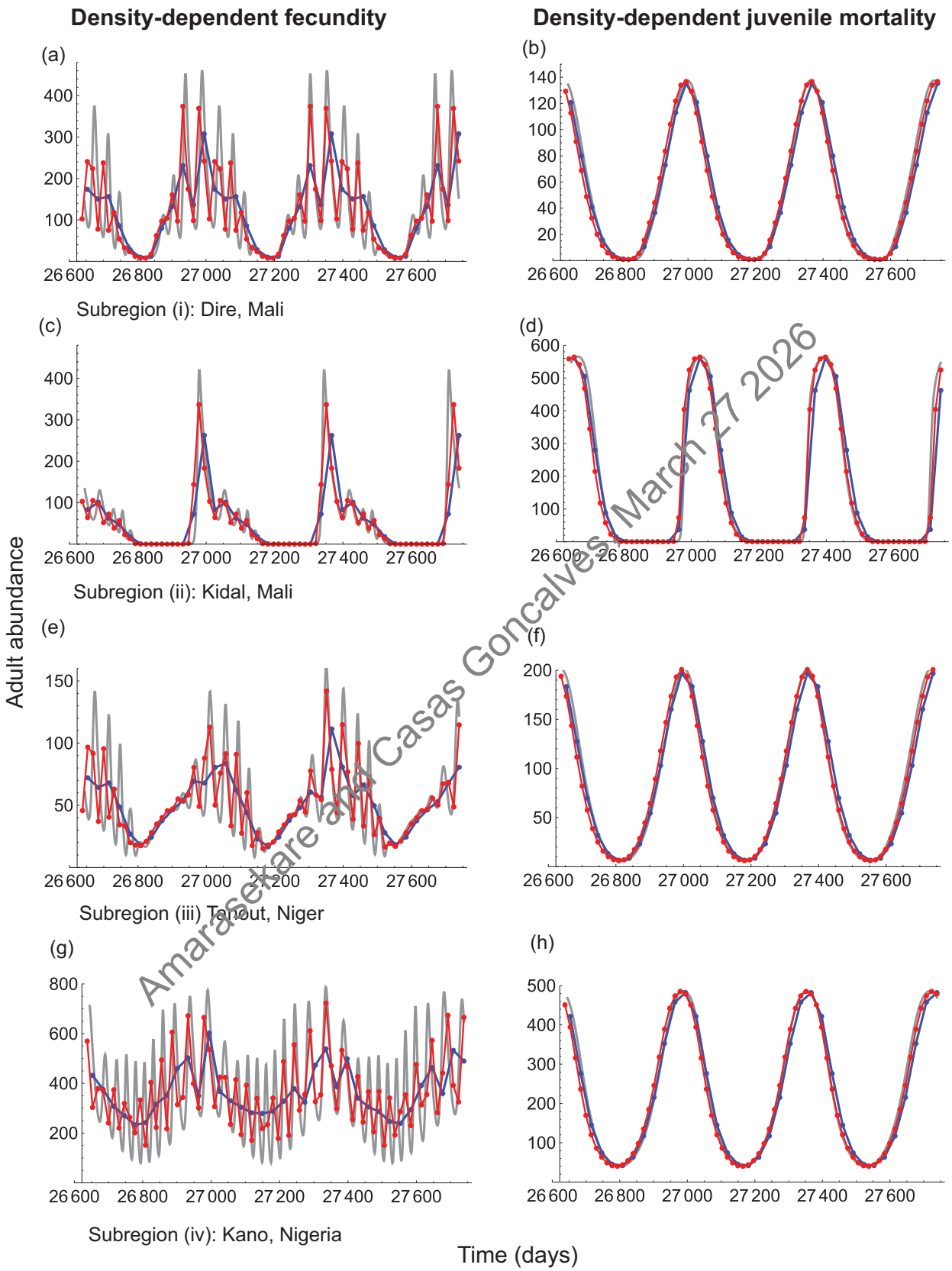

Figure 5

A framework for predicting the effects of climate warming on arthropod disease vectors

Priyanga Amarasekare[1,3] **and Guilherme Casas Goncalves**[2]

[1] Los Angeles, California, USA, [2] Sao Paulo, Brazil

[3] Corresponding author; E-mail: pamarasekare@gmail.com

ABSTRACT. Predicting the effects of climate warming on vector-borne disease transmission is a crucial research priority. Predictions that can reliably inform policy need to be based on vector biology, but models that incorporate biological realism are often difficult to test with the limited amount of information available for most disease vectors. Here we present a framework for predicting warming effects on vector population dynamics based solely on the vector's life history trait responses to temperature and the characteristics of the vector's thermal environment. We show that life history trait responses alone can make reasonably accurate predictions of a vector population's propensity for extinction under warming, while trait responses combined with the life stage at which density-dependence operates can predict whether vector populations exhibit intrinsic cycles in the absence of temperature variation. By incorporating the vector's life history traits into a population model that explicitly incorporates the vector's developmental delay, we show that the interplay between intrinsic cycles and temperature variation can lead to distinctive signatures in vector abundance patterns that can be detected in time series data without having to fit the model to such data. Importantly, we can use the model to predict the level of warming at which population regulation fails altogether, causing vector extinction. We find that the threshold warming level for extinction is lower when warming is driven by hot extremes compared to other scenarios.

Keywords: Climate warming, developmental delays, disease vectors, ectotherm, thermal niche, life history traits, population regulation

Introduction

Vector-borne diseases pose significant risks to public health and wildlife management on a global scale (Caminade et al., 2016). Most disease vectors are arthropods (e.g., mosquitoes, ticks, flies) with complex life cycles consisting of distinct life stages (e.g., eggs, larvae/nymphs, adults). The time delay induced by development from egg to adult is a distinctive feature of such life cycles. Developmental

delays drive phenology, the seasonal timing of life history events (Scranton and Amarasekare, 2017). They also induce delays in the operation of density-dependent feedbacks underlying population regulation, generating intrinsic oscillations in the absence of any environmental variation (Gurney et al., 1983; Nisbet and Gurney, 1983; Nisbet, 1997; Murdoch et al., 2003). Because arthropods are ectotherms whose body temperature depends on the environmental temperature, climate warming is likely to have direct and immediate effects on vector developmental delays. If we are to make reliable predictions about warming effects on vector-borne disease transmission, we need to understand how temperature effects on vector developmental delays translate into vector phenology and population dynamics.

Delay differential equations (DDEs) provide a natural mathematical context for incorporating developmental delays into models of population dynamics. Such models have a long history in the study of insect population dynamics and host-parasitoid interactions (Gurney et al., 1983; Nisbet and Gurney, 1983; Nisbet, 1997; Murdoch, 1992; Murdoch et al., 2003, 2006). They have also been used in investigations of vector population dynamics (Beck-Johnson et al., 2013; Ewing et al., 2016; Beck-Johnson et al., 2017). However, the biological realism afforded by DDE models also makes them mathematically complex, making it difficult to fit them to time series data. The challenge is to leverage the realism of DDE models to generate predictions that can be tested with the minimum amount of empirical information.

Here we present a theoretical framework for predicting warming effects on vector phenology and population dynamics based solely on the vector's life history trait responses to temperature and the characteristics of the vector's thermal environment (e.g., mean temperature and amplitude of seasonal fluctuations). We show that life history trait responses alone can make reasonably accurate predictions of a vector population's propensity for extinction under warming, while trait responses combined with the life stage at which density-dependence operates can predict whether developmental delays can generate intrinsic population cycles. By incorporating the temperature responses of life history traits

and competition into a DDE model, we can identify qualitatively distinctive patterns of phenology and population dynamics, the signatures of which can be detected in time series data.

Conceptual framework

Our goal is to develop a framework for generating predictions about warming effects based on the vector's life history and its thermal environment. To this end, we focus on vector biology and defer the mathematical details to the Supplementary Information. We begin by showing how we can use the vector's life history trait responses to temperature to predict its fundamental thermal niche. We next investigate vector population dynamics in the absence of temperature variation, identifying the conditions under developmental delays generate intrinsic population cycles. We end with an analysis of vector population dynamics under seasonal variation and warming, making testable predictions about how the interplay between intrinsic cycles and temperature variation influences vector phenology and population dynamics.

Temperature responses of vector life history traits

Most disease vectors are ectotherms whose body temperature depends on the environmental temperature. Their life history traits exhibit plastic responses to temperature variation (thermal reaction norms; Stearns, 1992; Roff, 1992) arising from temperature effects on the underlying biochemical processes (Johnson and Lewin, 1946; Sharpe and DeMichele, 1977; Schoolfield et al., 1981; Van der Have and de Jong, 1996; Ratkowsky et al., 2005). This biochemical dependence allows us to derive mechanistic descriptions of trait responses based on first principles of thermodynamics (Johnson and Lewin, 1946; Sharpe and DeMichele, 1977; Schoolfield et al., 1981; Van der Have and de Jong, 1996; Van der Have, 2002; Van der Have and de Jong, 1996; Ratkowsky et al., 2005) (Appendix A). This characterization reveals two distinct types of life history trait responses to temperature. Rate-controlled responses, which are driven primarily by temperature effects on biochemical rate processes (e.g., reaction kinetics, en-

zyme inactivation), exhibit monotonic or left-skewed responses to temperature (Sharpe and DeMichele, 1977; Schoolfield et al., 1981; Van der Have and de Jong, 1996; Van der Have, 2002; Kingsolver, 2009; Kingsolver et al., 2011). For instance, above the low temperature threshold for viability, the mortality rate increases with increasing temperature while the maturation rate increases to a maximum followed by a rapid decline (Appendix A). Regulatory responses, which are driven by biochemical regulatory processes that prevent reactions from proceeding to their maxima (e.g., neural and hormonal regulation; Hochachka and Somero 2002; Long and Fee 2008; Nijhout 1994), exhibit more symmetrically unimodal responses to temperature (e.g., the birth rate; Appendix A). Several large-scale data analyses show that the qualitative nature of life history trait responses (e.g., monotonic, left-skewed, Gaussian) is conserved across ectotherm taxa Gillooly et al. (2001, 2002); Savage et al. (2004); Dell et al. (2011); Englund et al. (2011). This allows us to develop a mechanistic framework for predicting warming effects on ectotherm disease vectors that can apply broadly across taxa, habitats and latitudes.

The vector's fundamental thermal niche

The vector's fundamental thermal niche is the range of temperatures within which it can maintain a positive intrinsic growth rate. When population growth is density-independent, the long-run growth rate of the population constitutes its intrinsic growth rate (Amarasekare and Coutinho, 2013). When the thermal environment is invariant, i.e., the vector population experiences the same temperature, on average, with few or no fluctuations around the mean, we can derive the temperature dependence of the intrinsic growth rate in terms of the temperature responses of its constituent life history traits:

$$r(T) = -d_A(T) + \frac{W\left(b(T)\tau_J(T)e^{(d_A(T)-d_J(T))\tau_J(T)}\right)}{\tau_J(T)} \quad (1)$$

where W is the principal (positive) branch of the Lambert W function or the product logarithm (Corless et al., 1996), $\tau_J(T)$ is the temperature-dependent developmental delay, $b(T)$ and $d_X(T)$ $(X = J, A)$ are the temperature responses of birth and and mortality rates, and $m_J(T) = \frac{1}{\tau_J(T)}$ is the maturation rate (see Appendix A for details).

Note that $r(T)$ is the sum of two components, with a negative contribution through adult mortality ($d_A(T)$) and a positive contribution through the multiplicative effects of birth, juvenile mortality, adult mortality, and the developmental delay. Importantly, the lower and upper temperature limits at which the negative contribution equals the positive contribution constitute the thermal limits above and below which the vector population goes extinct ($T_{min_{r=0}}$ and $T_{max_{r=0}}$), and the temperature at which the positive contribution exceeds the negative contribution by the greatest amount constitutes the temperature at which $r(T)$ is maximized ($T_{\mathrm{r_{max}}}$). Knowing the $T_{\mathrm{r_{max}}}$ for a given vector species is important because it is the temperature at which the vector can recover from low density at the fastest rate.

The key point is that we can characterize the FTN of any ectotherm disease vector based solely on the temperature responses of its life history rates. By comparing the upper thermal limit to viability and the temperature at which $r(T)$ is maximized with the mean and maximum temperatures under a given warming scenario, we can predict whether a given vector population is likely to go extinct under that warming scenario.

Vector population dynamics in constant thermal environments

Vector populations are regulated by negative density-dependent feedbacks driven by intra-specific competition at the juvenile or adult stage. In mosquito vectors for example, competition between adult females for blood meals from hosts can cause vector birth rate to decline with increasing adult density; competition between larvae for food can cause the juvenile mortality rate to increase with increasing juvenile density. Importantly, because vector life cycles are characterized by a developmental delay,

there can be a delay in the operation of these negative feedback mechanisms, leading to population cycles even in the absence of any abiotic environmental variation (Gurney et al., 1983; Nisbet and Gurney, 1983; Nisbet, 1997; Murdoch et al., 2003).

The mechanisms underlying population cycles are as follows. When density-dependence operates through the birth rate, its effects on the adult population is delayed by a generation because of the time delay due to juvenile development. When lifetime fecundity (birth rate * adult longevity) is high and the developmental delay is long relative to adult longevity, this leads to delayed feedback cycles with a period $2-4$ times the developmental delay (Murdoch et al., 2003). When density-dependence operates through juvenile mortality, its effects are felt immediately on the juvenile population. When lifetime fecundity is high, this can lead to direct feedback cycles with a period $1-1.5$ times the developmental delay (Murdoch et al., 2003).

We can make two predictions based on these findings. First, we expect vector species with high lifetime fecundity and long juvenile developmental periods relative to adult longevity to exhibit population cycles even in the absence of temperature variation (Appendix B). Second, vector populations in which females are more limited by hosts than larvae are by their food resources are more likely to exhibit delayed feedback cycles while populations in which larvae are more food-limited than adults are host-limited are more likely to exhibit generation cycles.

Vector population dynamics in variable thermal environments

When temperature varies over time, the developmental delay varies with both temperature and time. In this case, modelling vector population dynamics requires using DDE models with variable time delays (Appendix C). The key question is how temperature variation affects the negative feedback processes that underlie population regulation, especially when delays in the operation of these feedbacks lead to intrinsic cycles.

We expect vector populations experiencing direct or delayed negative feedback to exhibit bounded growth under typical seasonal variation (i.e., populations do not drift to zero or reach outbreak densities). We also expect vector populations exhibiting intrinsic cycles in the absence of temperature variation to retain the signature of those cycles under typical seasonal variation. For instance, populations may still cycle with the same period and amplitude but attain higher maximum and minimum abundances during favorable periods and *vice versa* during unfavorable periods. We expect vector populations that attain stable point equilibria in the absence of temperature variation to follow the seasonal pattern of temperature variation with a single peak in abundance during the most favorable time of the year.

We expect climate warming to weaken the negative feedback processes that underlie population regulation, altering phenological patterns and disrupting bounded population growth. In populations exhibiting intrinsic cycles in the absence of temperature variation, higher mortality and longer developmental delays should cause abundances to fall below the cycle minima during the hottest parts of the year and to increase above the cycle maxima during the cooler parts of the year, with prolonged periods below cycle minima as warming proceeds. In populations exhibiting stable point equilibria in the absence of temperature variation, we expect longer periods of low abundances during the hottest periods the year and smaller peaks in abundance during the cooler periods as warming increases.

Our framework is general and its predictions apply to any ectotherm disease vector. We use the Malaria vector as a case study to illustrate how it can be used to predict the vector's FTN, its propensity for intrinsic cycling, and population dynamics under seasonal variation and warming based solely on information on the vectors life history trait responses to temperature and characteristics of its thermal environment.

Methods

Biology and previous studies of the Malaria vector (*Anopheles* species)

The malaria vector has a stage-structured life cycle with juvenile (eggs, larvae, pupae) and adult stages. Intra-specific competition can occur at the adult stage when females compete for blood meals from hosts and/or at the larval stage when larvae compete for their food resources (Beck-Johnson et al., 2013, 2017). Yamana et al. (2016) investigated the effects of climate warming on malaria prevalence in four geographic subregions in west Africa. They used extensive field observations to develop a mechanistic model of malaria transmission that included temperature, hydrology, and an agent-based model of vector population dynamics. Based on their findings, Yamana et al. (2016) predicted hotter and drier conditions in subregion (i), with an attendant decrease in malaria outbreaks. In subregion (ii) where vector reproduction and survival were already limited due to hot and dry conditions, they predicted malaria transmission to be unsustainable under future climate conditions. In subregion (iv) where the climate was highly suitable for disease transmission, Yamana et al. (2016) predicted future temperature increases to have minimal effect. They considered subregion (iii) the most critical because of strong inter-annual variability in transmission and because the increase in mosquito breeding due to projected increases in rainfall was similar in magnitude to the increase in mortality due to increases in temperature, thus making future outcomes uncertain. Based on these findings, Yamana et al. (2016) predicted that climate warming was unlikely to increase malaria burden in west Africa.

Temperature responses of life history traits

We used non-linear regression (nls package in R; R Core Team, 2016) to fit mechanistic response functions (Appendix A) to published data on temperature responses of life history traits for the Malaria vector (*Anopheles* species; Mordecai et al., 2013; Ciota et al., 2014; Shapiro et al., 2017). We used the nls.multstart package (Padfield et al., 2020) to allow for multiple initial conditions for each parameter.

This analysis assumes Gaussian error around predictions of trait means and a reference trait value measured at a temperature typically determined by the investigator.

We used trait response parameters to calculate the malaria vector's developmental delay, adult longevity, lifetime fecundity and the fraction of juveniles surviving to adulthood at the mean habitat temperature for eight locations across the four subregions in west Africa previously studied by Yamana et al. (2016) (Table 1).

Temperature response of the vector's fundamental thermal niche (FTN)

We incorporated life history trait response parameters into Equation (1) to characterize the FTN of the malaria vector. We calculated the lower and upper thermal limits to population viability and the temperature at which the intrinsic growth rate is maximized.

Vector population dynamics in constant thermal environments

We used the DDE model with fixed developmental delays (Appendix B) to investigate vector population dynamics in the absence of temperature variation. We parameterized the model with trait response data at the mean habitat temperature for each location to determine whether vector populations exhibited direct or delayed feedback cycles (see Appendix B for details). We calculated the amplitude and cycle period for each population that exhibited intrinsic cycles.

Vector population dynamics in variable thermal environments

We used the stage-structured DDE model with time-varying developmental delays (Appendix C) to investigate vector phenology and population dynamics under typical seasonal variation and warming. We parameterized the model with trait response parameters and simulated population dynamics at each locality over 75 years.

Characterizing temperature variation

We obtained monthly temperature data for the eight locations in west Africa from the NOAA climate prediction center (https://www.cpc.ncep.noaa.gov) and records from local weather stations closest to each location (Yamana et al., 2016). We depicted seasonal temperature variation using the sinusoidal function $T(t) = M_T - A_T \cos\frac{2\pi t - S}{yr}$ where t is the time in days, M_T is the mean habitat temperature in K, A_T is the amplitude of seasonal fluctuations, S is the phase shift when the warmest day occurs later in the year, and $yr = 365$ days. Taking the Julian date of the mid-point of each month as the independent variable (time), we estimated M_T, A_T and S for each of the eight locations using non-linear least squares regression (R Core Team, 2016) and allowing for multiple initial conditions with the nls.multstart package (Padfield et al., 2020).

We depict climate warming by modifying the seasonal temperature regime as follows: $T(t) = (M_T + m\,t) - (A_T + a\,t)\cos\frac{2\pi t - S}{yr}$ where $m = (\text{mhigh} + \text{mlow})/2$ and $a = (\text{mhigh} - \text{mlow})/2$ represent respectively, the daily rate of increase in mean and amplitude. The quantities $\text{mlow} = s_1/(n * yr)$ and $\text{mhigh} = s_2/(n * yr)$ where s_1 and s_2 are, respectively, the number of degrees by which minimum and maximum temperatures increase in n years.

We consider warming to manifest as an increase in the mean annual temperature and/or an increase in minimum and maximum temperatures. We consider three scenarios:

1. Baseline: minimum and maximum temperatures increase at the same rate ($s_1 = s_2$), resulting in an increase in the mean temperature while the amplitude stays the same.

2. Higher minimum temperature: the minimum temperature increases faster than the maximum temperature ($s_1 > s_2$), resulting in an increase in the mean temperature and a decrease in the amplitude. We term this the warmer winters scenario.

3. Higher maximum temperature: the maximum temperature increases faster than the maximum

temperature ($s_1 < s_2$), resulting in an increase in both the mean temperature and amplitude. We term this the hot extremes scenario.

According to the latest IPCC predictions (IPCC, 2023), the best estimate for warming is a 1.4° C increase in the mean habitat temperature (M_T) by year 2100 (75 years), the intermediate is 2.7° C, and the worst estimate is 4.4° C. We implement the three warming scenarios such that M_T increases by $1.4 - 4.4°$ over period of 75 years. For example, in the hot extremes (warmer winters) scenario, the mean increases by 2.7° when the maximum temperature increases by 3.6° (1.8°) and the minimum temperature by 1.8° (3.6°). We get the baseline scenario when both minimum and maximum temperatures increase by 2.7° over 75 years.

We use the DDE model with variable time delays (Appendix C) to generate predictions on the effects of these warming scenarios on the malaria vector the four subregions in west Africa. We compare our predictions with those made by (Yamana et al., 2016) in their study.

Results

Temperature responses of vector life history traits

The mechanistic temperature response functions (Appendix A) provide an excellent fit to data on the malaria vector's birth, maturation and mortality rates (Fig.1a-d). The mean habitat temperatures of the eight locations are at or near the optimal temperature for the birth rate (28.2° C; Fig. 1a) and below the temperature at which the maturation rate is maximal (30° C; Fig. 1b). The high mean temperatures mean that the vector experiences high juvenile and adult mortality, with juvenile mortality increasing faster with increasing temperature compared to adult mortality (Fig.1c-d, Table A1). These data suggest that even a small increase in mean temperature could lead to declines in birth and maturation and increases in juvenile and adult mortality (Fig.1a-d), with detrimental consequences for population viability.

The vector's fundamental thermal niche

By parameterizing Equation (1) with life history trait response data, we find that the temperature at which $r(T)$ is maximized ($T_{r_{max}}$) is 28.2° C, the same temperature as the birth rate optimum (T_{opt_b}), and the upper thermal limit for viability ($T_{max_{r=0}}$) is 33.9° C, barely 1° above the temperature above which the maturation rate starts to decline with increasing temperature ($T_{H_{m_J}} = 33.0°$ C; Table A1). These findings suggest that T_{opt_b} and $T_{H_{m_J}}$ can provide good approximations of $T_{r_{max}}$ and $T_{max_{r=0}}$. Importantly, this means that we can use life history trait response data to predict the temperature at which the vector population can increase from low densities at the fastest rate ($T_{r_{max}}$) and the temperature at which warming will cause deterministic extinction of the vector population ($T_{max_{r=0}}$).

By comparing the vector's $T_{r_{max}}$ and $T_{max_{r=0}}$ with the mean habitat temperature (M_T) and amplitude of seasonal fluctuations (A_T), we can predict the effects of warming on the population viability of the malaria vector. Save for the two locations in subregion (iv), vector populations in all other locations have $M_T > T_{r_{max}}$ indicating slower recovery from low abundances. Populations in subregion (ii) exhibit the largest seasonal fluctuations with maximum temperatures exceeding $T_{max_{r=0}}$ even in the absence of warming (Fig. 1e-l; Table 1). Populations within subregions (i) and (iii) also differ in seasonal fluctuations, with those exhibiting higher fluctuations exhibiting maximal temperatures closer to $T_{max_{r=0}}$ (Fig. 1e-l).

Based on this comparison, we expect even a moderate increase in M_T (e.g., M_T increasing by 2.7° over 75 years; see above) to cause vector extinction in subregion (ii) even without an increase in A_T due to hot extremes. We expect a moderate increase in M_T coupled with hot extremes to cause extinction in regions (i) and (iii). We do not expect warming-induced extinction in subregion (iv) where $M_T \ll T_{r_{max}}$ and seasonal fluctuations are sufficiently small that maximum temperatures are unlikely to exceed $T_{max_{r=0}}$ even when a moderate increase in M_T is coupled with hot extremes (Fig. 1m-t).

Vector population dynamics in constant thermal environments

As noted above, the vector's developmental delay can cause delays in the operation of density-dependent feedbacks, leading to intrinsic population cycles even in the absence of temperature variation. Importantly, we can predict a given vector population's propensity to exhibit such cycles based solely on the temperature responses of its life history traits and the mean habitat temperature.

We see that lifetime fecundity of the malaria vector is high even in the warmest locations, and that the developmental delay exceeds adult longevity in the warmer locations and slightly exceeds unity in the coolest locations (subregion (iv); Fig. 1m). The reason why the delay and longevity are more similar in the coolest locations is because the mean habitat temperature is well below the temperature at which the delay is minimized (and the maturation rate is maximized; Fig. 1n) and hence the delay and longevity are both decreasing with increasing temperature. Since the rate at which this decrease occurs decelerates as the delay approaches its minimum while longevity continues to decline exponentially, the delay starts to exceed longevity in the warmer locations (Fig. 1n). Based on these findings, we expect vector populations in all eight locations to exhibit intrinsic cycles.

Verifying the accuracy of this prediction with the fixed-delay the DDE model parameterized with the vector's trait response data (Appendix B) shows that when density-dependence operates on the adult stage (e.g., females competing for blood meals from hosts causing the birth rate to decrease with increasing adult density), populations from all eight locations exhibit delayed feedback cycles with periods approximately four times the developmental delay at the mean habitat temperature (Table 1, Figure 2). When density-dependence operates on the juvenile stage (e.g., when larvae compete for food), all eight populations reach stable point equilibria (Figure 2).

Knowing a vector population's propensity for intrinsic cycles in the absence of temperature variation is important for predicting its populations dynamics under seasonal variation and warming. Since temperature variation can only affect the strength of density-dependence but not the life stage it op-

erates at (e.g., juvenile vs. adult) or its nature (e.g., delayed vs. direct negative feedback), we expect signatures of direct and delayed density-dependent feedbacks to be evident in vector abundance patterns under typical seasonal variation. We also expect such signatures to be retained under warming until and unless warming is strong enough to weaken density-dependence to a level at which bounded growth no longer occurs.

It is difficult in practice to determine which life stage density-dependence operates on or how strong the negative feedback is. We can, however, make inferences based on available information. For instance, we can use data on human population density in different locations to determine whether competition for blood meals is likely to be the main source of population regulation. We expect weaker competition for blood meals in locations of high human density and *vice versa*. For example, human population density is high in locations within subregion (iv), low in subregions (i) and (ii), and variable in subregion (iii) with low to moderate densities (Yamana et al., 2016). Since adult females are unlikely to be limited by blood meals in high density locations, we expect larval competition to be the main source of population regulation in such locations. If this is the case, we expect vector populations in locations of low human density to exhibit delayed feedback cycles and populations in locations of high human density to attain stable point equilibria in the absence of temperature variation. We therefore expect distinct differences in phenology and population dynamics between these locations.

Vector population dynamics under seasonal variation

We used the DDE model with variable developmental delays (Appendix C) to investigate vector population dynamics under typical seasonal variation in the eight locations. As predicted, we find signatures of delayed and direct density-dependent feedback in the time series of vector abundances (Fig. 2, Fig. C1).

Density-dependence operates on vector birth rate

When density-dependence operates on the vector's birth rate, we see seasonal variation superimposed on delayed feedback cycles such that delay cycles retain the same period but have lower minima and maxima during the warmest part of the year and higher minima and maxima during the cooler parts of the year. Signatures of delay cycles are strongest in the two locations experiencing the lowest mean temperature (subregion (iv), Fig.2(g), Fig. C1(g) and (h)) and weakest in the two locations experiencing the highest amplitude of seasonal fluctuations (subregion (ii), Fig.2c), Fig. C1c and d). In subregion (iv), delay cycles persist throughout the year. While the minimum abundance drops slightly below the cycle minimum during the warmest part of the year, the maximum abundance never exceeds the cycle maximum (Fig.2(g), Fig. C1(g) and (h)). In subregion (ii), delay cycles are suppressed during the warmest period of the year, leading to extended periods of abundances falling well below the cycle minima followed by a single short peak of high abundance (Fig. 2c, Fig. C1(c) and (d)). In subregion (i), the population experiencing larger seasonal fluctuations exhibits a longer period of abundances below the cycle minimum (compare Fig. 2a, Fig. C1(a) and (b)), while in subregion (iii), the population experiencing lower fluctuations but the highest mean temperature of all locations (Koure, Niger) exhibits a longer period of abundances below the cycle minimum (compare Fig. C1(e) and (f)).

Higher temperatures suppress delay cycles via the following mechanism. Juvenile mortality increases and the maturation rate decreases with increasing temperature (Fig. 1b and c), leading to a smaller fraction of juveniles surviving to adulthood. At the same time, higher adult mortality means a smaller adult population and weaker competition for blood meals, weakening negative feedback and suppressing delay cycles. Since the birth rate is also lower at higher temperatures, the adult population remains low during the warmer period, recovering only after temperatures drop to levels at which birth and maturation can exceed mortality.

Density-dependence operates on vector's juvenile mortality rate

As predicted, when density-dependence operates on juvenile mortality and vector populations reach stable point equilibria in the absence of temperature variation, we see only seasonal cycles with abundances reaching a maximum during the cooler part of the year and a minimum during the warmer part of the year (Fig. 2b, d, f and h, Fig. C2) However, these seasonal cycles retain signatures of direct density-dependent feedback. In locations where $M_T < T_{r_{max}}$ (subregion (iv)), minimum seasonal abundance does not fall below the equilibrium abundance; this is also the case in locations within subregions (i) and (iii) where $M_T > T_{r_{max}}$ but A_T is low. In locations where $M_T < T_{r_{max}}$ but A_T is high (subregion (ii)), abundances fall below the equilibrium abundance during the warmest months of the year (Fig. 2f, Fig. C2).

As in the case when density-dependence operates on the birth rate, populations in subregion (ii) exhibit long periods of low abundances followed by a short period of high abundances. Similarly, the population experiencing larger seasonal fluctuations in region (i) (Dire, Mali) and the population with the highest mean temperature in subregion (iii) (Koure, Niger) show longer periods of low abundances compared to their counterparts within the same subregion.

Of note, when density-dependence operates on juvenile mortality, adult vector abundances are lower than when density-dependence operates on the birth rate. This is because vector populations experience high juvenile mortality even at their current mean habitat temperatures (Fig. 1c), further increases in mortality due to competition reduces the fraction of juveniles surviving to adulthood. Vector populations in subregion (iv), which experience the lowest mean temperatures, exhibit the highest adult abundance.

Combining this information with existing data on human population density (Yamana et al., 2016), we can predict the type of phenological pattern we expect to see in the different locations. In subregions (i) and (ii) where human population density is low and delayed feedback cycles are likely, we expect a

pattern driven by seasonal forcing of the delay cycles (Fig. 2a,d). In subregion (iv) where population human density is high and feedback cycles are unlikely, we expect a pattern dominated by seasonal variation (Fig. 2g,Fig. C2g and h). In subregion (iii) where human population density is variable, the location with the lower density (Tanout, Niger) is likely to exhibit feedback cycles (Fig. 2e, Figs. C2e and f) and hence a phenological pattern similar to subregion (i), while the location with higher density (Koure, Niger) is likely to exhibit a pattern similar to subregion (iv) (Fig. C2f and g).

Detecting signatures of population dynamics in census data

A key question is whether we can detect the signatures predicted by the LDE model in vector census data. Using the daily time series from the model to calculate monthly vector abundances, we find that when density-dependence operates on the birth rate, monthly census data can accurately capture the distinctive abundance pattern arising from the interplay between delay cycles and seasonal temperature variation. However, monthly data, while accurately capturing population minima, tend to underestimate the maxima (Fig. 5). We find that biweekly census data can more accurately capture population maxima. When density-dependence operates on juvenile mortality, monthly data are sufficient to capture the peaks and troughs driven by seasonal variation (Fig. 5).

Vector population dynamics under climate warming

We find that low levels of warming (e.g., M_T increasing by 1.4° C over 75 years) do not cause vector extinctions in any of the eight locations (Fig. 3, Figs. C3 and C4). This is true regardless of whether density-dependence operates on the vector's birth rate or the juvenile mortality rate. Warming does amplify the seasonal pattern of lower abundances during the hottest months and higher abundances during the cooler months. An increase in M_T accompanied by an increase in A_T due to hot extremes is the most detrimental warming scenario, causing long periods of extremely low abundances followed short-period outbreaks in subregion (ii). Populations in the coolest locations (subregion (iv)) are largely

immune to these warming effects.

As predicted based on the vector's FTN, moderate levels of warming (2.7° C) cause five out of eight populations to go extinct due to hot extremes by 2100 (Fig. 4, Figs. C5 and C6). Two out of eight populations go extinct under all three warming scenarios. These include one population in subregion (ii) with high M_T and A_T, and one in subregion (iii) with the highest M_T of all locations. Also as predicted based on the vector's FTN, vector populations in subregion (iv) persist under all warming scenarios but with abundances falling below cycle minima during the warmest months of the year. Hot extremes cause longer periods of low abundances compared to other warming scenarios. These outcomes ensue regardless of which life stage density-dependence operates on. The one exception to our predictions is the remaining population in subregion (iii) (Tanout, Niger), which persists under all warming scenarios albeit with an extended period of low abundances followed by short-period outbreaks under baseline and hot extremes scenarios (Fig. 4, Figs. C5 and C6). This is likely due to the fact that this population exhibits the highest $r_{T_{\max}}$ of all locations, which gives it the ability to recover from low densities at the fastest rate.

High levels of warming (4.4° C over 75 years) cause the extinction of all but the two populations in subregion (iv). These two populations, though extant, experience warming-induced disruption of bounded growth. Vector abundances fall below cycle minima for extended periods of time and increase above cycle maxima to outbreak levels under baseline and hot extremes scenarios (Fig. C7 and C8). Across all levels of warming, the warmer winters scenario is the least detrimental to vector population viability.

In comparing our findings with the predictions made by Yamana et al. (2016), the vector's FTN provides reasonably accurate predictions of its ability to sustain malaria transmission. For instance, we find that vector populations in subregion (i) are likely to go extinct due to hot extremes even under moderate levels of warming, consistent with Yamana et al. (2016)'s predicttion of significantly reduced

malaria transmission in this subregion. The FTN shows that vector populations in subregion (ii) already experience temperatures near the upper limit of population viability, supporting the Yamana et al. (2016)'s previous prediction that malaria transmission is unlikely to sustainable in this region. Interestingly, we also find subregion (iii) to exhibit the most variable outcomes, with one population remaining viable even when moderate levels of warming are accompanied by hot extremes while the other goes extinct. In the case of subregion (iv) which was predicted to exhibit no change, we find that hot extremes can disrupt bounded population growth leading to prolonged periods of low abundances during which the vector population could go extinct due to demographic stochasticity. This comparison shows that our trait-based approach can provide reasonably accurate predictions of warming effects on field populations of disease vectors.

Summary of results

We find that the vector's life history trait responses and the characteristics of the vector's thermal environment are sufficient to predict warming effects on vector population dynamics and persistence.

1. Data on the vector's life history trait responses to temperature are sufficient to predict vector extinction under warming. Using trait response data for the malaria vector, we find that the temperatures at which birth and maturation rates are maximized (T_{opt_b} and $T_{H_{m_J}}$) provide good approximations of the temperature at which the vector can recover from low densities at the fastest rate ($T_{r_{max}}$) and the upper thermal limit for viability ($T_{max_{r=0}}$).

   By comparing these metrics with the mean habitat temperature (M_T) and the amplitude of seasonal fluctuations (A_T), we can predict which vector populations are likely to go extinct under different levels (M_T increasing by $1.4^\circ, 2.7^\circ$ or 4.4° over 75 years) and scenarios (baseline, warmer winters, hot extremes) of warming. These predictions are borne out by the analyses of a DDE model that incorporates trait response data and the life stage at which density-dependence

operates.

2. Life history trait response data can predict whether vector populations exhibit intrinsic cycles in the absence of temperature variation. High lifetime fecundity and a long developmental delay relative to adult longevity can lead to delayed feedback cycles when density-dependence operates at the adult stage and direct feedback cycles when density-dependence operates at the juvenile stage.

   The malaria vector exhibits high lifetime fecundity and a long developmental delay in all eight locations, indicating the propensity for intrinsic cycles. A DDE model parameterized with trait response data shows that all eight populations exhibit delayed feedback cycles when females compete for host blood meals, and stable point equilibria when larvae compete for food resources. Using data on human population density in different locations, we can predict which vector populations are likely exhibit delayed feedback cycles and which are likely to attain stable equilibria in the absence of temperature variation.

3. The combination of life history trait response data and characteristics of the thermal regime are sufficient to predict vector population dynamics under seasonal variation and warming.

   We find that locations in which vector populations are likely to undergo delayed feedback cycles exhibit a qualitatively different phenological pattern under seasonal variation compared to locations in which vector populations attain stable point equilibria.

   We find that vector populations experiencing warming tend to exhibit qualitatively similar abundance patterns as under typical seasonal variation when density-dependence operates at the juvenile stage and qualitatively different patterns when density-dependence operates at the adult stage.

4. We find that monthly census data of vector abundances are sufficient to detect which life stage density-dependence is likely to be strongest at and whether a given population is likely to exhibit intrinsic population cycles.

Discussion

Vector-borne diseases comprise a significant portion of the global disease burden (Caminade et al., 2016; World Health Organization, 2019). Predicting whether climate warming will increase or decrease this burden is a crucial priority for public health and wildlife management. Predictions that can reliably inform policy need to be based on vector biology, but models that incorporate biological realism are often difficult to test with the limited amount of information available for most disease vectors. For instance, most disease vectors are arthropods with complex life cycles characterized by developmental delays that drive both vector phenology and population dynamics. Population models that can incorporate developmental delays can generate predictions on phenology and dynamics. But, their biological realism comes at the cost of being parameter-rich, making it difficult to fit these models to census data.

Here we present a theoretical framework for predicting warming effects on disease vectors based solely on the temperature responses of the vector's life history traits and characteristics of the vector's thermal environment. Its novelty lies in elucidating mechanisms underlying warming effects on vector phenology and population dynamics from first principles rather than inferring mechanisms from data. It has the advantage of identifying qualitative signatures of warming effects on vector abundance patterns that can be detected in time series data, without having to fit complex models to such data. Perhaps most important, it shows us that the vector species' life history features contain insights that are crucial for predicting their ability to transmit diseases in the face of climate warming.

Our key findings are as follows. First, by characterizing the vector's fundamental thermal niche (FTN) based on its constituent life history traits (birth, maturation, mortality) we can predict the ther-

mal limits to vector population viability and the temperature at which the population can recover from low densities at the fastest rate. This allows us to predict the vector's propensity to go extinct under a given climate warming scenario, and whether or not it can recover from warming-induced decreases in abundance. Second, by comparing the vector's developmental delay with its lifetime fecundity and adult longevity, we can predict whether vector populations are prone to intrinsic population cycles. Third, by incorporating the vector's life history traits into a population model that explicitly incorporates the vector's developmental delay, we can predict the time to vector extinction under a given climate warming scenario and expected patterns of population dynamics when vector populations exhibit intrinsic cycles as opposed to stable point equilibria in the absence of temperature variation. We show that the interplay between intrinsic cycles and temperature variation can lead to distinctive signatures in vector abundance patterns that can be detected in time series data without having to fit the model to such data.

By testing the applicability of our framework with temperature response data for the malaria vector (*Anopheles* species), we find that the optimal temperature for the birth rate and the upper temperature limit above which the maturation rate starts to decrease with increasing temperature provide reasonably accurate predictions of the temperature at which the vector population can recover from low densities at the fastest rate and the upper thermal limit for vector viability. By incorporating the vector's life history trait responses to temperature into a stage-structured population model constructed with delay differential equations (DDEs), we find that the vector's FTN, which can be characterized using life history trait response data alone, can accurately predict the vector's propensity to go extinct under a given climate change scenario. We also find that the vector's developmental delay relative to its lifetime fecundity and adult longevity can accurately predict its propensity to exhibit delay-driven population cycles, and that for the malaria vector's trait response parameters, we expect to see delayed feedback cycles with a period of approximately four times the developmental delay when density-dependence operates on at

the adult stage (through competition for host blood meals by females), and stable point equilibria when density-dependence operates on the juvenile stage (through larval competition for food resources). The model predicts qualitatively distinct patterns of vector phenology and abundance depending on whether competition occurs at the adult or juvenile stages. Importantly, signatures of these qualitative differences can emerge in monthly census data, allowing us to infer what life stage density-dependence is most likely to operate at and whether vector populations exhibit intrinsic population cycles in the absence of temperature variation. The key point is that by elucidating mechanisms from first principles rather than inferring them from the data, we can make informed predictions about warming effects on disease vectors without having to fit complex models to time series data.

Given that this framework hinges on life history trait responses to temperature, the question arises as to the feasibility of quantifying these responses for disease vectors and the applicability of trait response data obtained in laboratory experiments to real world situations. As for feasibility, temperature responses of vector life history traits and disease transmission rates have been quantified for a number of Dipteran and Hemipteran vectors, and used to predict thermal limits to viability and Basic Reproductive Number (R_0; Mordecai et al. (2013); Ciota et al. (2014); Shapiro et al. (2017)). As for applicability, applying our framework to the malaria vector shows that life history trait response data can be reliably used to characterize real vector populations. For instance, we used laboratory-measured trait responses to predict the temperature at which the malaria vector's intrinsic growth rate is maximized ($T_{r(T)_{\max}}$), which is also the temperature at which the vector population can increase from low densities the fastest. When we compare $T_{r_{max}}$ with the mean habitat temperatures of vector populations across the four subregions previously studied by Yamana et al. (2016), we find that all populations have mean temperatures at or near $T_{r(T)_{\max}}$, exactly what we would expect for tropical ectotherms adapted to their typical thermal environment (Deutsch et al., 2008; Amarasekare and Savage, 2012). We also find that the maximum intrinsic growth rate ($r(T)_{\max}$) is higher for vector populations experiencing mean habi-

tat temperatures closer to $T_{r(T)_{\max}}$, also what we would expect for tropical ectotherms (Deutsch et al., 2008; Amarasekare and Savage, 2012; Amarasekare and Johnson, 2017). Moreover, we find that the upper thermal limit for viability predicted by trait response data coincides with the observed maximum habitat temperature for all vector populations, except those in subregion (ii) that experience higher-amplitude seasonal fluctuations than are typical for tropical habitats. Lastly, laboratory-measured trait response data can also correctly predict the propensity for intrinsic population cycles. Taken together, these findings suggest that trait response data measured in laboratory experiments can reliably be used to predict the viability, phenology and population dynamics of real vector populations. Indeed, there is a long tradition of using such data to predict the prevalence and transmission of vector-borne diseases (Mordecai et al., 2013, 2017; Johnson et al., 2015; Shocket et al., 2018, 2020; Tesla et al., 2018; Cator et al., 2020).

A related issue is whether knowledge of vector population dynamics in the absence of temperature variation, particularly whether populations exhibit intrinsic cycles, is useful for predicting warming effects on real vector populations. There are two reasons why this knowledge is important. The first is population regulation. Populations cannot persist in the absence of regulation via density-dependent feedbacks. These feedbacks enable populations to increase when rare and decrease when abundant, such that they exhibit bounded growth. Knowing what these bounds are is essential for predicting how well regulated a given population is in its typical thermal environment, and how severe warming would have to be to disrupt regulation altogether. For instance, life history trait data suggest that malaria vector populations in all four subregions have the propensity to exhibit delayed feedback cycles at their respective mean habitat temperatures. By comparing the maximum daily/monthly temperature each population is likely to experience with the upper thermal limit for viability, we can predict how many days/months of the year the population is likely to experience temperatures above this limit. We would expect abundances to fall below cycle minima during this period, and that is exactly what we find when

we simulate a DDE model parameterized with trait response data for each vector population. The key point is that knowing the bounds of population growth dictated by density-dependent feedbacks allows us to predict how severe warming would have to be for population regulation to fail.

It has been shown that as long as populations are regulated by density-dependent feedbacks, they will converge to a time-dependent asymptotic trajectory even in a nonstationary environment (AEDT; Chesson 2017, 2019). We do indeed see this when we simulate the DDE model parameterized with trait response data for various levels of climate warming. For low levels of warming, vector populations do indeed converge to qualitatively distinct trajectories depending on whether they attain stable point equilibria or delayed feedback cycles in the absence of temperature variation. We find that higher levels of warming progressively weaken density-dependent feedbacks, leading to long periods of low abundances followed by short-period outbreaks, a prediction we can test with information we can obtain with monthly censuses of vector abundances. Importantly, we can use the DDE model to predict the level of warming at which population regulation fails altogether, causing vector extinction. We find that the threshold warming level for extinction is lower when warming is driven by hot extremes compared to other scenarios.

The second reason why it is important to characterize vector population dynamics in the absence of temperature variation is because populations with a propensity for intrinsic cycles lead to qualitatively distinct phenological patterns compared to those that do not. Importantly, these differences can be detected in population census data, allowing us to infer which life stage density-dependence is most likely to operate on, information that cannot otherwise be obtained without detailed field studies. By comparing monthly census data with predicted trajectories of bounded growth from a DDE model, we can determine whether abundances fall below expected cycle minima and how long it takes the population to recover. By comparing the time spent below cycle minima in the observed time series with those predicted by a DDE model that incorporates climate warming scenarios, we can gauge how

susceptible a given vector population is to warming-induced extinction. The point is that we can learn a great deal about a vector population's susceptibility to extinction through information on its FTN and bounded population growth, without having to fit a complex population model to census data.

As noted in the Introduction, delay differential equations (DDEs) provide the most biologically realistic mathematical approach for modelling the dynamics of disease vectors and other arthropods whose life cycles are characterized by developmental delays. They are mathematically complex, particularly when developmental delays vary over time due to seasonal variation and warming. But they are necessary for making informed predictions about warming effects because models based on ordinary differential equations (ODEs) cannot capture the delay-induced phenological patterns that underlie patterns of disease transmission. There are well-developed numerical methods for simulating DDE models (e.g., the pydde package in Python) that are freely available. The great advantage of a DDE-based framework is that we can leverage the realism of DDE models to both generate and test predictions with the minimum amount of empirical information.

In conclusion, we have presented a theoretical framework for predicting the effects of climate warming on arthropod disease vectors that utilizes information on vector life history traits and characteristics of the vector's thermal environment to make predictions that can be tested with census data without having to fit models to data. The framework is general and can be applied to insect pests and pollinators in addition to arthropod disease vectors. In ongoing work we have successfully applied the framework to predict warming effects on west Nile vector populations across different latitudes and climate regimes (Amarasekare and Goncalves in Prep.), and we plan to apply it to insect pests from tropical, Mediterranean and temperate latitudes.

References

Amarasekare, P., and R. Coutinho. 2013. The intrinsic growth rate as a predictor of population viability under climate warming. Journal of Animal Ecology 82:1240–1253.

Amarasekare, P., and C. Johnson. 2017. Evolution of thermal reaction norms in seasonally varying environments. American Naturalist 189:E31–E45.

Amarasekare, P., and V. Savage. 2012. A mechanistic framework for elucidating the temperature dependence of fitness. American Naturalist 179:178–191.

Beck-Johnson, L., W. Nelson, K. Paaijmans, A. Read, M. Thomas, and O. Bjornstad. 2013. The effect of temperature on anopheles mosquito population dynamics and the potential for malaria transmission. PLoS One 8:e79276.

———. 2017. The importance of temperature fluctuations in understanding mosquito population dynamics and malaria risk. Open Science 4:160969.

Caminade, C., M. McIntyre, and A. Jones. 2016. Climate change and vector-borne diseases: Where are we next heading? The Journal of Infectious Diseases 214:1300–1301.

Cator, L. J., L. R. Johnson, E. A. Mordecai, F. El Moustaid, T. R. Smallwood, S. L. LaDeau, M. A. Johansson, P. J. Hudson, M. Boots, M. B. Thomas, A. G. Power, and S. Pawar. 2020. The role of vector trait variation in vector-borne disease dynamics. Frontiers in Ecology and Evolution 8.

Chesson, P. 2017. Aedt: A new concept for ecological dynamics in the ever-changing world. PLoS biology 15.

———. 2019. Contributions to nonstationary community theory. Journal of Biological Dynamics 13:123–150.

Ciota, A., A. Kilpatrick, and L. Kramer. 2014. Modelling the effect of temperature on the seasonal
616 population dynamics of temperate mosquitoes. Journal of Medical Entomology 51:55–62.

Corless, R., G. Gonnet, D. Hare, D. Jeffrey, and D. Knuth. 1996. On the lambert w function. Advances
618 in Computational Mathematics 5:329–359.

Dell, A., S. Pawar, and V. M. Savage. 2011. Systematic variation in the temperature dependence of
620 physiological and ecological traits. Proceedings of the National Academy of Sciences 108:10591–
10596.

622 Deutsch, C. J., J. Tewksbury, R. B. Huey, K. Sheldon, C. Ghalambor, D. Haak, and P. R. Martin.
2008. Impacts of climate warming on terrestrial ectotherms across latitude. Proc Natl Acad Sci USA
624 105:6668–6672.

Englund, G., G. Ohlund, C. Hein, and D. S. 2011. Temperature dependence of the functional response.
626 Ecology Letters 14:914–921.

Ewing, D., C. Cobbold, B. Purse, M. Nunn, and S. White. 2016. Modelling the effect of temperature on
628 the seasonal population dynamics of temperate mosquitoes. Journal of Theoretical Biology 400:65–
79.

630 Gillooly, J. F., J. H. Brown, G. B. West, V. M. Savage, and E. L. Charnov. 2001. Effects of size and
temperature on metabolic rate. Science 293:2248–2251.

632 Gillooly, J. F., E. L. Charnov, G. B. West, , V. M. Savage, and J. H. Brown. 2002. Effects of size and
temperature on developmental time. Science 293:2248–2251.

634 Gurney, W., R. Nisbet, and J. Lawton. 1983. The systematic formulation of tractable single-species
population models incorporating age structure. Journal of Animal Ecology 52:479–495.

636 Hochachka, P., and G. Somero. 2002. Biochemical Adaption. Oxford University Press.

IPCC. 2023. Climate Change 2023: Synthesis Report. Contribution of Working Groups I, II and III
638 to the Sixth Assessment Report of the Intergovernmental Panel on Climate Change [Core Writing Team, H. Lee and J. Romero (eds.)]. IPCC, Geneva, Switzerland.

640 Johnson, F., and I. Lewin. 1946. The growth rate of e. coli in relation to temperature, quinine and coenzyme. Journal of Cellular and Comparative Physiology 28:47–75.

642 Johnson, L., T. Ben-Horin, K. Lafferty, A. McNally, E. Mordecai, K. Paaijmans, S. Pawar, and S. Ryan. 2015. Understanding uncertainty in temperature effects on vector-853 borne disease: a bayesian
644 approach. Ecology 96:203–213.

Kingsolver, J. 2009. The well-temperatured biologist. American Naturalist 174:755–768.

646 Kingsolver, J., A. Woods, L. B. Buckley, L. Potter, H. MacLean, and J. Higgins. 2011. Complex life cycles and the responses of insects to climate change. Integrative and Comparative Biology 51:719–
648 732.

Long, M., and M. Fee. 2008. Using temperature to analyse temporal dynamics in the songbird motor
650 pathway. Nature 456:189–194.

Mordecai, E. A., J. M. Cohen, M. V. Evans, P. Gudapati, L. Johnson, C. A. Lippi, K. Miazgowicz,
652 C. C. Murdock, J. R. Rohr, S. J. Ryan, V. M. Savage, M. S. Shocket, A. S. Ibarra, M. B. Thomas, and D. P. Weikel. 2017. Detecting the impact of temperature on transmission of zika, dengue, and
654 chikungunya using mechanistic models. PLOS Neglected Tropical Diseases 11.

Mordecai, E. A., K. Paaijmans, L. Johnson, C. Balzer, T. Ben-Horin, E. Moor, M. A., S. Pawar, S. Ryan,

T. Smith, and K. Lafferty. 2013. Optimal temperature for malaria transmission is dramatically lower than previously predicted. Ecology Letters 16:22–30.

Murdoch, W. 1992. Ecological theory and biological control. Pages 197–221 *in* S. Jain and L. Botsford, eds. Applied Population Biology. Kluwer Academic Publishers.

Murdoch, W., C. J. Briggs, and N. R. M. 2003. Consumer resource dynamics. Princeton University Press, Princeton New Jersy.

Murdoch, W. W., S. Swarbrick, and C. J. Briggs. 2006. Biological control: lessons from a study of calofornia red scale. Population Ecology 48:297–305.

Nijhout, H. 1994. Insect hormones. Princeton University Press.

Nisbet, R. 1997. Sdelay-differential equations for structured populations. Pages 89–116 *in* S. Tuljapurkar and H. Caswell, eds. Structured-population models in marine, terrestrial, and freshwater systems. Chapman and Hall, New York.

Nisbet, R. M., and W. Gurney. 1983. The systematic formulation of population-models for insects with dynamically varying instar duration. Theoretical Population Biology 23:114–135.

Padfield, D., H. O'Sullivan, and S. Pawar. 2020. rtpc and nls.multstart: A new pipeline to fit thermal performance curves in r. Methods in Ecology and Evolution 12:1138–1143.

R Core Team. 2016. R: A language and environment for statistical computing. R Foundation for Statistical Computing, Vienna .

Ratkowsky, D., J. Olley, and T. Ross. 2005. Unifying temperature effects on the growth rate of bacteria and the stability of globular proteins. Journal of Theoretical Biology 233:351–362.

676 Roff, D. 1992. The evolution of life histories: theory and analysis. Chapman and Hall.

Savage, V. M., J. F. Gillooly, J. H. Brown, G. B. West, and E. L. Charnov. 2004. Effects of body size
678 and temperature on population growth. American Naturalist 163:429–441.

Schoolfield, R., J. Sharpe, and C. Magnuson. 1981. Non-linear regression of biological temperature-
680 dependent rate models based on absolute reaction-rate theory. Jounal of Theoretical Biology 88:719–
731.

682 Scranton, K., and P. Amarasekare. 2017. Predicting phenological shifts in a changing climate. Pro-
ceedings of the National Academy of Sciences 114:13212–13217.

684 Shapiro, L. L. M., S. A. Whitehead, and M. B. Thomas. 2017. Quantifying the effects of temperature
on mosquito and parasite traits that determine the transmission potential of human malaria. PLoS
686 biology 15:e2003489.

Sharpe, P., and D. DeMichele. 1977. Reaction kinetics of poikilotherm development. Journal of Theo-
688 retical Biology 64:649–670.

Shocket, M. S., S. J. Ryan, and E. A. Mordecai. 2018. Temperature explains broad patterns of ross
690 river virus transmission. Elife 7:e37762.

Shocket, M. S., A. B. Verwillow, M. G. Numazu, H. Slamani, J. M. Cohen, F. El Moustaid, J. Rohr, L. R.
692 Johnson, and E. A. Mordecai. 2020. Transmission of west nile and five other temperate mosquito-
borne viruses peaks at temperatures between 23 c and 26 c. Elife 9.

694 Stearns, S. 1992. The Evolution of Life Histories. Oxford University Press.

Tesla, B., L. R. Demakovsky, E. A. Mordecai, S. J. Ryan, M. H. Bonds, C. N. Ngonghala, M. A. Brind-

ley, and C. C. Murdock. 2018. Temperature drives zika virus transmission: evidence from empirical and mathematical models. Proceedings of the Royal Society B: Biological Sciences 285:20180795.

Van der Have, T. 2002. A proximate model for thermal tolerance in ectotherms. Oikos 98:141–155.

Van der Have, T. M., and G. de Jong. 1996. Adult size in ectotherms: temperature effects on growth and differentiation. Journal of Theoretical Biology 183:329–340.

World Health Organization. 2019. World Malaria Report 2019. World Health Organization.

Yamana, T., A. Bomblies, and E. Eltahir. 2016. Climate change unlikely to increase malaria burden in west africa. Nature Climate Change 6:1012–1016.

Table 1: Characteristics of vector populations in the four geographical subregions of west Africa[1].

Sub-region	Location	MT	AT	S	-(MT)	Transmission category	Human density	Cycle period	Cycle amplitude
(i)	Dire, Mali	302.35	3.79	-122.22	0.3339	Moderate	Low	35	594
(i)	Linguere, Senegal	302.59	2.43	-51.18	0.3291	Moderate	Low	35	620
(ii)	Kidal, Mali	301.88	6.85	45.41	0.3407	Low	Low	37	218
(ii)	Agadez, Niger	302.23	6.30	9.73	0.336	Low	Low	36	581
(iii)	Tanout, Niger	301.57	3.81	-101.63	0.3432	Moderate	Low	37	206
(iii)	Koure, Niger	303.00	2.71	-143.53	0.318	Moderate	Medium	35	666
(iv)	Kano, Nigeria	299.50	4.07	-201.11	0.3315	High	High	44	743
(iv)	Karan, Mali	300.16	2.18	-423.52	0.3395	High	Medium	42	407

[1] Subregions, locations, and data on transmission category and human population density are from Yamana *et al.,* (2016).

Figure legends

Figure 1. Life history trait responses, fundamental thermal niche (FTN) and propensity for intrinsic cycles in malaria vector populations across four geographic subregions in west Africa. Panels (a)-(d) depict, respectively, the temperature responses of the vector's birth, maturation, juvenile, mortality, and adult mortality rates. In panels (a) and (c), the vertical dashed line depicts the optimal temperature for

the birth rate and in panels (b) and (e), upper temperature threshold for the maturation rate. Panels (e)-(l) depict the FTN of eight populations in the four subregions. In these panels, the solid circle depicts the mean habitat temperature (M_T) of the focal population, the blue shaded region depicts the range of M_T across the eight populations, and the pink region, the expected range under a 2.7° increase in M_T due to hot extremes. Panel (m) depicts the vector's lifetime fecundity (black curve) and the ratio of adult longevity to the developmental delay (red curve) as a function of temperature (in K), and panel (n), adult longevity (black curve) and developmental delay as a function of temperature. In panel (m), the blue vertical line depicts the optimal temperature for reproduction, and in panel (n), the upper temperature limit above which the developmental delay starts to increase with increasing temperature. In both panels, the points on each curve correspond to the mean habitat temperature experienced by the eight vector populations. Parameter values are given in Tables 1 and A1.

Figure 2. Population dynamics of the malaria vector in constant and seasonal thermal environments when density-dependence operates on the vector's birth rate (left column) and juvenile mortality rate (right column). Dynamics are shown for four populations for each of the four subregions. Dynamics for all eight populations are given in Figs. C1 and C2. Parameter values are given in Tables 1 and A1.

Figure 3. Malaria vector population dynamics under low levels of warming (increase in mean temperature by 1.4° over 75 years) for the warmer winters (blue), baseline (orange) and hot extremes (red) scenarios when density-dependence operates on the vector's birth rate (left column) and juvenile mortality rate (right column). Dynamics for all eight populations across the four subregions are given in Figs. C3 and C4. Parameter values are given in Tables 1 and A1.

Figure 4. Malaria vector population dynamics under moderate levels of warming (increase in mean temperature by 2.7° over 75 years) for the warmer winters (blue), baseline (orange) and hot extremes (red) scenarios when density-dependence operates on the vector's birth rate (left column) and juvenile mortality rate (right column). Dynamics for all eight populations across the four subregions are given

in Figs. C5 and C6. Parameter values are given in Tables 1 and A1.

Figure 5. Average monthly and biweekly abundances of malaria vector populations calculated from the daily time series predicted by the DDE model when density-dependence operates on the birth rate (left column) or the juvenile mortality rate (right column). The solid blue points denote monthly abundances and the red points, biweekly abundances. The points are connected for ease of comparison with the daily time series (gray). Parameter values are given in Tables 1 and A1.

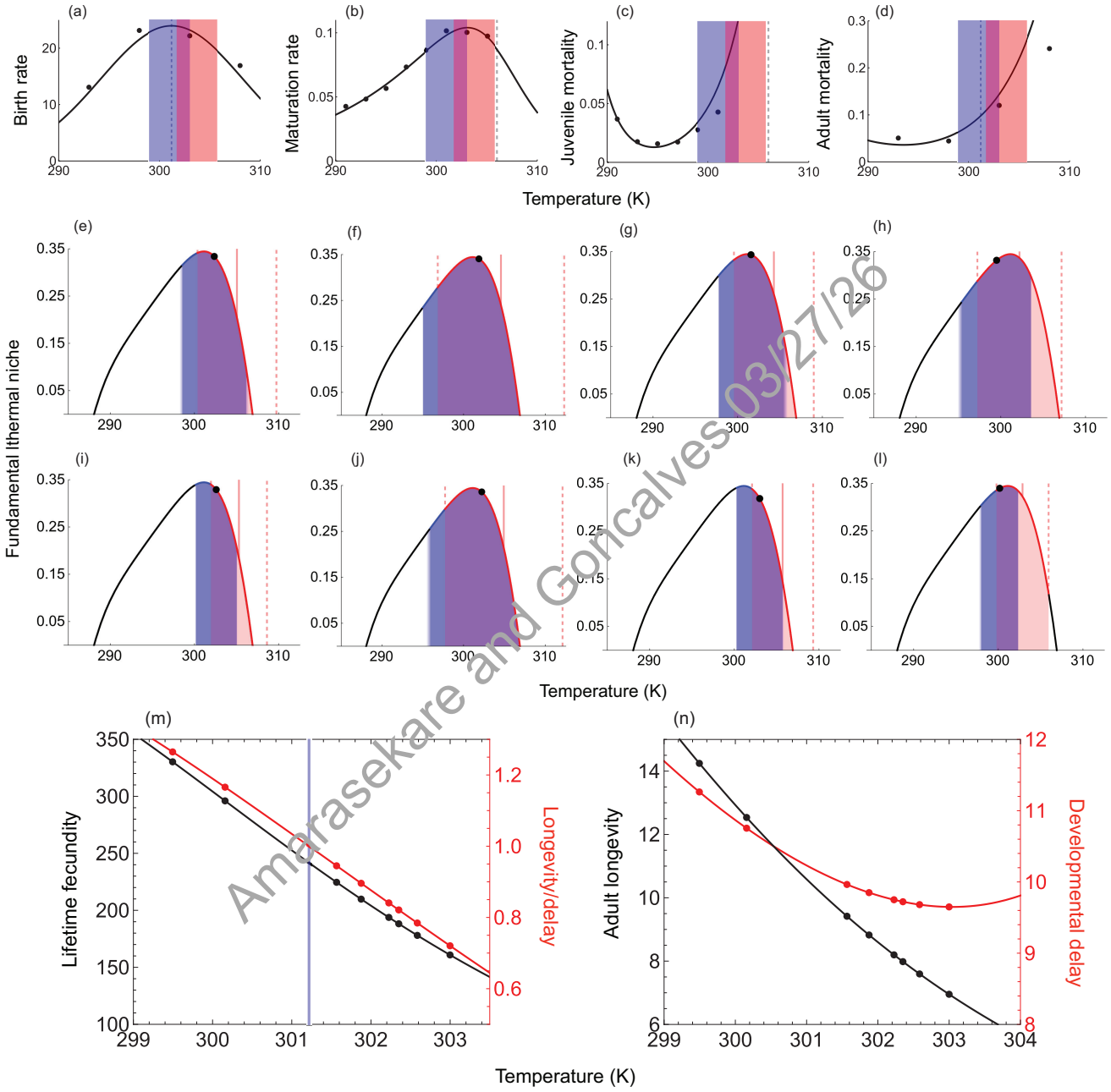

Figure 1

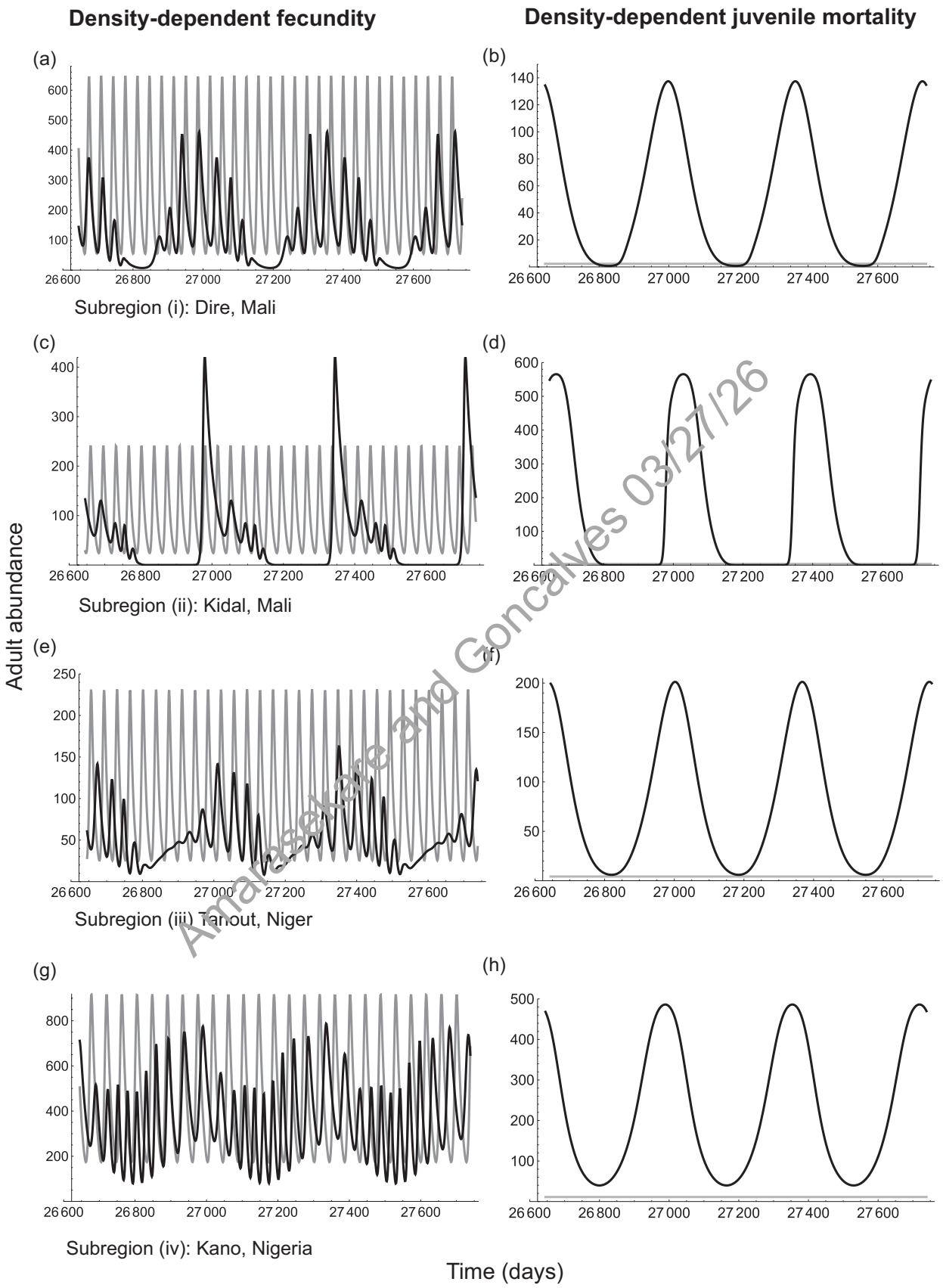

Figure 2

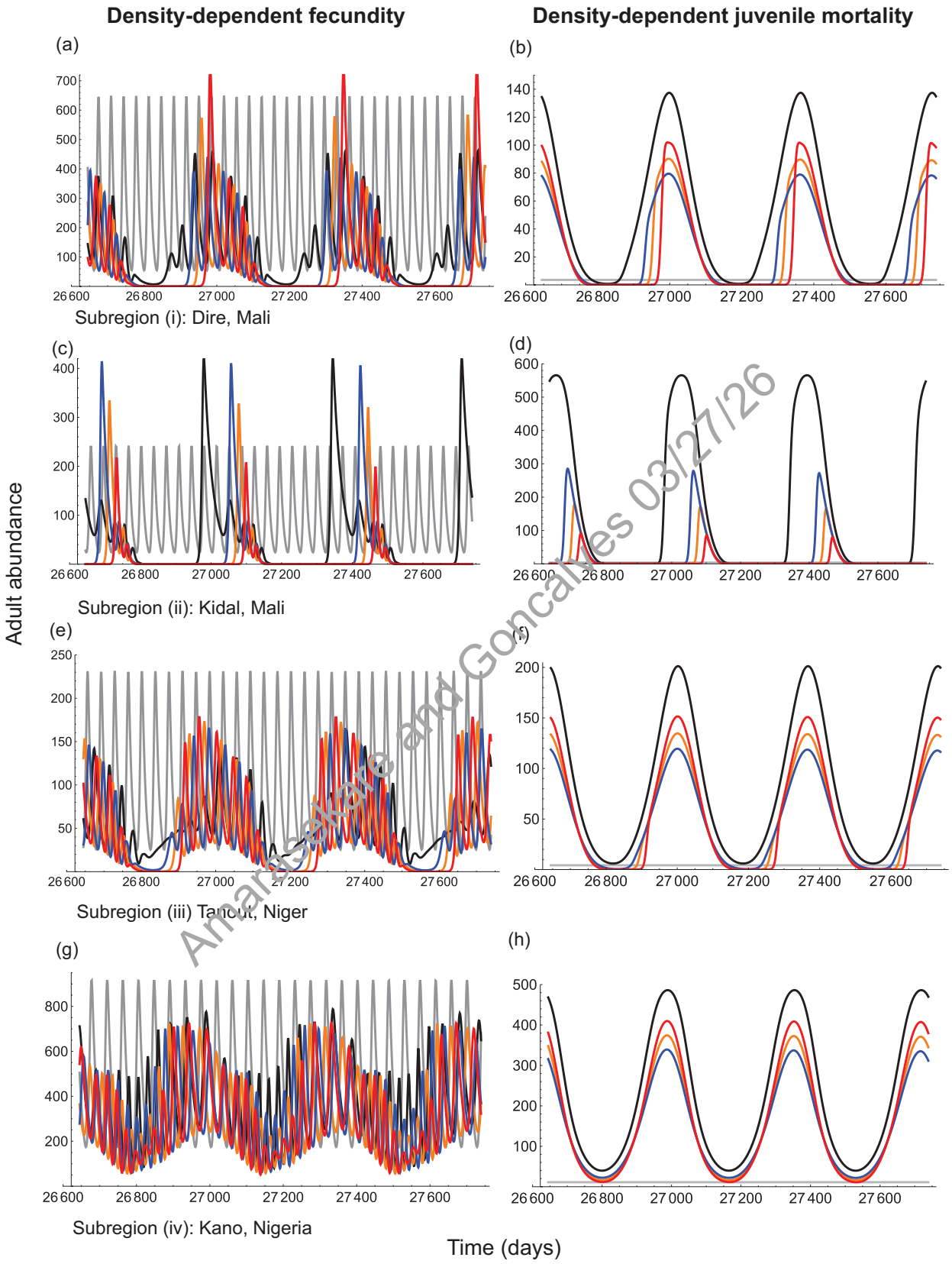

Figure 3

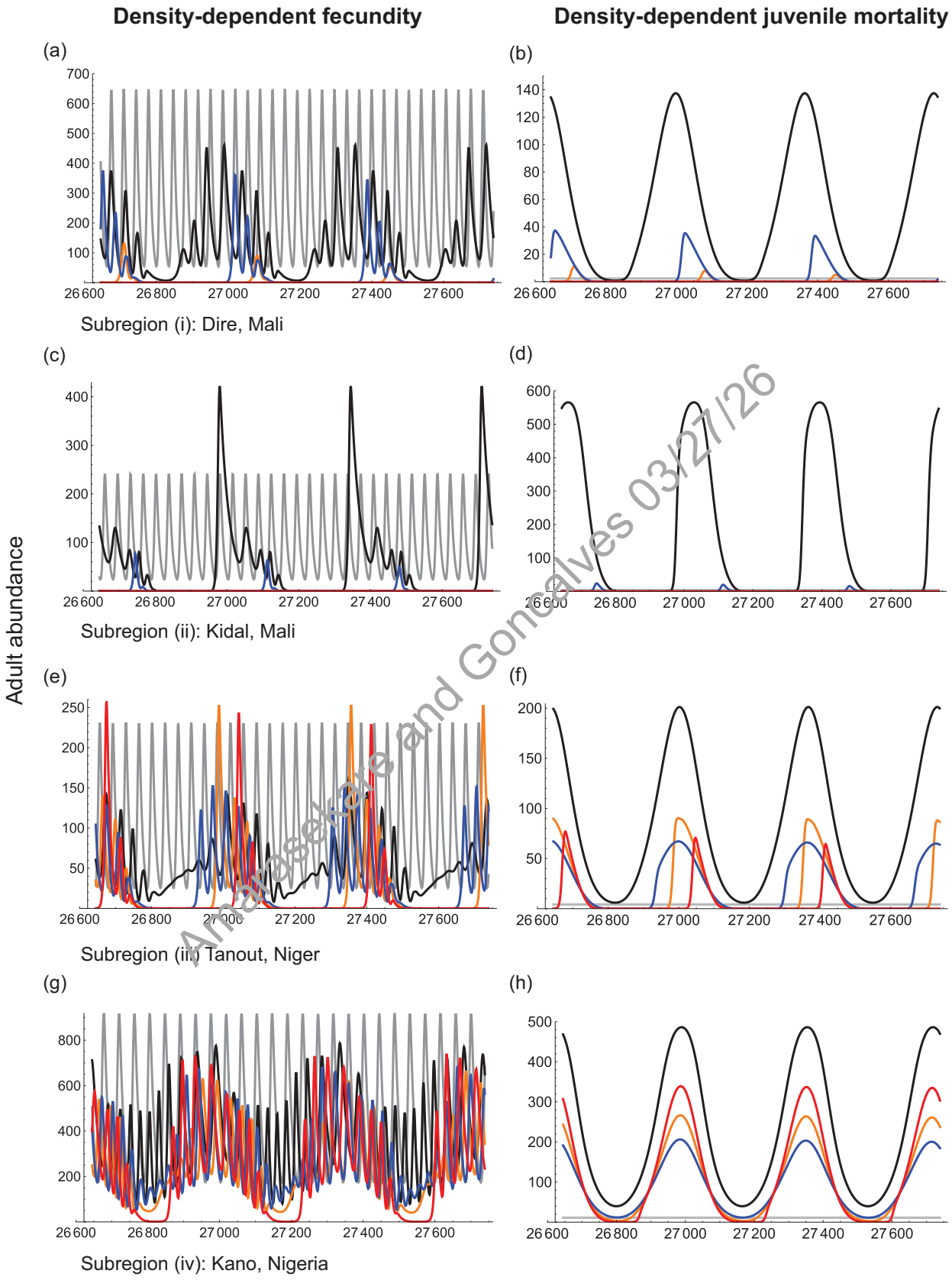

Figure 4

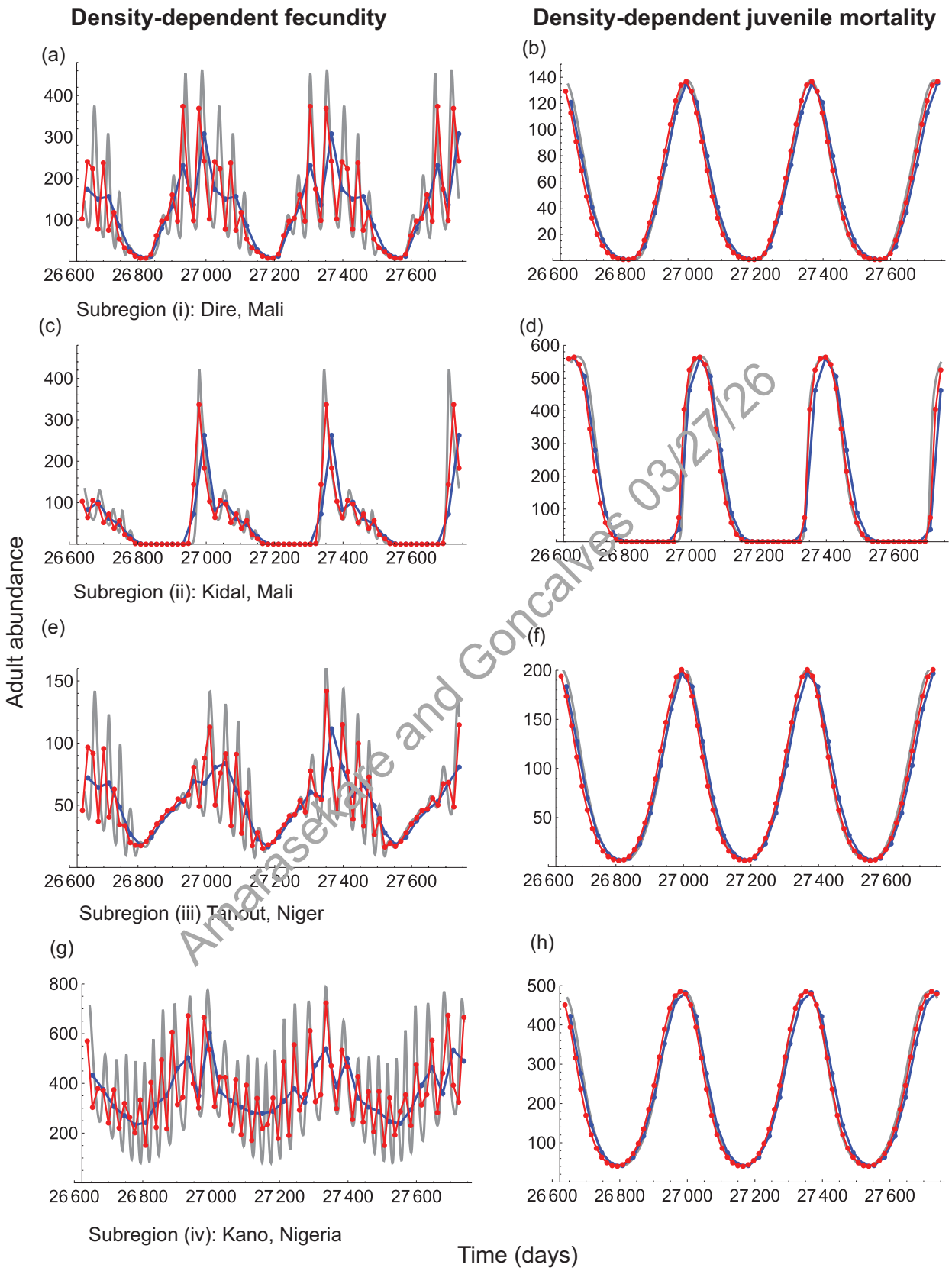

Figure 5

ONLINE APPENDIX A: Mechanistic descriptions of vector trait responses to temperature

Temperature-dependence of vector life history traits

Temperature response of mortality

In all ectotherms, density-independent per capita mortality rate increases with temperature (Savage et al., 2004 and references in Gillooly et al., 2001, 2002) within temperature range over which the underlying biochemical processes are fully functional and reproduction and development can occur (Johnson and Lewin, 1946; Ratkowsky et al., 2005; Schoolfield et al., 1981; Sharpe and DeMichele, 1977). Below this range, mortality increases with decreasing temperature due to the freezing of body fluids and other related phenomena (Savage et al., 2004 and references in Gillooly et al., 2001, 2002). The complete mortality response can be described by the following modification to the Boltzmann-Arrhenius function for reaction kinetics:

$$d_X(T) = d_{X\mathrm{T_R}} e^{A_{d_X}\left(\frac{1}{T_{R_X}} - \frac{1}{T}\right)} \left(1 + e^{A_{L_X}\left(\frac{1}{T_{L_X}} - \frac{1}{T}\right)}\right) \tag{A.1}$$

where $d_X(T)$ $X = J, A$ is the mortality rate at temperature T (in K), A_{d_X} is the Arrhenius constant, which quantifies how fast the mortality rate increases with increasing temperature, $\mathrm{T_{R_X}}$ is a reference (baseline) temperature at which mortality is equal to $d_{X\mathrm{T_R}}$. The reference temperature occurs within the range where enzymes are 100% active (typically between $20 - 30^{\circ}C$, $24 - 25^{\circ}C$ being the most common; Johnson and Lewin, 1946; Ratkowsky et al., 2005; Schoolfield et al., 1981; Sharpe and DeMichele, 1977). The parameter $\mathrm{T_{L}}_X$ is the temperature threshold at which mortality starts to increase with decreasing temperature, and A_{L_X} quantifies how quickly the mortality rate decreases with decreasing temperature. Note that $A_{d_X} > 0$ and $A_{L_X} < 0$.

Temperature response of the birth rate

A large number of studies spanning a range of ectothermic taxa show that the per capita birth rate exhibits a unimodal response to temperature (Amarasekare and Savage, 2012; Carriere and Boivin, 1997; Dannon et al., 2010; Dell et al., 2011; Dreyer and Baumgartner, 1996; Englund et al., 2011; Hou and Weng, 2010; Jandricic et al., 2010; Morgan et al., 2001), which is well-described by a Gaussian function:

$$b(T) = b_{\text{Topt}} e^{-\frac{(T - T_{\text{opt}_b})^2}{2{s_b}^2}} \tag{A.2}$$

where T_{opt_b} is the temperature at which the birth/attack rate is maximal (b_{Topt}), and s_b determines how fast or slowly the response decays from the optimum.

Temperature response of the maturation rate

Maturation rate of ectotherms exhibits a left-skewed temperature response (Kingsolver, 2009; Kingsolver et al., 2011; Schoolfield et al., 1981; Sharpe and DeMichele, 1977; Van der Have, 2002; Van der Have and de Jong, 1996) that results from the reduction in reaction rates at low and high temperature extremes due to enzyme inactivation. This response is well-described by a thermodynamic rate process model (Ratkowsky et al., 2005; Schoolfield et al., 1981; Sharpe and DeMichele, 1977):

$$m(T) = \frac{\frac{m_{T_R} T}{T_R} e^{A_{m_J}\left(\frac{1}{T_R} - \frac{1}{T}\right)}}{1 + e^{A_L\left(\frac{1}{T_{L/2}} - \frac{1}{T}\right)} + e^{A_H\left(\frac{1}{T_{H/2}} - \frac{1}{T}\right)}} \tag{A.3}$$

where $m(T)$ is the maturation rate at temperature T (in $^\circ K$), m_{T_R} is the maturation rate at the reference temperature T_R at which the enzyme is 100% active, A_{m_J} (enthalpy of activation divided by the universal gas constant R) quantifies temperature sensitivity, $T_{L/2}$ and $T_{H/2}$ are, respectively, the low and high temperatures at which the enzyme is 50% active, and A_L and A_H are the enthalpy changes associated with low and high temperature enzyme inactivation divided by R (Johnson and Lewin, 1946; Ratkowsky et al., 2005; Schoolfield et al., 1981; Sharpe and DeMichele, 1977; Van der Have, 2002; Van der Have and de Jong, 1996). Note that $A_L < 0$ and $A_H > 0$.

Temperature response of intra-specific competition

Vector self-limitation can arise from intra-specific competition at juvenile or adult stages. Previous work on insects (Amarasekare, 2015; Amarasekare and Coutinho, 2014; Gao et al., 2016; Johnson et al., 2016) suggests that self-limitation is likely to be strongest at the optimal temperature for reproduction (i.e., $T_{\text{opt}_\text{q}} = T_{\text{opt}_\text{b}}$ with the same response breadth as the birth rate (i.e., $s_q = s_b$).

Table A1: Parameters of the temperature response functions for the malaria vector (*Anopheles* species).

Vector birth rate	
$b(T) = b_{\text{Topt}} e^{-\frac{(T-T_{\text{opt}_\text{b}})^2}{2{s_b}^2}}$	
$b_{T_{\text{opt}}} = 23.88 \pm 1.57 (p = 0.042)$	$T_{\text{opt}_\text{b}} = 301.22 \pm 0.64 (p = 0.0014)$
$s_b = 7.81 \pm 1.0 (p = 0.08)$	
Vector maturation rate	
$m(T) = \frac{\frac{m_{T_R}}{T_R} T e^{A_{m_J}\left(\frac{1}{T_R} - \frac{1}{T}\right)}}{1 + e^{A_H\left(\frac{1}{T_H} - \frac{1}{T}\right)}}$	
$\text{T}_{\text{R}m} = 297K$	$m_{\text{T}_\text{R}} = 0.07$
$A_m = 8423 \pm 725.2 (p = 8.3e-05)$	$A_H = 41010 \pm 5886 (p = 0.00094)$
$T_H = 306.0 \pm 39.67 (p = 6.9e-14)$	
Vector mortality rate	
$d_X(T) = d_{X\text{T}_\text{R}} e^{A_{d_X}\left(\frac{1}{\text{T}_{\text{R}X}} - \frac{1}{T}\right)} \left(1 + e^{A_{L_X}\left(\frac{1}{\text{T}_{\text{L}X}} - \frac{1}{T}\right)}\right)$	
(X=J, A)	
Juvenile mortality rate	
$\text{T}_{\text{R}J} = 297K$	$d_{J_{\text{T}_\text{R}}} = 0.02$
$A_{d_J} = 29284.68 \pm 1387.51 (p = 2.9e-05)$	$A_{L_J} = -74869.43 \pm 35198.11 (p = 0.1)$
$T_{LJ} = 294.12 \pm 1.4 (p = 3.1e-09)$	
Adult mortality rate	
$\text{T}_{\text{R}J} = 298K$	$d_{\text{T}_\text{R}} = 0.04$
$A_d = 20710.62 \pm 441.89 (p = 8.3e-08)$	$A_L = -35973.81 \pm 7717.18 (p = 0.005)$
$T_L = 294.25 \pm 3.51 (p = 4.6e-09)$	

Literature Cited

Amarasekare, P. 2015. Temperature effects on consumer-resource interactions. Journal of Animal Ecology 84:665–679.

Amarasekare, P., and R. Coutinho. 2014. Effects of temperature on intra-specific competition in ectotherms. American Naturalist 184:E50–E65.

Amarasekare, P., and V. Savage. 2012. A mechanistic framework for elucidating the temperature dependence of fitness. American Naturalist 179:178–191.

Beck-Johnson, L., W. Nelson, K. Paaijmans, A. Read, M. Thomas, and O. Bjornstad. 2013. The effect of temperature on anopheles mosquito population dynamics and the potential for malaria transmission. PLoS One 8:e79276.

Carriere, Y., and G. Boivin. 1997. Evolution of thermal sensitivity of parasitization capacity in egg parasitoids. Evolution 51:2028–2032.

Dannon, E. A., M. Tamo, A. van Huis, and M. Dicke. 2010. Functional response and life history parameters of *Apanteles taragamae*, a larval parasitoid of *Maruca vitrata*. BioControl 55:363–378.

Dell, A., S. Pawar, and V. M. Savage. 2011. Systematic variation in the temperature dependence of physiological and ecological traits. Proceedings of the National Academy of Sciences 108:10591–10596.

Dreyer, H., and J. Baumgartner. 1996. Temperature influence on cohort parameters and demographic characteristics of the two cowpea coreids *Clavigralla tomentosicollis* and *C. shadabi*. Entomologia Experimentalis et Applicata 78:201–213.

Englund, G., G. Ohlund, C. Hein, and D. S. 2011. Temperature dependence of the functional response. Ecology Letters 14:914–921.

Gao, D., Y. Lou, D. He, T. Porco, Y. Kuang, G. Chowell, and S. Ryan. 2016. Prevention and control of zika as a mosquito-borne and sexually transmitted disease: a mathematical modelling analysis. Scientific Reports 6:28070–28080.

Gillooly, J. F., J. H. Brown, G. B. West, V. M. Savage, and E. L. Charnov. 2001. Effects of size and temperature on metabolic rate. Science 293:2248–2251.

Gillooly, J. F., E. L. Charnov, G. B. West, , V. M. Savage, and J. H. Brown. 2002. Effects of size and temperature on developmental time. Science 293:2248–2251.

Gurney, W., R. Nisbet, and J. Lawton. 1983. The systematic formulation of tractable single-species population models incorporating age structure. Journal of Animal Ecology 52:479–495.

Hou, Y., and Z. Weng. 2010. Temperature-dependent development and life table parameters of *Octodonta nipae* (coleoptera: Chrysomelidae). Environmental Entomology 39:1676–1684.

Jandricic, S. E., S. P. Wraight, K. C. Bennett, and J. P. Sanderson. 2010. Developmental times and life table statistics of *Aulacorthum solani* (hemiptera: Aphididae) at six constant temperatures, with recommendations on the application of temperature-dependent development models. Environmental Entomology 39:1631–1642.

Johnson, C., R. Coutinho, E. Berlin, E. Dolphin, J. Heyer, B. Kim, A. Leung, J. Sabellon, and P. Amarasekare. 2016. Effects of temperature and resource variation on insect population dynamics: the bordered plant bug as a case study. Functional Ecology 30:1122–1131.

Johnson, F., and I. Lewin. 1946. The growth rate of e. coli in relation to temperature, quinine and coenzyme. Journal of Cellular and Comparative Physiology 28:47–75.

Kingsolver, J. 2009. The well-temperatured biologist. American Naturalist 174:755–768.

Kingsolver, J., A. Woods, L. B. Buckley, L. Potter, H. MacLean, and J. Higgins. 2011. Complex life cycles and the responses of insects to climate change. Integrative and Comparative Biology 51:719–732.

Morgan, D., K. F. A. Walters, and J. N. Aegerter. 2001. Effect of temperature and cultivar on the pea aphid, *Acyrthosiphon pisum* (hemiptera: Aphididae) life history. Bulletin of Entomological Research 91:47–52.

Murdoch, W., C. J. Briggs, and N. R. M. 2003. Consumer resource dynamics. Princeton University Press, Princeton New Jersy.

Nisbet, R. 1997. Sdelay-differential equations for structured populations. Pages 89–116 *in* S. Tuljapurkar and H. Caswell, eds. Structured-population models in marine, terrestrial, and freshwater systems. Chapman and Hall, New York.

Nisbet, R. M., and W. Gurney. 1983. The systematic formulation of population-models for insects with dynamically varying instar duration. Theoretical Population Biology 23:114–135.

Ratkowsky, D., J. Olley, and T. Ross. 2005. Unifying temperature effects on the growth rate of bacteria and the stability of globular proteins. Journal of Theoretical Biology 233:351–362.

Savage, V. M., J. F. Gillooly, J. H. Brown, G. B. West, and E. L. Charnov. 2004. Effects of body size and temperature on population growth. American Naturalist 163:429–441.

Schoolfield, R., J. Sharpe, and C. Magnuson. 1981. Non-linear regression of biological temperature-dependent rate models based on absolute reaction-rate theory. Jounal of Theoretical Biology 88:719–731.

Sharpe, P., and D. DeMichele. 1977. Reaction kinetics of poikilotherm development. Journal of Theoretical Biology 64:649–670.

Van der Have, T. 2002. A proximate model for thermal tolerance in ectotherms. Oikos 98:141–155.

Van der Have, T. M., and G. de Jong. 1996. Adult size in ectotherms: temperature effects on growth and differentiation. Journal of Theoretical Biology 183:329–340.

ONLINE APPENDIX B: DDE model for vector population dynamics in the absence of temperature variation

We consider an ectotherm disease vector whose life cycle consists of a juvenile stage and an adult stage. Examples include arthropod vectors such as mosquitoes, ticks and sandflies. The juvenile

stage typically includes an egg, larval and pupal stage. Since self-limitation typically operates at the larval or adult stage, egg and pupal stages act merely as time lags. We can therefore depict life cycle dynamics in terms of a single juvenile stage. When the thermal environment is constant, i.e., the vector population experiences the same temperature, on average, with few or no fluctuations around the mean ($T(t) = T$), stage-structured population dynamics are given by:

$$\begin{aligned}
\frac{dJ(t)}{dt} &= b\big(T, A(t)\big)A(t) - M_J(t) - d_J\big(T(t), J(t)\big)J(t) \\
\frac{dA(t)}{dt} &= M_J(t) - d_A(T)A(t) \\
M_J(t) &= b\big((t - \tau_J(T)), A(t - \tau_J(T))\big)A(t - \tau_J(T))e^{-d_J(T)\tau_J(T)}
\end{aligned} \tag{B.1}$$

where the state variables $J(t)$ and $A(t)$ represent juvenile and adult abundances, $b(T), \tau_J(T), d_J(T)$ and $d_A(T)$ depict the temperature responses of birth, maturation, juvenile mortality and adult mortality, and the functions $b(T, A(t))$ and $d_J(T, J(t))$ depict the joint effects of temperature and density on per capita birth and juvenile mortality rates. Note that $\tau_J(T) = \frac{1}{m_J(T)}$ where $m_J(T)$ is the temperature response of the per capita maturation rate.

Vector self-regulation can occur at the adult or juvenile stage. In most arthropod vectors (e.g., mosquitos, ticks, sandflies), the females' ability to produce viable eggs depends on access to blood meals (Beck-Johnson et al., 2013). Since blood meal availability is determined by host abundance, which is typically constant on the time scale of vector-host dynamics, the number of viable eggs produced is likely to decrease as vector density increases. Self-regulation at the juvenile stage can occur when larval competition for food or space causes the juvenile mortality rate to increase with juvenile density. Following previous work on insect population dynamics (see references in Murdoch et al. (2003)), we use the following functions to depict density-dependence in birth and juvenile mortality rates: $b(T, A(t)) = b(T)e^{-q(T)A(t)}$ and $d_J(T)(1 + q(T)J(t))$ where $q(T)$ is the temperature-dependent per capita competition coefficient.

This model, parameterized with data on temperature effects on life history traits and competition, can predict the population dynamics and steady states (e.g., point equilibria, limit cycles) at the mean habitat temperature for any ectotherm disease vector. See main text for an application of the model to the malaria vector.

Literature Cited

Amarasekare, P. 2015. Temperature effects on consumer-resource interactions. Journal of Animal Ecology 84:665–679.

Amarasekare, P., and R. Coutinho. 2014. Effects of temperature on intra-specific competition in ectotherms. American Naturalist 184:E50–E65.

Amarasekare, P., and V. Savage. 2012. A mechanistic framework for elucidating the temperature dependence of fitness. American Naturalist 179:178–191.

Beck-Johnson, L., W. Nelson, K. Paaijmans, A. Read, M. Thomas, and O. Bjornstad. 2013. The effect of temperature on anopheles mosquito population dynamics and the potential for malaria transmission. PLoS One 8:e79276.

Carriere, Y., and G. Boivin. 1997. Evolution of thermal sensitivity of parasitization capacity in egg parasitoids. Evolution 51:2028–2032.

Dannon, E. A., M. Tamo, A. van Huis, and M. Dicke. 2010. Functional response and life history parameters of *Apanteles taragamae*, a larval parasitoid of *Maruca vitrata*. BioControl 55:363–378.

Dell, A., S. Pawar, and V. M. Savage. 2011. Systematic variation in the temperature dependence of physiological and ecological traits. Proceedings of the National Academy of Sciences 108:10591–10596.

Dreyer, H., and J. Baumgartner. 1996. Temperature influence on cohort parameters and demographic characteristics of the two cowpea coreids *Clavigralla tomentosicollis* and *C. shadabi*. Entomologia Experimentalis et Applicata 78:201–213.

Englund, G., G. Ohlund, C. Hein, and D. S. 2011. Temperature dependence of the functional response. Ecology Letters 14:914–921.

Gao, D., Y. Lou, D. He, T. Porco, Y. Kuang, G. Chowell, and S. Ryan. 2016. Prevention and control of zika as a mosquito-borne and sexually transmitted disease: a mathematical modelling analysis. Scientific Reports 6:28070–28080.

Gillooly, J. F., J. H. Brown, G. B. West, V. M. Savage, and E. L. Charnov. 2001. Effects of size and temperature on metabolic rate. Science 293:2248–2251.

Gillooly, J. F., E. L. Charnov, G. B. West, , V. M. Savage, and J. H. Brown. 2002. Effects of size and temperature on developmental time. Science 293:2248–2251.

Gurney, W., R. Nisbet, and J. Lawton. 1983. The systematic formulation of tractable single-species population models incorporating age structure. Journal of Animal Ecology 52:479–495.

Hou, Y., and Z. Weng. 2010. Temperature-dependent development and life table parameters of *Octodonta nipae* (coleoptera: Chrysomelidae). Environmental Entomology 39:1676–1684.

Jandricic, S. E., S. P. Wraight, K. C. Bennett, and J. P. Sanderson. 2010. Developmental times and life table statistics of *Aulacorthum solani* (hemiptera: Aphididae) at six constant temperatures, with recommendations on the application of temperature-dependent development models. Environmental Entomology 39:1631–1642.

Johnson, C., R. Coutinho, E. Berlin, E. Dolphin, J. Heyer, B. Kim, A. Leung, J. Sabellon, and P. Amarasekare. 2016. Effects of temperature and resource variation on insect population dynamics: the bordered plant bug as a case study. Functional Ecology 30:1122–1131.

Johnson, F., and I. Lewin. 1946. The growth rate of e. coli in relation to temperature, quinine and coenzyme. Journal of Cellular and Comparative Physiology 28:47–75.

Kingsolver, J. 2009. The well-temperatured biologist. American Naturalist 174:755–768.

Kingsolver, J., A. Woods, L. B. Buckley, L. Potter, H. MacLean, and J. Higgins. 2011. Complex life cycles and the responses of insects to climate change. Integrative and Comparative Biology 51:719–732.

Morgan, D., K. F. A. Walters, and J. N. Aegerter. 2001. Effect of temperature and cultivar on the pea aphid, *Acyrthosiphon pisum* (hemiptera: Aphididae) life history. Bulletin of Entomological Research 91:47–52.

Murdoch, W., C. J. Briggs, and N. R. M. 2003. Consumer resource dynamics. Princeton University Press, Princeton New Jersy.

Nisbet, R. 1997. Sdelay-differential equations for structured populations. Pages 89–116 *in* S. Tuljapurkar and H. Caswell, eds. Structured-population models in marine, terrestrial, and freshwater systems. Chapman and Hall, New York.

Nisbet, R. M., and W. Gurney. 1983. The systematic formulation of population-models for insects with dynamically varying instar duration. Theoretical Population Biology 23:114–135.

Ratkowsky, D., J. Olley, and T. Ross. 2005. Unifying temperature effects on the growth rate of bacteria and the stability of globular proteins. Journal of Theoretical Biology 233:351–362.

Savage, V. M., J. F. Gillooly, J. H. Brown, G. B. West, and E. L. Charnov. 2004. Effects of body size and temperature on population growth. American Naturalist 163:429–441.

Schoolfield, R., J. Sharpe, and C. Magnuson. 1981. Non-linear regression of biological temperature-dependent rate models based on absolute reaction-rate theory. Jounal of Theoretical Biology 88:719–731.

Sharpe, P., and D. DeMichele. 1977. Reaction kinetics of poikilotherm development. Journal of Theoretical Biology 64:649–670.

Van der Have, T. 2002. A proximate model for thermal tolerance in ectotherms. Oikos 98:141–155.

Van der Have, T. M., and G. de Jong. 1996. Adult size in ectotherms: temperature effects on growth and differentiation. Journal of Theoretical Biology 183:329–340.

ONLINE APPENDIX C: DDE model for vector population dynamics under seasonal variation and warming

When temperature varies over time, the developmental delay varies with both temperature and time. In this case, stage-structured population dynamics are given by:

$$\begin{aligned}
\frac{dJ(t)}{dt} &= b\Big(T(t), A(t)\Big)A(t) - M_J(t) - d_J\Big(T(t), J(t)\Big)J(t) \\
\frac{dA(t)}{dt} &= M_J(t) - d_A(T(t), A(t))A(t) \\
M_J(t) &= b\Big(T(t-\tau_J(t)), A(t-\tau_J(t))\Big)A(t-\tau_J(t))s_J(t)\frac{m_J(T(t))}{m_J(T(t-\tau_J(t)))} \\
\frac{ds_J(t)}{dt} &= s_J(t)\left[\frac{m_J(T(t))d_J(T(t-\tau_J(t)), J(t-\tau_J(t)))}{m_J(T(t-\tau_J(t)))} - d_J(T(t), J(t))\Big)\right] \\
\frac{d\tau_J(t)}{dt} &= 1 - \frac{m_J(T(t))}{m_J(T(t-\tau_J(t)))}
\end{aligned} \tag{C.1}$$

where the state variables $J(t) and, A(t)$ represent juvenile and adult abundances, and the functions $b(T(t), A(t)), d_J(T(t), J(t))$ and $d_A(T(t), A(t))$ depict the joint effects of temperature and density on per capita birth and juvenile mortality rates.

Recruitment to the juvenile vector stage occurs via adult reproduction. The rate at which newborns are added to the juvenile population is a function of adult vector density ($A(t)$), which can be density-dependent. The parameter $\tau_J(t)$ depicts the juvenile developmental delay of the vector, and function $M_J(t)$, the rate at which juvenile vectors mature into adults, given by the recruitment rate into the juvenile stage $\tau_J(t)$ time units ago multiplied by the fraction of juveniles that survive the juvenile stage ($s_J(t)$). When temperature varies over time (e.g., seasonal variation, warming), the vector's developmental delays ($\tau_J(t)$) and through-stage survivorship ($s_J(t)$) vary with both temperature and time. The rate of change in survivorship is given by the differential equation $\frac{ds_J}{dt}$, and that in developmental delay, by $\frac{d\tau_J}{dt}$. In these equations, $m_J(T(t)) = \frac{1}{\tau_J(t)}$ depicts the instantaneous per capita maturation rate of the vector's juvenile stage. The ratio $\frac{m_J(T(t))}{m_J(T(t-\tau_J(t)))}$ determines how temperature affects maturation. If temperature increases over the duration of the juvenile stage, this ratio exceeds 1, stage duration is shorter, and more individuals survive to the adult stage. Conversely, if temperature

decreases over the duration of the juvenile period, the ratio falls below 1, stage duration is longer, and fewer individuals survive to the adult stage. Further details of deriving variable delay equations for stage-structured ecological systems are given in (Gurney et al., 1983; Murdoch et al., 2003; Nisbet, 1997; Nisbet and Gurney, 1983).

Vector self-regulation can occur at the adult or juvenile stage. In most arthropod vectors (e.g., mosquitos, ticks, sandflies), the females' ability to produce viable eggs depends on access to blood meals (Beck-Johnson et al., 2013). Since blood meal availability is determined by host abundance, which is typically constant on the time scale of vector-host dynamics, the number of viable eggs produced is likely to decrease as vector density increases. Self-regulation at the juvenile stage can occur when larval competition for food or space causes the juvenile mortality rate to increase with juvenile density. Following previous work on insect population dynamics (see references in Murdoch et al. (2003)), we use the following functions to depict density-dependence in birth and mortality rates: $b\big(T(t), A(t)\big) = b(T(t))e^{-q_b(T(t))A(t)}$ and $d_J\big(T(t),\, J(t)\big) = d_J(T(t))(1 + q_{d_J}(T(t))J(t))$ where $q(T(t))$ is the temperature and time-dependent per capita competition coefficient.

Literature Cited

Amarasekare, P. 2015. Temperature effects on consumer-resource interactions. Journal of Animal Ecology 84:665–679.

Amarasekare, P., and R. Coutinho. 2014. Effects of temperature on intra-specific competition in ectotherms. American Naturalist 184:E50–E65.

Amarasekare, P., and V. Savage. 2012. A mechanistic framework for elucidating the temperature dependence of fitness. American Naturalist 179:178–191.

Beck-Johnson, L., W. Nelson, K. Paaijmans, A. Read, M. Thomas, and O. Bjornstad. 2013. The effect of temperature on anopheles mosquito population dynamics and the potential for malaria transmission. PLoS One 8:e79276.

Carriere, Y., and G. Boivin. 1997. Evolution of thermal sensitivity of parasitization capacity in egg parasitoids. Evolution 51:2028–2032.

Dannon, E. A., M. Tamo, A. van Huis, and M. Dicke. 2010. Functional response and life history parameters of *Apanteles taragamae*, a larval parasitoid of *Maruca vitrata*. BioControl 55:363–378.

Dell, A., S. Pawar, and V. M. Savage. 2011. Systematic variation in the temperature dependence of physiological and ecological traits. Proceedings of the National Academy of Sciences 108:10591–10596.

Dreyer, H., and J. Baumgartner. 1996. Temperature influence on cohort parameters and demographic characteristics of the two cowpea coreids *Clavigralla tomentosicollis* and *C. shadabi*. Entomologia Experimentalis et Applicata 78:201–213.

Englund, G., G. Ohlund, C. Hein, and D. S. 2011. Temperature dependence of the functional response. Ecology Letters 14:914–921.

Gao, D., Y. Lou, D. He, T. Porco, Y. Kuang, G. Chowell, and S. Ryan. 2016. Prevention and control of zika as a mosquito-borne and sexually transmitted disease: a mathematical modelling analysis. Scientific Reports 6:28070–28080.

Gillooly, J. F., J. H. Brown, G. B. West, V. M. Savage, and E. L. Charnov. 2001. Effects of size and temperature on metabolic rate. Science 293:2248–2251.

Gillooly, J. F., E. L. Charnov, G. B. West, , V. M. Savage, and J. H. Brown. 2002. Effects of size and temperature on developmental time. Science 293:2248–2251.

Gurney, W., R. Nisbet, and J. Lawton. 1983. The systematic formulation of tractable single-species population models incorporating age structure. Journal of Animal Ecology 52:479–495.

Hou, Y., and Z. Weng. 2010. Temperature-dependent development and life table parameters of *Octodonta nipae* (coleoptera: Chrysomelidae). Environmental Entomology 39:1676–1684.

Jandricic, S. E., S. P. Wraight, K. C. Bennett, and J. P. Sanderson. 2010. Developmental times and life table statistics of *Aulacorthum solani* (hemiptera: Aphididae) at six constant temperatures, with rec-

ommendations on the application of temperature-dependent development models. Environmental Entomology 39:1631–1642.

Johnson, C., R. Coutinho, E. Berlin, E. Dolphin, J. Heyer, B. Kim, A. Leung, J. Sabellon, and P. Amarasekare. 2016. Effects of temperature and resource variation on insect population dynamics: the bordered plant bug as a case study. Functional Ecology 30:1122–1131.

Johnson, F., and I. Lewin. 1946. The growth rate of e. coli in relation to temperature, quinine and coenzyme. Journal of Cellular and Comparative Physiology 28:47–75.

Kingsolver, J. 2009. The well-temperatured biologist. American Naturalist 174:755–768.

Kingsolver, J., A. Woods, L. B. Buckley, L. Potter, H. MacLean, and J. Higgins. 2011. Complex life cycles and the responses of insects to climate change. Integrative and Comparative Biology 51:719–732.

Morgan, D., K. F. A. Walters, and J. N. Aegerter. 2001. Effect of temperature and cultivar on the pea aphid, *Acyrthosiphon pisum* (hemiptera: Aphididae) life history. Bulletin of Entomological Research 91:47–52.

Murdoch, W., C. J. Briggs, and N. R. M. 2003. Consumer resource dynamics. Princeton University Press, Princeton New Jersy.

Nisbet, R. 1997. Sdelay-differential equations for structured populations. Pages 89–116 *in* S. Tuljapurkar and H. Caswell, eds. Structured-population models in marine, terrestrial, and freshwater systems. Chapman and Hall, New York.

Nisbet, R. M., and W. Gurney. 1983. The systematic formulation of population-models for insects with dynamically varying instar duration. Theoretical Population Biology 23:114–135.

Ratkowsky, D., J. Olley, and T. Ross. 2005. Unifying temperature effects on the growth rate of bacteria and the stability of globular proteins. Journal of Theoretical Biology 233:351–362.

Savage, V. M., J. F. Gillooly, J. H. Brown, G. B. West, and E. L. Charnov. 2004. Effects of body size and temperature on population growth. American Naturalist 163:429–441.

Schoolfield, R., J. Sharpe, and C. Magnuson. 1981. Non-linear regression of biological temperature-dependent rate models based on absolute reaction-rate theory. Jounal of Theoretical Biology 88:719–731.

Sharpe, P., and D. DeMichele. 1977. Reaction kinetics of poikilotherm development. Journal of Theoretical Biology 64:649–670.

Van der Have, T. 2002. A proximate model for thermal tolerance in ectotherms. Oikos 98:141–155.

Van der Have, T. M., and G. de Jong. 1996. Adult size in ectotherms: temperature effects on growth and differentiation. Journal of Theoretical Biology 183:329–340.

Figure Legends

Fig. C1. Population dynamics of the malaria vector in constant and seasonal thermal environments when density-dependence operates on the vector's birth rate. Delayed feedback cycles are depicted in gray and seasonal variation in abundance in black. Parameter values are given in Tables 1 and A1.

Fig. C2. Population dynamics of the malaria vector in constant and seasonal thermal environments when density-dependence operates on the vector's juvenile mortality rate. Delayed feedback cycles are depicted in gray and seasonal variation in abundance in black. Parameter values are given in Tables 1 and A1.

Fig. C3. Malaria vector population dynamics under low levels of warming (increase in mean temperature by 1.4° over 75 years) for the warmer winters (blue), baseline (orange) and hot extremes (red) scenarios when density-dependence operates on the vector's birth rate. Parameter values are given in Tables 1 and A1.

Fig. C4. Malaria vector population dynamics under low levels of warming (increase in mean temperature by 1.4° over 75 years) for the warmer winters (blue), baseline (orange) and hot extremes (red) scenarios when density-dependence operates on the vector's juvenile mortality rate. Parameter values are given in Tables 1 and A1.

Fig. C5. Malaria vector population dynamics under moderate levels of warming (increase in mean temperature by 2.7° over 75 years) for the warmer winters (blue), baseline (orange) and hot extremes (red) scenarios when density-dependence operates on the vector's birth rate. Parameter values are given in Tables 1 and A1.

Fig. C6. Malaria vector population dynamics under moderate levels of warming (increase in mean temperature by 2.7° over 75 years) for the warmer winters (blue), baseline (orange) and hot extremes (red) scenarios when density-dependence operates on the vector's juvenile mortality rate. Parameter values are given in Tables 1 and A1.

Fig. C7. Malaria vector population dynamics under high levels of warming (increase in mean temperature by 4.4° over 75 years) for the warmer winters (blue), baseline (orange) and hot extremes (red) scenarios when density-dependence operates on the vector's birth rate. Parameter values are

given in Tables 1 and A1.

Fig. C8. Malaria vector population dynamics under high levels of warming (increase in mean temperature by 4.4° over 75 years) for the warmer winters (blue), baseline (orange) and hot extremes (red) scenarios when density-dependence operates on the vector's juvenile mortality rate. Parameter values are given in Tables 1 and A1.

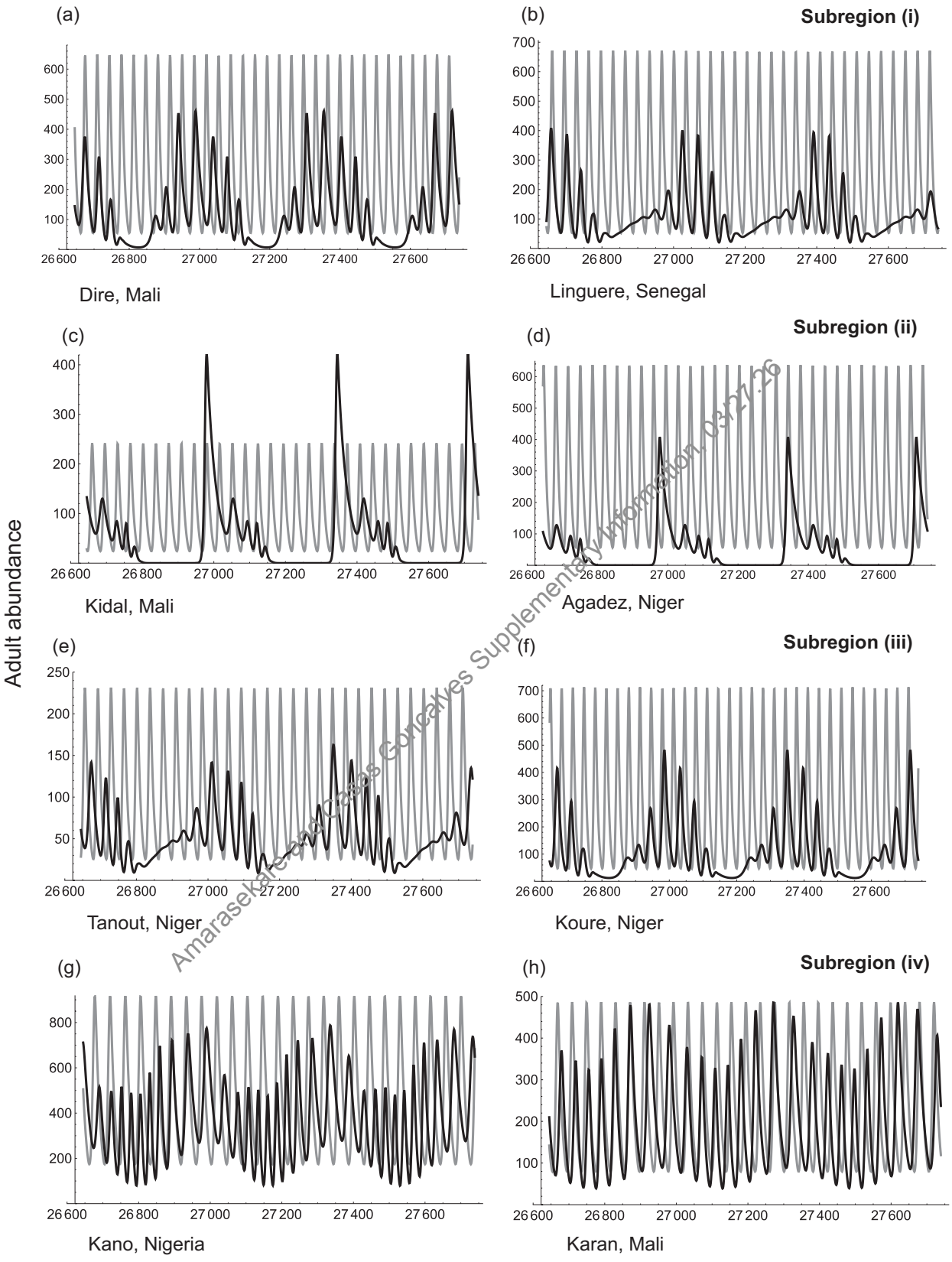

Figure C1

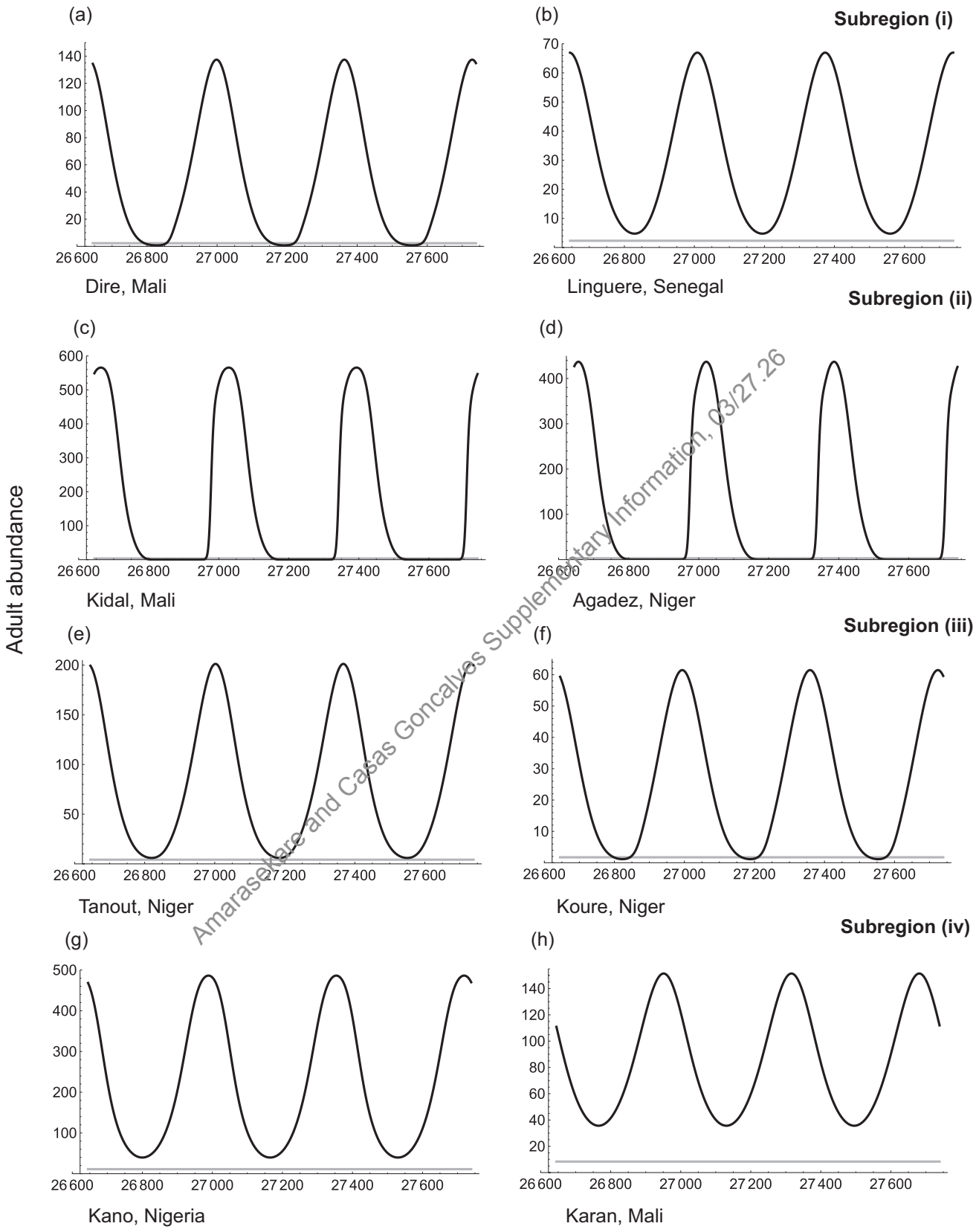

Figure C2

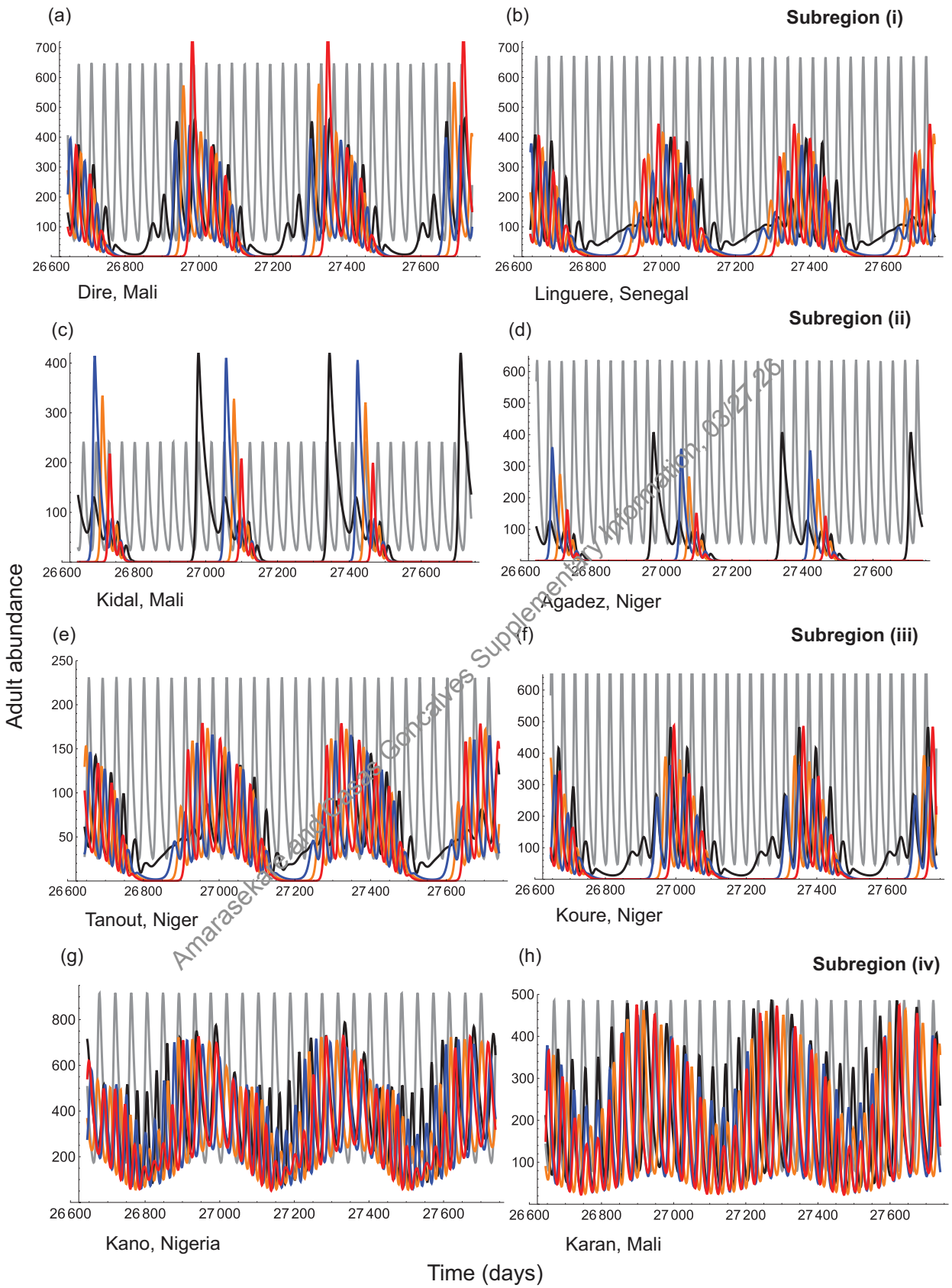

Figure C3

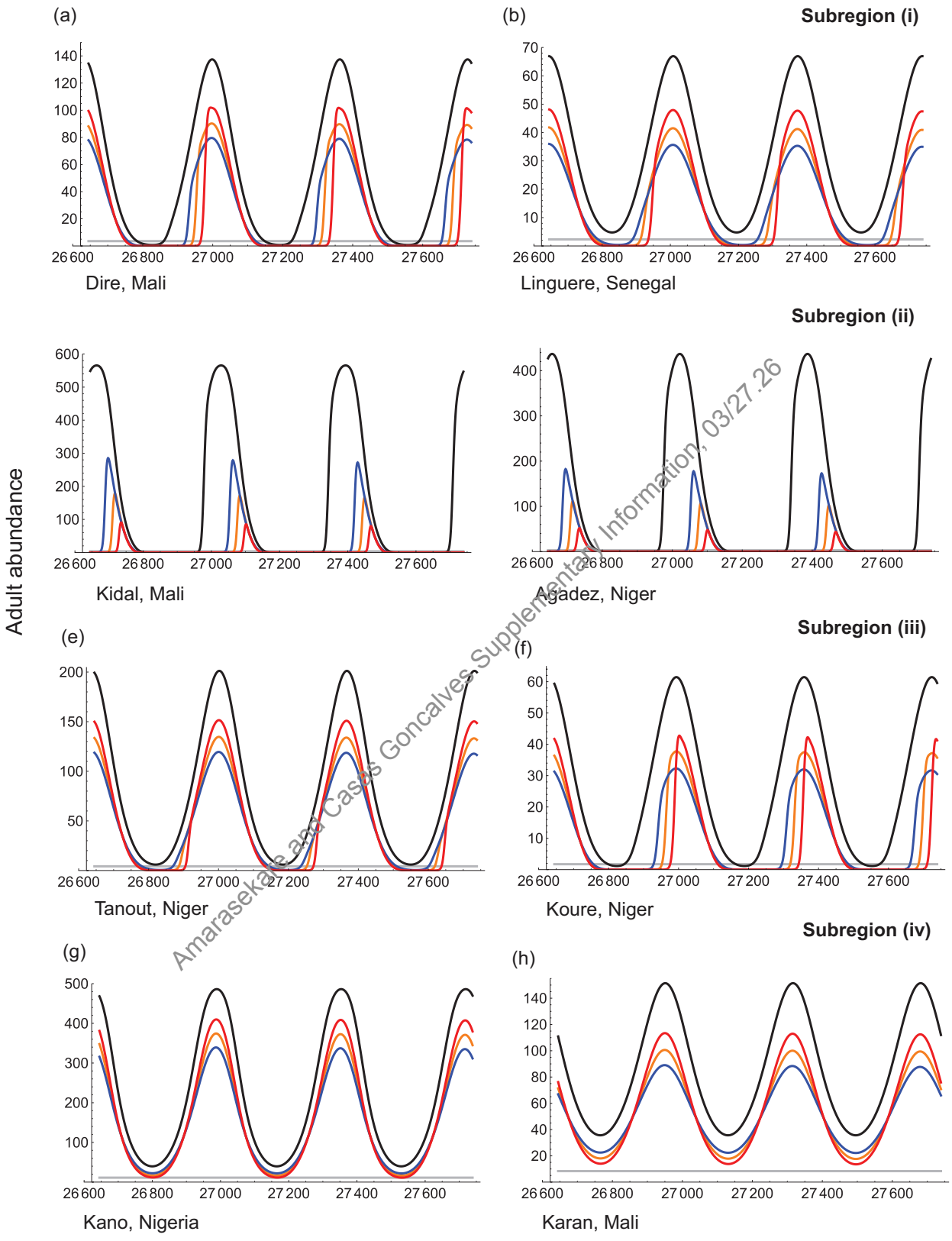

Figure C4

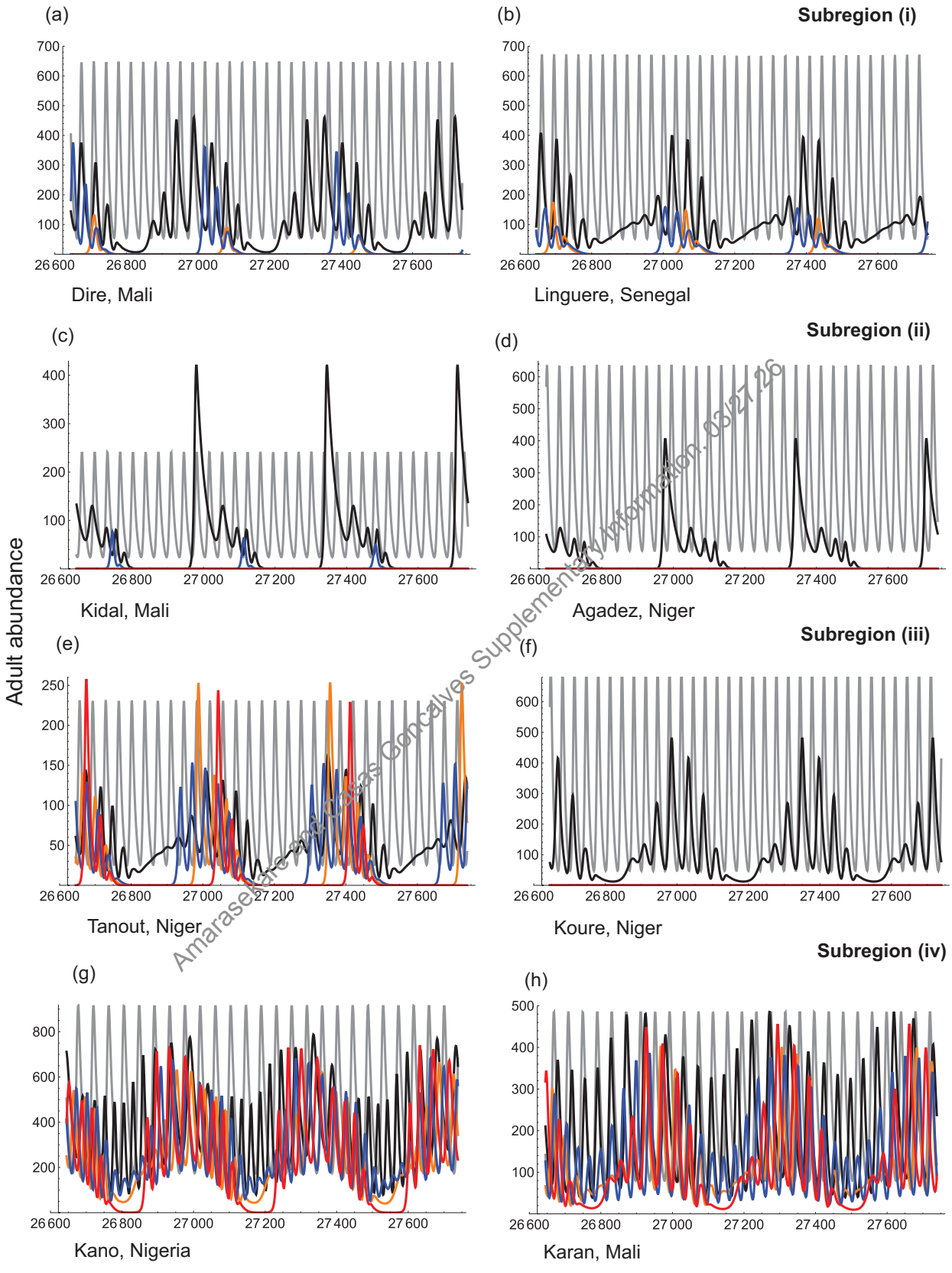

Figure C5

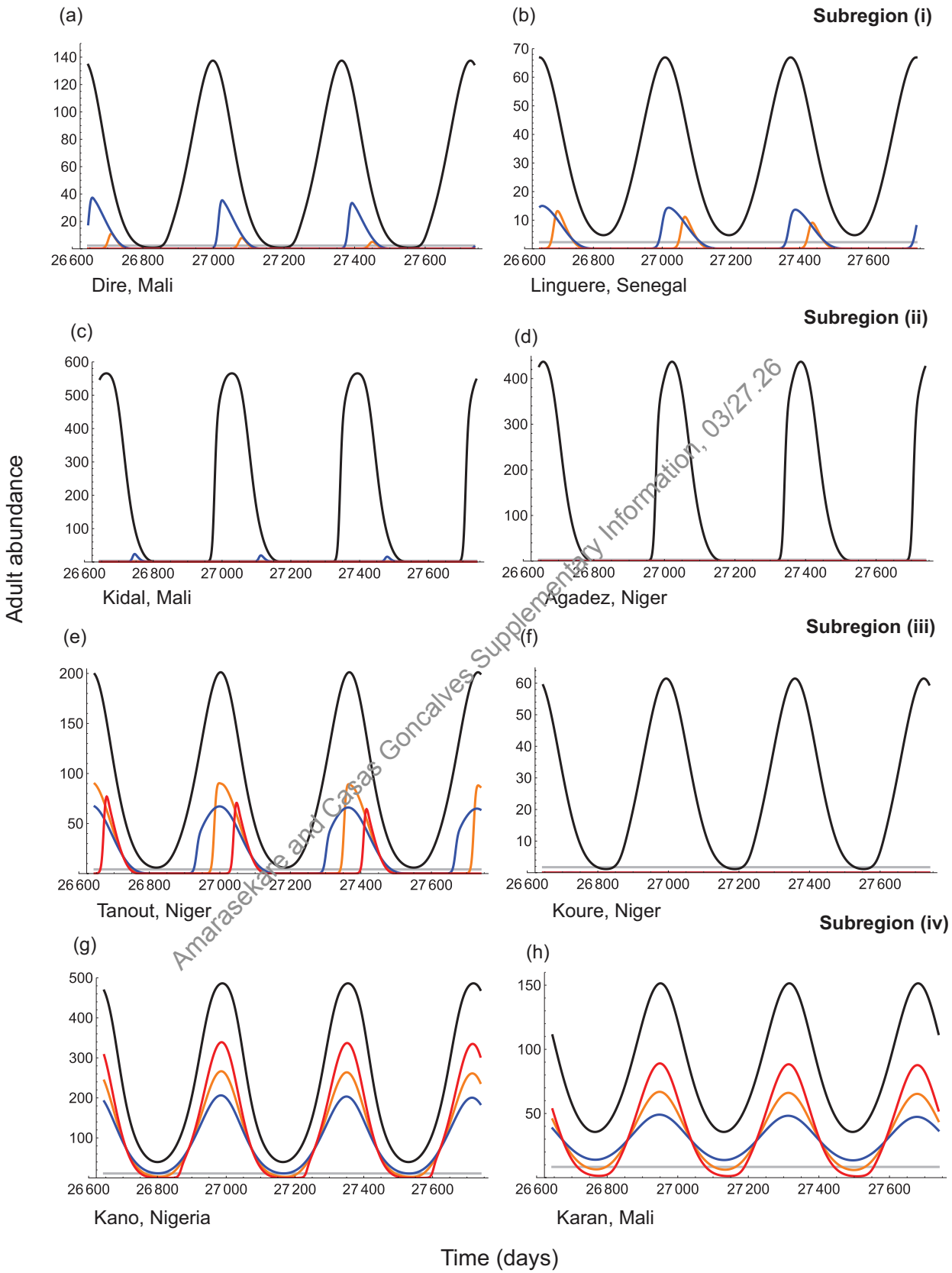

Figure C6

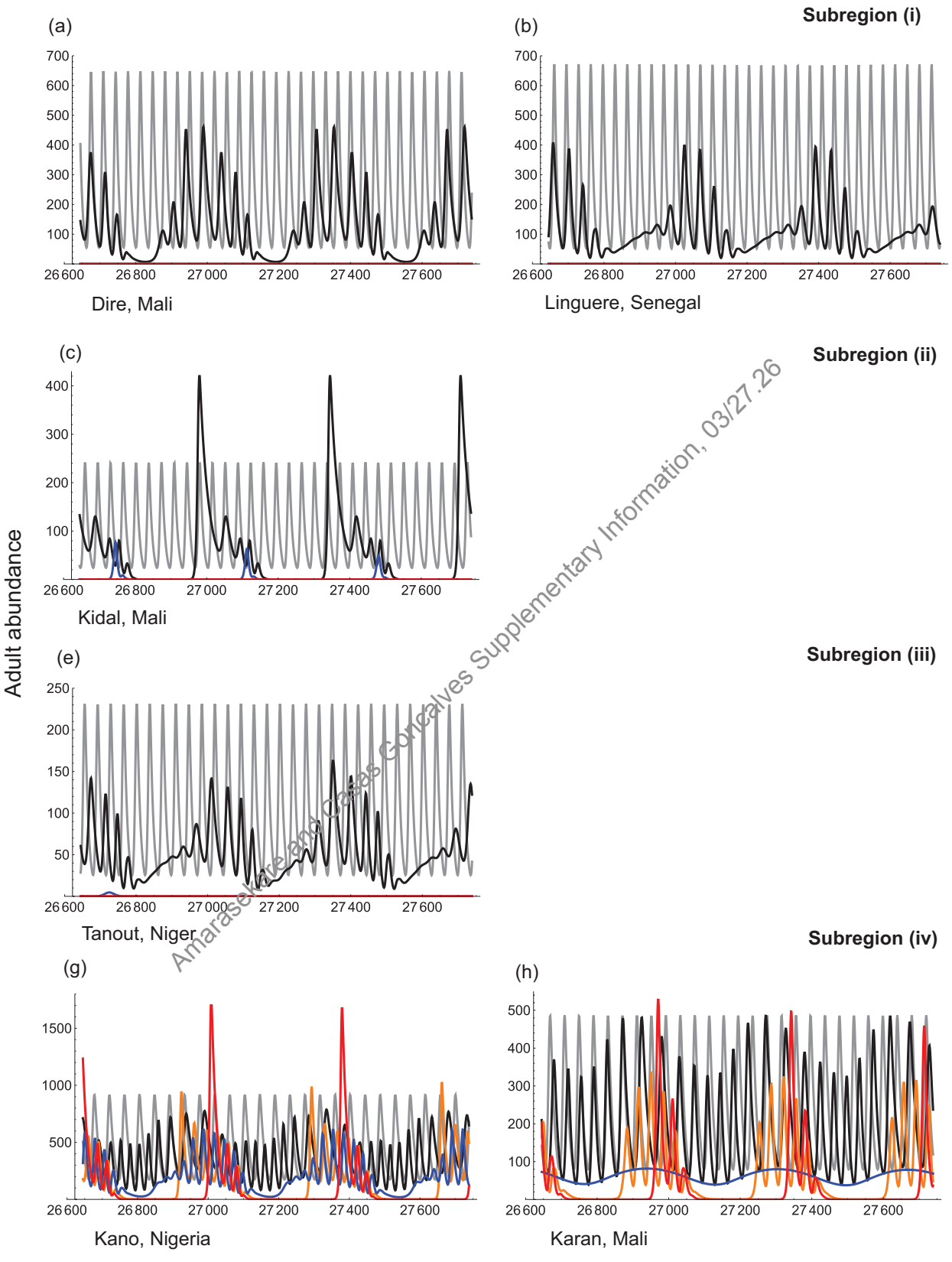
Subregion (i)
(a)
(b)
Dire, Mali
Linguere, Senegal
Subregion (ii)
(c)
Kidal, Mali
Subregion (iii)
(e)
Tanout, Niger
Subregion (iv)
(g)
(h)
Kano, Nigeria
Karan, Mali
Adult abundance
Time (days)
Amarasekare and Coutinho Supplementary Information, 03/27.26

Figure C7

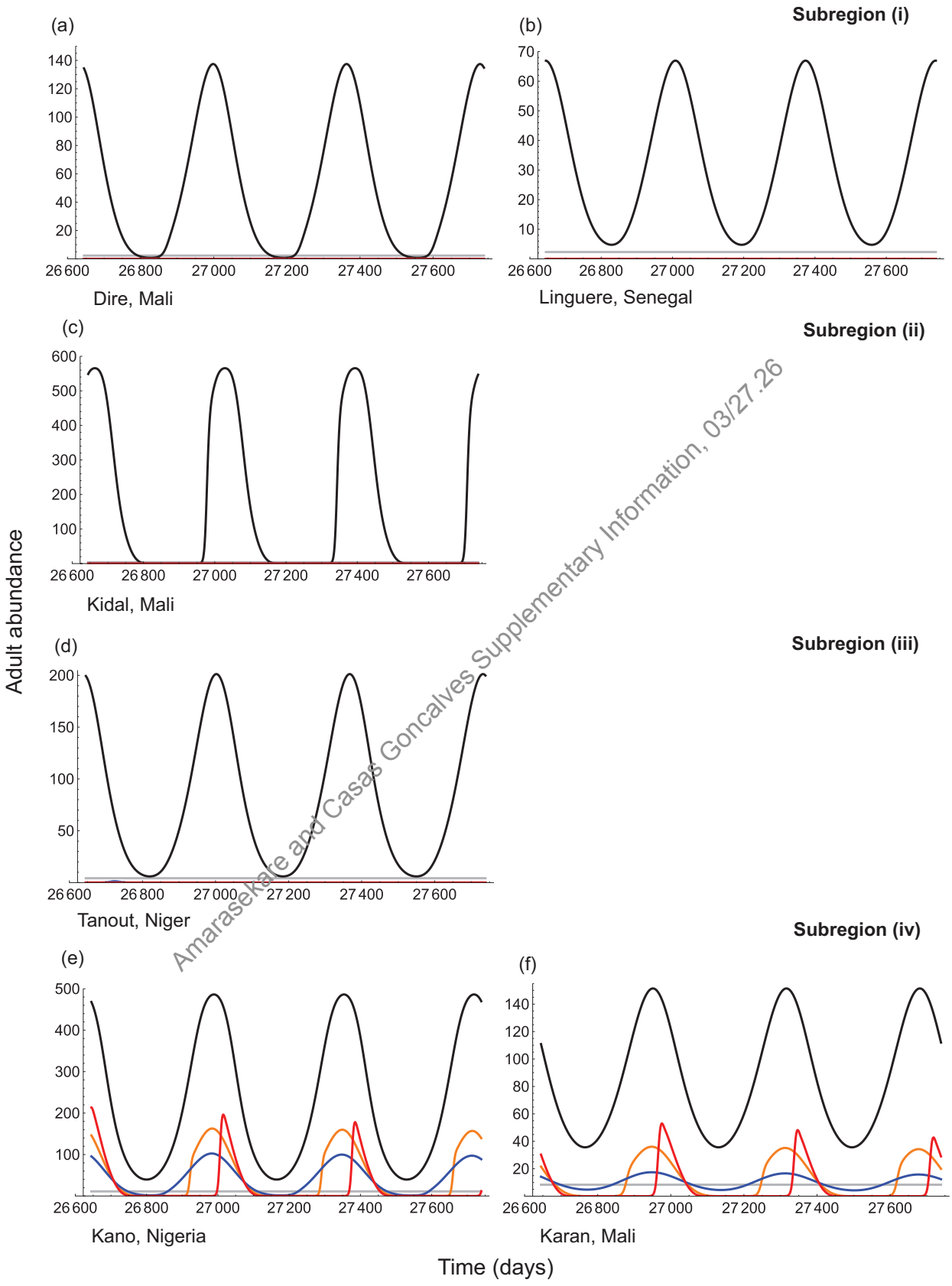

Figure C8